General Disclaimer

One or more of the Following Statements may affect this Document

- This document has been reproduced from the best copy furnished by the organizational source. It is being released in the interest of making available as much information as possible.

- This document may contain data, which exceeds the sheet parameters. It was furnished in this condition by the organizational source and is the best copy available.

- This document may contain tone-on-tone or color graphs, charts and/or pictures, which have been reproduced in black and white.

- This document is paginated as submitted by the original source.

- Portions of this document are not fully legible due to the historical nature of some of the material. However, it is the best reproduction available from the original submission.

Produced by the NASA Center for Aerospace Information (CASI)

08

STIF

III

E7.5 10.359
CR-143161

IN SITU SPECTRORADIOMETRIC QUANTIFICATION OF ERTS DATA

(E75-10359) IN SITU SPECTRORADIOMETRIC QUANTIFICATION OF ERTS DATA Final Report, Jul. 1972 - Jan. 1975 (Long Island Univ.) 169 p HC $6.25 CSCL 05B G3/43

N75-28497

Unclas 00359

Edward F. Yost
Science Engineering Research Group
C.W. Post Center
Long Island University
Greenvale, New York 11548

"Made available under NASA sponsorship in the interest of early and wide dissemination of Earth Resources Survey Program information and without liability for any use made thereof."

February 1975
Final Report under Contract NAS5-21793

Original photography may be purchased from:
EROS Data Center
10th and Dakota Avenue
Sioux Falls, SD 57198

ORIGINAL CONTAINS COLOR ILLUSTRATIONS

1069A

RECEIVED
JUL 30 1975
SIS/902.6

Prepared for:

GODDARD SPACE FLIGHT CENTER
Greenbelt, Maryland 20771

TECHNICAL REPORT STANDARD TITLE PAGE

1. Report No.	2. Gov. Acession No.	3. Recipient's Catalog No.
4. Title and Subtitle "In Situ Spectroradiometric Quantification of ERTS Data"		5. Report Date February 1975 6. Performing Organization Code
7. Author(s) Edward F. Yost		8. Performing Organization Report No. TR-21
9. Performing Organization Name & Address Science Engineering Research Group C.W. Post Center-Long Island University Greenvale, New York 11548		10. Work Unit No. 11. Contract or Grant No. NAS5-21793
12. Sponsoring Agency Name & Address Mr. Edmund F. Szajna Goddard Space Flight Center Greenbelt, Maryland 20771		13. Type of Report and Period Covered Type III July 1972 - January 1975 14. Sponsoring Agency Code

15. Supplementary Notes

16. Abstract

Analyses of ERTS-1 photographic data were made to quantitatively relate ground reflectance measurements to photometric characteristics of the images. Digital image processing of photographic data resulted in a nomograph to correct for atmospheric effects over arid terrain. Optimum processing techniques to derive maximum geologic information from desert areas were established. Additive color techniques to provide quantitative measurements of surface water between different orbits were developed which have been accepted as the standard flood mapping techniques using ERTS.

17. Key Words (Selected by Author(s))	18. Distribution Statement
Spectroradiometric Quantification of Data	

19. Sec. Classif. (of this report)	20. Sec. Classif. (of this page)	21. No. of Pages	22. Price*
U	U		

*For sale by the Clearinghouse for Federal Scientific and Technical Information, Springfield, Virginia 22151.

Preface

The primary objective of this Interpretation Techniques Development Study was to quantitatively relate the photographic characteristics of the ERTS-1 images to measurements of reflectance as well as geologic terrain classifications, as exist on geologic maps, in south eastern Arizona.

Ground spectral reflectance measurements of the Willcox Playa were made on two different dates. These data collected at twelve stations within the Playa were made on the same day as ERTS-1 coverage. Simultaneous soil samples analyzed for moisture content showed that change in spectral reflectance was not correlated with soil moisture but rather represents standing surface water.

Reflectance measurements of three tree species in the Prescott National Forestwere collected prior to the launch of ERTS-1. These reflectance spectra could not be correlated with ERTS-1 images at locations where known plantations of these trees existed.

A computerized "System 800" was used to quantitatively examine ERTS-1 image density characteristics. This system used TV digitization of four ERTS-1 photographic images in registration into 294,912 pixels for each photo, each pixel having 8 bits (256 levels). The data were stored in a computer disc, and processed by PDP-11 computer using a variety of statistical and display programs. Output was on a 8 color TV display. This system was used to make both spectral and temporal analysis of the Willcox Playa as well as the Prescott National Forest and Phoenix, Arizona. Relative atmospheric effects in each of the four bands weredetermined along with the statistical characteristics of the brightness in each ERTS-1 band. These data were used to develop procedures to correct for atmospheric effects in each of the four bands.

Photo-optical additive color techniques were used to perform geologic interpretations using ERTS-1 black-and-white positives. Processing procedures were developed which when used to make positives from standard release negatives, when these positives were used in an additive color viewer, produced optimum color image characteristics of soils and rocks. Many features appearing in the imagery were found not to appear on the most recent geologic maps.

Additive color viewer procedures were developed which produced temporal changes of standing surface water between different ERTS-1 passes. These procedures were adopted by the U. S. Geological Survey, Water Resources Division as a standard procedure to be used in mapping floods using ERTS. The 1973 Mississippi Flood was mapped using the temporal additive color techniques developed in this study.

ORIGINAL PAGE IS
OF POOR QUALITY

TABLE OF CONTENTS

Section	Title	Page
1	INTRODUCTION	1
	Initial Data Analysis	1
	Ground Truth	1
	Digital Image Analysis	2
	Geologic Interpretation	3
	Image Characteristics Related to Reflectance Spectra	3
2	TECHNIQUES AND EQUIPMENT FOR ERTS-1 MULTISPECTRAL PHOTOGRAPHIC IMAGES	4
	Analysis of Photographic Characteristics of the ERTS-1 MSS Data	4
	Additive Color Analysis of ERTS MSS Imagery	16
	Digital Image Processing Equipment and Techniques	17
3	IN SITU SPECTRAL REFLECTANCE MEASUREMENTS AND GROUND TRUTH DATA	23
	Pre ERTS-1 Spectral Reflectance Measurements of the Willcox Playa	23
	Additional Reflectance Spectra of Willcox Playa	38
	Reflectance Spectra of Predominant Vegetation in the Prescott National Forest	50
4	DIGITAL IMAGE PROCESSING OF ERTS-1 PHOTOGRAPHIC DATA	57
	Willcox Playa Spectral Image Analysis	57
	Willcox Playa - Detailed Spectral Image Analysis	61
	Willcox Playa - Temporal Image Analysis	65
	Phoenix, Arizona Spectral Analysis	75
	Prescott, Arizona Spectral Analysis	77
	Atmospheric Effects in Desert Areas	80

ORIGINAL PAGE IS
OF POOR QUALITY

Section	Title	Page
5	ERTS GEOLOGIC INTERPRETATION USING OPTIMUM IMAGE CHARACTERISTICS	86
	Optimum Photographic Characteristics of ERTS for Geology	86
	Visual Analysis of ERTS Image for Geologic Information	87
	Objectives of the Geologic Investigation	91
	Discussion of Correlations and other findings in ERTS-1 Frame Number E-1317-17222	93
6	CONCLUSIONS	101
7	NEW TECHNOLOGY	107
	APPENDIX A: "SYSTEM 800" DESCRIPTIVE LITERATURE	
	APPENDIX B: "SYSTEM 800" COMPUTER PRINTOUTS WILLCOX, ARIZONA SPECTRAL ANALYSIS	
	APPENDIX C: "SYSTEM 800" COMPUTER PRINTOUTS WILLCOX, ARIZONA TEMPORAL ANALYSIS	
	APPENDIX D: "SYSTEM 800" COMPUTER PRINTOUTS PHOENIX, ARIZONA SPECTRAL ANALYSIS	
	APPENDIX E: "SYSTEM 800" COMPUTER PRINTOUTS PRESCOTT, ARIZONA SPECTRAL ANALYSIS	
	APPENDIX F: "SYSTEM 800" COMPUTER PRINTOUTS WILLCOX, ARIZONA SPECTRAL ANALYSIS OF ATMOSPHERIC EFFECTS	
	APPENDIX G: Mapping of the 1973 Mississippi River floods from ERTS, June 1973, Remote Sensing and Water Resources Management.	

LIST OF ILLUSTRATIONS

Number	Caption	Page
1	Characteristic curves of ERTS-1 release positives of MSS imagery of the Willcox Playa acquired on 27 September 1972	5
2	ERTS-1 bulk multispectral scanner images taken on 27 September 1972. The Willcox Playa is in the upper right of each photograph.	6
3	Additive color rendition using NASA bulk positives in which the (500-600 nm) band is projected as blue, the (600-700 nm) band as green, and the (700-800 nm) band as red.	8
4	Step wedge number versus density of multispectral scanner bulk positives of area covering the Willcox Playa, Arizona, taken on 14 October 1972	9
5	Contact prints of ERTS-1 multispectral scanner bulk images taken on the Willcox Playa, Arizona, on 14 October 1972. The Playa is in the upper left of each photo.	10
6	Composite additive color rendition of 14 October 1972 ERTS-1 imagery in which the 500-600 nm band is imaged as blue, the 600-700 nm band as green, and both the 700-800 nm and 800-1100 nm infrared bands as red.	12
7	Composite additive color image similar to that above in which the 500-600 nm band is imaged as red, the 600-700 nm band is imaged as blue, and only the 700-800 nm infrared band is imaged as green.	12
8	Contact prints of ERTS-1 multispectral scanner bulk images taken of the Willcox Playa, Arizona, on 2 November 1972. The Playa is in the lower right of the photo.	13
9	Step wedge number versus density curves of ERTS-1 bulk 70mm positive transparencies of Willcox Playa, Arizona, taken on 2 November 1972	14

Number	Caption	Page
10	Additive color rendition of 2 November 1972 ERTS-1 imagery in which the (500-600 nm) band is projected as blue, the (600-700 nm) band as green, and the (700-800 nm) band as red.	15
11	Spectral Data Model 64 viewer used for additive color analysis of ERTS-1 multispectral images.	16
12	The "System 800" digital processing equipment for multispectral photographs.	18
13	Arrangement of instruments for measuring the spectral distribution of incident and reflected solar radiation in the 380-1250 nm region of the spectrum.	25
14	Flow diagram of percent directional reflectance readings.	30
15	Computer output format of incident and reflectance spectra.	31
16	Computer plot of percent directional reflectance as a function of wavelength.	33
17	Spectral distribution of solar radiation incident at the Willcox Playa test site at different times during the day.	34
18	Location at which incident and reflectance spectra were measured.	35
19	Percent directional reflectance of two locations on the Willcox Playa, Arizona.	36
20	Percent directional reflectance of bare soil, grass and the Willcox Playa. Note the comparative spectral uniformity of the Playa compared to higher infrared reflectance of grass and bare soil.	37
21	Willcox Playa, looking east.	39
22	Locations in Willcox Playa, Arizona, where spectra was taken during Fall 1973.	40
23	Willcox Playa, viewed from road looking east.	41

Number	Caption	Page
24	Willcox Playa location 1A, soil moisture 5.9 percent.	42
25	Willcox Playa location 1B, soil moisture 5.5 percent	42
26	Willcox Playa location 1C, soil moisture 67.7 percent	42
27	Incident Sun Spectra taken in Willcox Playa on 9 October 1973	43
28	Percent directional reflectance at different locations in Willcox Playa on 9 October 1973.	44
29	Percent directional reflectance at different locations in Willcox Playa on 9 October 1973.	45
30	Percent reflectance at 650 nm vs. percent soil moisture.	46
31	Percent reflectance at 950 nm vs. percent soil moisture.	46
32	Incident Sun Spectra taken in Willcox Playa on 16 November 1973.	47
33	Percent directional reflectance at different locations in Willcox Playa on 16 November 1973.	48
34	Percent directional reflectance at different locations in Willcox Playa on 16 November 1973.	49
35	Percent directional reflectance of predominant vegetation species in the Prescott National Forest.	51
36	Truck-mounted telespectroradiometer.	52
37	Telespectroradiometer optical schematic.	54
38	Telespectroradiometer electronics block diagram.	56
39	Willcox Playa "System 800" Digital Image analysis of ERTS-1 5 June 1973. Band 4 and Band 5 negatives.	59
40	Willcox Playa "System 800" Digital Image analysis of ERTS-1 5 June 1973. Band 6 and Band 7 negatives.	60

ORIGINAL PAGE IS
OF POOR QUALITY

Number	Caption	Page
41	Digitized ERTS-1 4 September 1973, images of Willcox Playa from positive film transparancies showing statistical distribution of brightness levels (dark at top of Vertical scale in photos).	62
42	4 September 1973 ERTS-1 Positive Transparencies of Willcox Playa.	64
43	Willcox Playa Temporal Analysis - Digital Image Analysis of ERTS-1 Photographic Negatives Band 5 (.6 to .7γ) on four different levels.	66
44	Digitally averaged brightness values of the Willcox Playa, Arizona on two dates.	68
45	Total Picture Elements 294, 912 Willcox Playa Temporal ERTS Band 5.	69
46	Willcox Playa Temporal ERTS Band 5 - 1 Nov. 72, 18 Feb. 73, 18 May 73, 5 June 73.	70
47	Digitized ERTS-1 Band 4 images from positive film transparencies showing variations (.5 to .6γ) reflectance on four different takes.	72
48	Willcox Playa Temporal ERTS Band 4	73
49	ERTS-1 Band 4 mean and variance of digital brightness measurements of three locations in the Willcox Playa, Arizona on four different dates.	74
50	Prescott, Arizona - Positive ERTS-1 images acquired on 29 September 1972.	78
51	Prescott, Arizona - digitized brightness presentation for photographic negatives acquired by ERTS-1 on 29 September 1972.	79
52	Digital brightness levels of the four ERTS-1 bands compared to Band 7 for cloud tops, terrain in sun, and terrain in shadow.	82
53	Scene brightness range of sunlit desert terrain minus similar terrain in shadow. The range of Band 7 is used as 100 percent.	83
54	Atmospheric correction factor for ERTS bands.	85
55	Variability of the digital brightness in each ERTS band.	85

Number	Caption	Page
56	Photographic characteristics of positives made from NASA Release Negatives to produce optimum additive color image for geologic interpretation.	88
57	Variation of geologic image quality with increasing gamma.	89
58	ERTS image produced using optimum reprocessing of black-and-white positive images.	90
59	ERTS-1 images of south eastern Arizona on which is superimposed an overlay of known geology from existing geologic maps.	94
60	Additional geologic information contained in ERTS-1 image but not appearing on state geologic maps.	96
61	Lithologic outlines for the Geologic map of the Southern Part of the Mule Mountains, Arizona, superimposed on an enlargement of ERTS additive color rendition of that area.	98
62	Comparison of in situ spectral reflectance measurements normalized to 950 nm and ERTS-1 image brightness data normalized to Band 7.	102
63	Multi-date additive color image of the Willcox Playa showing changes in standing water.	103

LIST OF TABLES

Number	Caption	Page
1	Soil Moisture at different locations in Willcox Playa, Arizona.	41
2	Digital Brightness Classification of ERTS-1 multispectral images of Willcox Playa taken on 4 September, 1973.	63
3	Statistics of the 4 September 1973 ERTS-1 positives of the Willcox Playa, Arizona.	63
4	Digital brightness classification of multidate imagery of Willcox Playa.	67
5	Digital brightness classification of multidate imagery of Willcox Playa.	71
6	The mean and standard deviation of the relative brightness of the Willcox Playa on four different dates as recorded in ERTS-1 Band 4 imagery.	74
7	Digital brightness statistics of clouds and shadows appearing in Phoenix, Arizona 14 April 1973 positives.	75
8	Digital brightness classification of urban section of ERTS-1 imagery of Phoenix, Arizona taken on 14 April 1973.	76
9	Brightness difference between cloud tops (x) and shadows (x.) in Phoenix, Arizona 14 April 1973.	76
10	Digital brightness classification of Prescott National Forest on ERTS-1 negatives taken 29 September 1972	77
11	Digital brightness of ERTS-1 images of Southern Arizona taken on 4 September 1972.	80
12	The mean and standard deviation of image brightness measurements of desert terrain in shadow and illuminated by sunlight.	81

ORIGINAL PAGE IS
OF POOR QUALITY

Number	Caption	Page
13	Terrain and shadow measurements normalized to equal cloud brightness measurements.	82
14	Computational steps to arrive at correction factors to compensate for atmospheric scattering of low brightness desert terrain.	83
15	Photographic characteristics of ERTS positives reproduced to give optimum additive color picture for geologic interpretation.	87
16	In situ spectral reflectance measurements and corresponding ERTS-1 image density measurements.	101

Section I

Introduction

This report presents the results of an Interpretation Techniques Development study, the initial objective of which was to quantitatively relate photographic characteristics of the ERTS-1 images to measurements of the reflectance, and of the characteristics of ground objects. Positive and negative Multispectral Scanner (MSS) images taken principally over the Willcox Playa, Arizona as received from Goddard Space Flight Center were the basic input to this project.

Initial Data Analysis

An analysis of the ERTS-1 photographic characteristics was performed initially, the purpose being to establish optimum procedures for printing positives of semi-arid desert-like terrain. A procedure was developed which when used to print positive transparencies from NASA ERTS-1 release negatives produced excellent composite color images when projected on an Additive Color Viewer screen.

An extensive qualitative interpretative analysis was performed using an Additive Color Viewer and the reprocessed positive images. The purpose here was to examine spectral reflectance image characteristics of a large and relatively homogenous object such as the Willcox Playa.

Ground Truth

The principal area of interest in this study, the Willcox Playa, is a large dry lake located in southeastern Arizona. The central part of the Playa has a hard and compact crust. The outer areas of the

ORIGINAL PAGE IS
OF POOR QUALITY

Playa contain soft, dry and porous surfaces which become flooded during the infrequent rains.

Reflectance spectra were taken in situ on the Playa before the launch of ERTS-I and during 1973. These latter measurements were made at twelve sample stations in the Playa and correlated with soil moisture measurements simultaneously taken.

Reflectance measurements were also taken at the Prescott National Forest in north central Arizona. Three plant species were measured in situ. This data was later used as a quantitative data base against which the digitally processed ERTS-I photographic data were examined.

Digital Image Analysis

In order to quantitatively examine image density characteristics, digital image processing procedures were developed using TV digitization of the images in registration, storage in a PDP-11 computer disc, image processing, statistical analysis and display programs.

Using this digital image processing system, both a spectral and temporal analysis of the reflectance characteristics of the Willcox Playa were performed. An analysis of the cloud shadow characteristics was carried out using imagery of Phoenix, Arizona. Imagery of the Prescott National Forest was also digitally analyzed. The relative effect of the atmosphere in each of the four spectral bands was measured using imagery of the Willcox Playa. The statistics of the relative screen brightness range in each of the four ERTS-I bands were established for desert areas and a procedure was developed to correct for atmospheric effects in each of the four bands.

ORIGINAL PAGE IS
OF POOR QUALITY

Geologic Interpretation

A geologic interpretation was performed using ERTS-1 black-and-white positives which had been reprocessed to provide optimum additive color image characteristics for exposed soils and rocks found in the southern Arizona desert. This reprocessing procedure has been precisely set forth herein. A considerable amount of image detail identified by color signature differences was rendered visible on the additive Color Viewer screen. Many features appearing in the imagery did not appear on the most recent geologic maps.

Image Characteristics Related to Reflectance Spectra

An analysis of the image characteristics of the Willcox Playa in relation to in situ ground spectra was made. A procedure was developed whereby temporal additive color composites would show the presence of standing water. These procedures for depicting the presence of surface water were used for mapping the 1973 Mississippi flood.

ORIGINAL PAGE IS
OF POOR QUALITY

Section 2

Techniques and Epuipment

for ERTS-I Multispectral Photographic Images

Multispectral Scanner (MSS) imagery exposed on different dates was received from the Goddard Space Flight Center in both positive and negative form. The spectral bands included the 500-600 nm, 600-700 nm, 700-800 nm, and 800-1100 nm spectral bands. Candidate frames from these ERTS photographic products were selected, taking into consideration the extent of cloud coverage. The selected frames were employed for densitometric additive color and digital image analysis and correlation with ground reflectance spectra.

Analysis of Photographic Characteristics of the ERTS-I MSS Data

A photographic analysis of the ERTS-I MSS photographic data acquired over the Willcox test site was performed. The purpose was to establish the best procedures for printing positives of semi-arid desert like terrain such as exists around Willcox, Arizona.

Release positives of MSS Bands 4, 6 and 7 acquired on 27 September 1972 were the first images analyzed. Graphs relating step wedge grey scale numbers on the data block to density were generated from the data block. These curves are shown in Figure 1.

The graphs in Figure 1 show that the reproduction techniques of printing and processing the release positives yielded photographs which were well matched for the three bands. However, the relatively high minimum density (approximately 0.4) did not allow sufficient image brightness when the positives were used in an additive color viewer. The small change in density at the higher grey scale values (i.e. for increasing relative log exposure) reveals that the release positives were reproduced to give greatest density range for the low brightness detail in the scene

ORIGINAL PAGE IS
OF POOR QUALITY

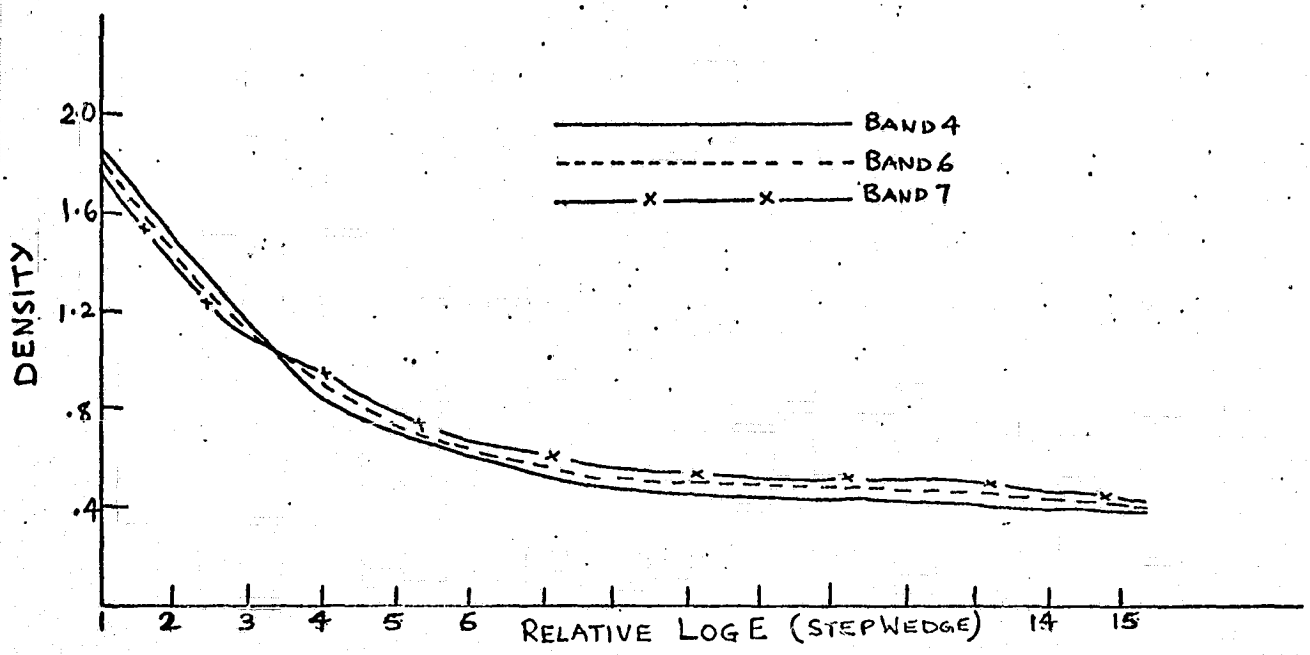
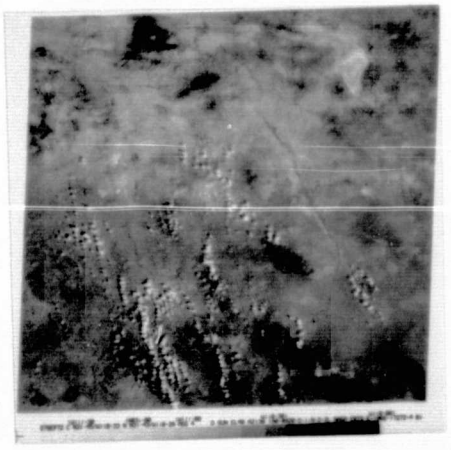


Figure 1. Characteristic curves of ERTS-1 release positives of MSS imagery of the Willcox Playa acquired on 27 September 1972.

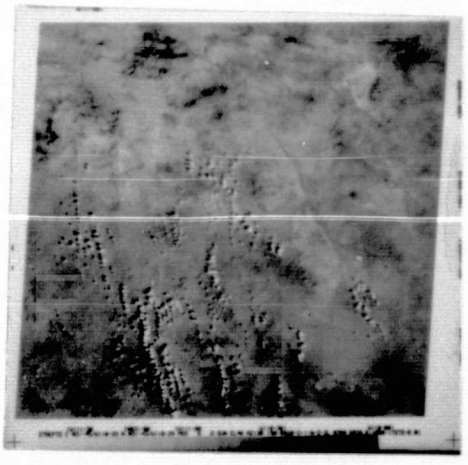
at the expense of the higher brightness detail.

A densitometric evaluation of the reproduction of the release positives of MSS Bands 4, 5, 6 and 7 was performed. Contact prints from the 70mm multispectral scanner release negatives are shown in Figure 2. Great care was taken to match the densities of the step wedges on the prints to match those of the release positive transparencies.

In Band 4 (500-600nm), it is apparent that most of the terrain is in highlight. In terms of the step wedge number versus density curve (Figure 1), the densities lie along the portion of the curve where the density differences are not large. The imagery, therefore, appears lacking in contrast, especially in the darker cultivated land region to the right of the Willcox Playa. The optimization of density differences in the scene, particularly the highlight regions, can be accomplished by increasing the exposure of the positive image while maintaining the development parameters constant. The density range of a

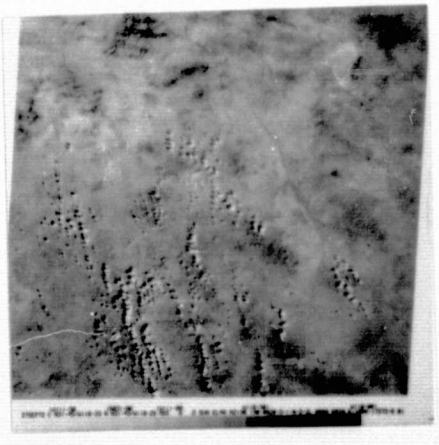


500-600 nm Band



600-700 nm Band

ORIGINAL PAGE IS
OF POOR QUALITY



700-800 nm Band



800-1100 nm Band

Figure 2. ERTS-1 bulk multispectral scanner images taken on 27 September 1972. The Willcox Playa is in the upper right of each photograph.

large portion of the scene lies between the #1 and #8 steps of the grey scale while the mountain ridges have a lower density corresponding to the #13 step. The density differences between most of the terrain objects do not exceed .12 in Band 4. If exposed on the straight line portion of the percent transmission versus density curve, the density differences produced could have been as large as 3.0.

A similar examination of Band 5 (600-700 nm) shows considerably more image detail than is present on Band 4. This increase in detail results from an improved contrast between objects in the scene (for example, the cultivated area to the right of the Playa). This increased contrast does not result from any difference in processing, rather it is caused by the fact that the negative material was given sufficient exposure to place the objects of interest more nearly on the straight line portion of the percent transmission versus density curve. The density range of most of the scene lies between steps #9 and #12. The image density range is .3 in Band 5.

Both near-infrared release positives, Bands 6 and 7 (700-800 nm and 800-1100 nm) were partly exposed in the reproduction, although the contrast is the same as Band 5. The high reflectance of the cultivated crops adjacent to the Playa can barely be differentiated from the barren clay flat of the dry lake bed. This is because both objects, in spite of their inherent spectral brightness differences, lie along the toe of the step wedge number versus density curve. Densitometric measurements of the Playa image reveals that it has an average density of .52, while the crops have a density of .5. These values correspond to steps #8 and #7 on the data block step wedge. If the printing exposure had been increased, the density differences between these two objects could have been increased from .02 to .4 in both Band 6 and 7.

The set of NASA released positives shown in Figure 2 were placed into the Spectral Data Model 64 viewer for recombination in additive color. Figure 3 is a photograph of the viewer screen in which Band 4 (500-600 nm) was projected as blue, Band 5 (600-700 nm) as green, and Band 6 (700-800 nm) as red. This rendition is an approximation of that which would be achieved using color infrared film. Because of the incorrect printing exposure of the positives, the imagery lacks image detail, contrast, and color.

ORIGINAL PAGE IS
OF POOR QUALITY

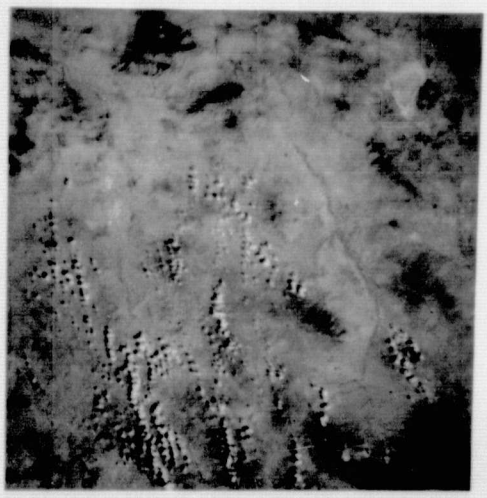


Figure 3. Additive color rendition using NASA bulk positives in which the (500-600 nm) band is projected as blue, the (600-700 nm) band as green, and the (700-800 nm) band as red.

The second set of ERTS multispectral scanner release positives which were analyzed was acquired on 14 October 1972 over the Willcox Playa test site. The nadir of these photos is considerably eastward of that taken on September 27th. The relative grey scale number versus density curves shown in Figure 4 were generated using the grey scale in the data block of each release positive.

ORIGINAL PAGE IS
OF POOR QUALITY

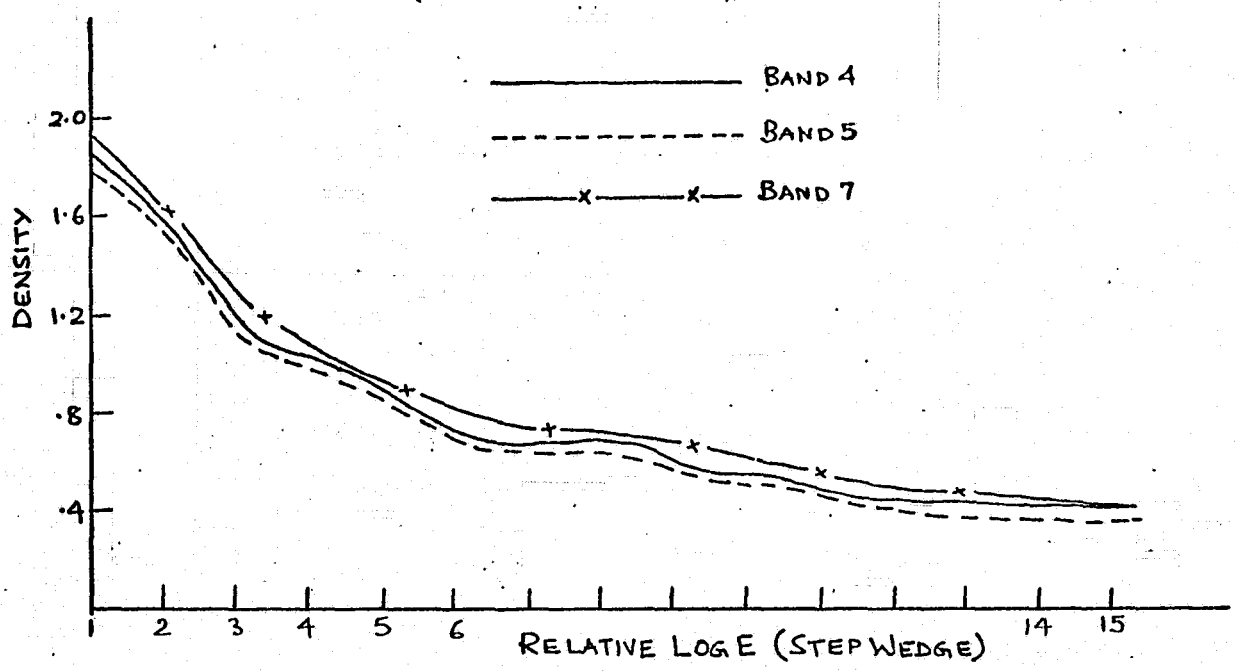
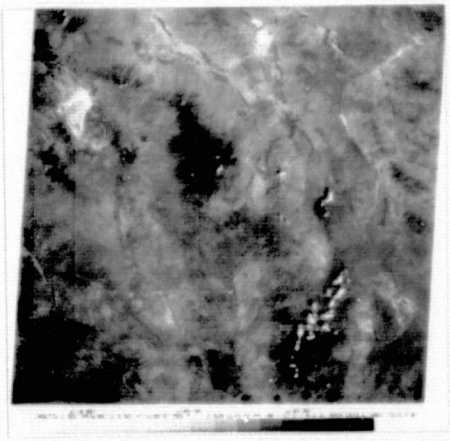


Figure 4. Density vs. step wedge number of multispectral scanner bulk positives of area covering the Willcox Playa, Arizona, taken on 14 October 1972.

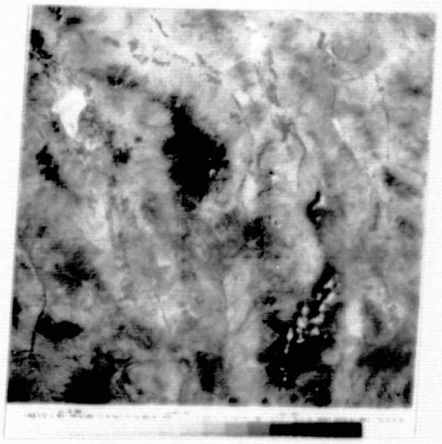
A comparison of this set of curves with those of Figure 1 shows that there exists a larger scene brightness range which is imaged on the upper portion of Figure 4. In other words, the exposure has been increased. There has also been an increase in the slope of the step wedge number versus density curve for these later release positives which are shown as contact prints in Figure 5. Each of the multispectral scanner positives are well matched in curve slope and minimum density.

Comparing Band 4 (500-600 nm) of Figures 5 and 2 shows a marked improvement in the image detail for the cultivated land areas to the southeast of the Willcox Playa; this, in spite of the relative increase in density, is a much better positive image for analysis in an additive color viewer.

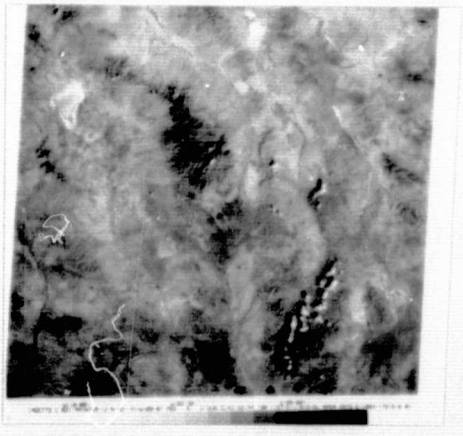
ORIGINAL PAGE IS
OF POOR QUALITY



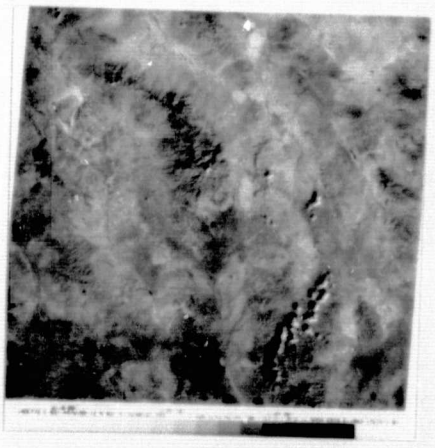
500 - 600 nm Band



600 - 700 nm Band



700 - 800 nm Band



800 - 1100 nm Band

Figure 5. Contact prints of ERTS-1 multispectral scanner bulk images taken on the Willcox Playa, Arizona, on 14 October 1972. The Playa is in the upper left of each photo.

The release positive for Band 5 (600-700 nm) shows that most of the scene lies between steps #6 and #10 on the transmission grey scale located at the bottom of the image. This represents a density difference of only .3. The most dense images in the photo correspond to step #13 which lies just at the start of the straight line portion of the percent transmission versus density curve shown in Figure 4. A significant portion of the curve is not being utilized at all. The highlight areas of the Willcox Playa are in the fog density level of the film so that the entire scene exists along that part of the curve which yields the least discrimination in terms of density. The base-plus-fog density level for all MSS bands exposed on 14 October is excessively high, being .49.

A simulation of color infrared film, shown by Figure 6, was generated by projecting the (500-600 nm) band as blue, the (600-700 nm) band as green, and both the (700-800 nm) and (800-1100 nm) infrared bands as red. The brightness of each near-infrared channel was reduced to half value so that when projected their combined brightness would be the same as a single infrared channel projected at full brightness. Figure 7 shows a false color presentation generated by projecting the (500-600 nm) green band as red, the (600-700 nm) red band as blue, and the (700-800 nm) infrared band as green.

MSS release positives obtained on 2 November 1972 were typical of the photographic characteristics of all subsequent release positives. The nominal nadir of the imagery is directly north of the 27 September imagery. Contact prints of the four release positives are shown in Figure 8 and the grey scale number versus density curves associated with them are given in Figure 9. The exposure of the positive images,

ORIGINAL PAGE IS
OF POOR QUALITY

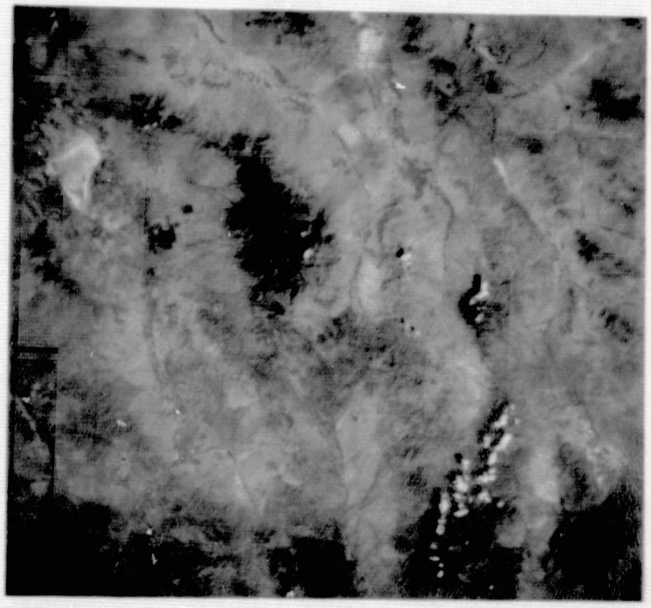
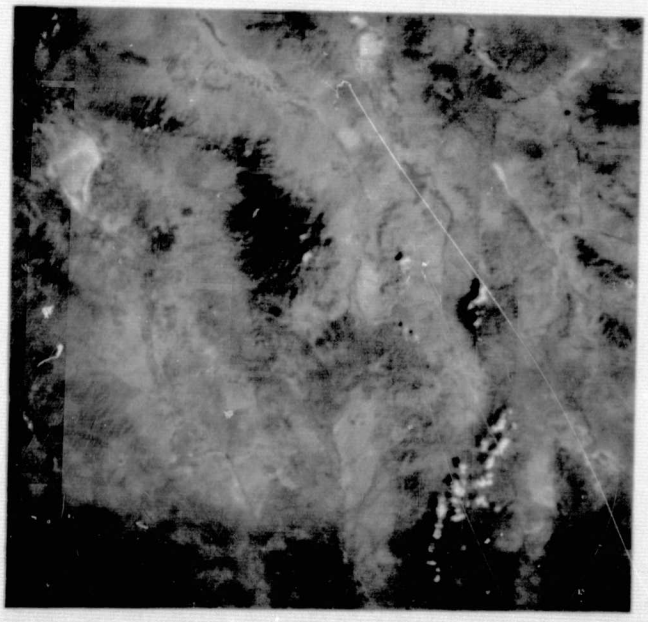


Figure 6. Composite additive color rendition of 14 October 1972 ERTS-1 imagery in which the 500-600 nm band is imaged as blue, the 600-700 nm band as green, and both the 700-800 nm and 800-1100 nm infrared bands as red.

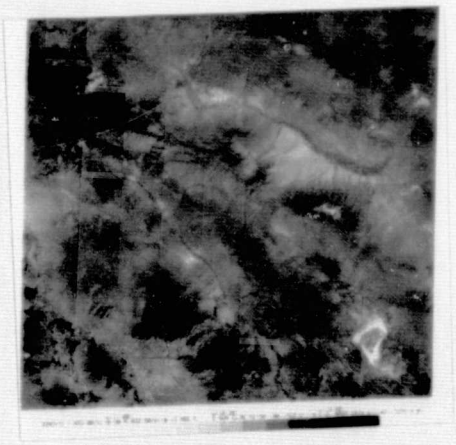


ORIGINAL PAGE IS
OF POOR QUALITY

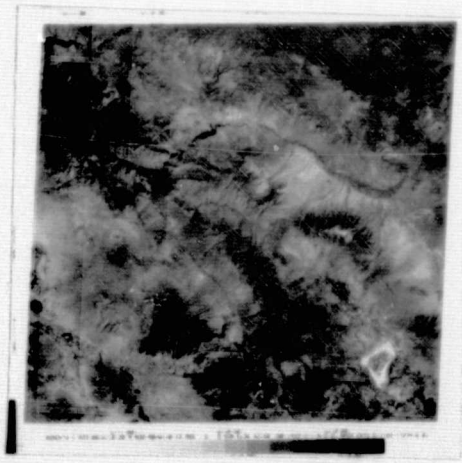
Figure 7. Composite additive color image similar to that above in which the 500-600 nm band is imaged as red, the 600-700 nm band is imaged as blue, and only the 700-800 nm infrared band is imaged as green.

ORIGINAL PAGE IS
OF POOR QUALITY

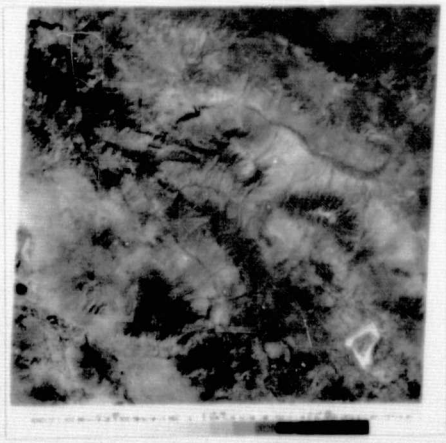
ORIGINAL PAGE IS
OF POOR QUALITY



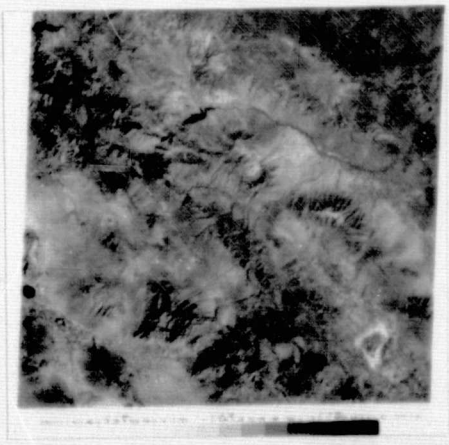
500-600 nm Band



600-700 nm Band



700-800 nm Band



800-1100 nm Band

Figure 8. Contact prints of ERTS-1 multispectral scanner bulk images taken of the Willcox Playa, Arizona, on 2 November 1972. The Playa is in the lower right of the photo.

ORIGINAL PAGE IS
OF POOR QUALITY

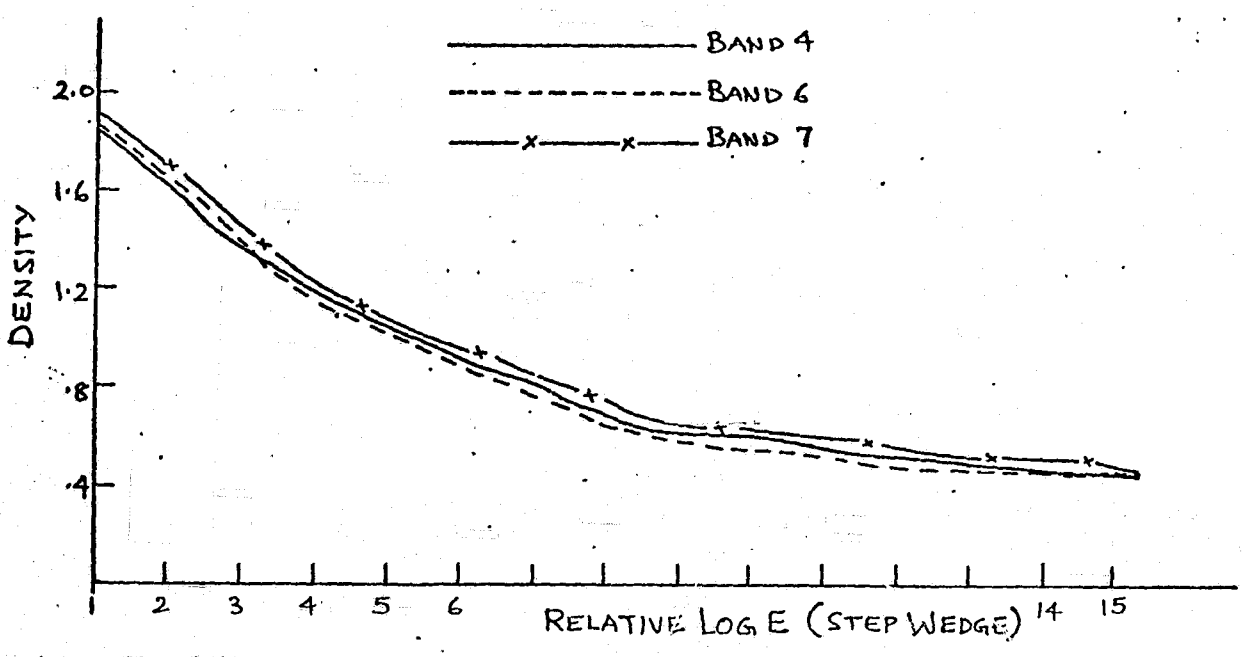


Figure 9. Density versus step wedge number curves of ERTS-1 bulk 70mm positive transparencies of Willcox Playa, Arizona, taken on 2 November 1972.

as well as the processing conditions, are almost identical with those of 14 October, except that the minimum density is .1 lower.

The overall density of Band 4 (500-600 nm) lies between the #8 and #12 steps of the grey scale which represents a density difference of .52. The center of the Playa has an average density of 1.05 and shows considerably more contrast within it than either of the previous sets of scanner data. Exposure of Band 4 is excessive and no image detail lies along the straight line of the step wedge number versus density curve. The overall density range of the image detail in Band 6 lies between steps #7 and #13 on the positive grey scale. Band 5 appears to be much "sharper" than Band 4 in terms of inherent contrast, although the overall density ranges do not differ by more than .28. This is due to a contrast which exists as a result of the spectral reflectance

of the terrain.

A color infrared simulation of the 2 November 1972 imagery has been generated by projecting Band 4 (500-600 nm), Band 5 (600-700 nm), and Band 6 (700-800 nm) as blue, green, and red respectively in a Spectral Data Model 64 additive color viewer. Figure 10 is a color reproduction of this rendition created on the viewer screen. The multispectral screen brightness factor is low due to the high base-plus-fog factor. A change in the reflectance of the Playa can be seen by comparing this rendition to Figures 3 and 7.

Photographic reprocessing techniques were subsequently developed to enhance geological information. These are presented in Section 5.

ORIGINAL PAGE IS
OF POOR QUALITY

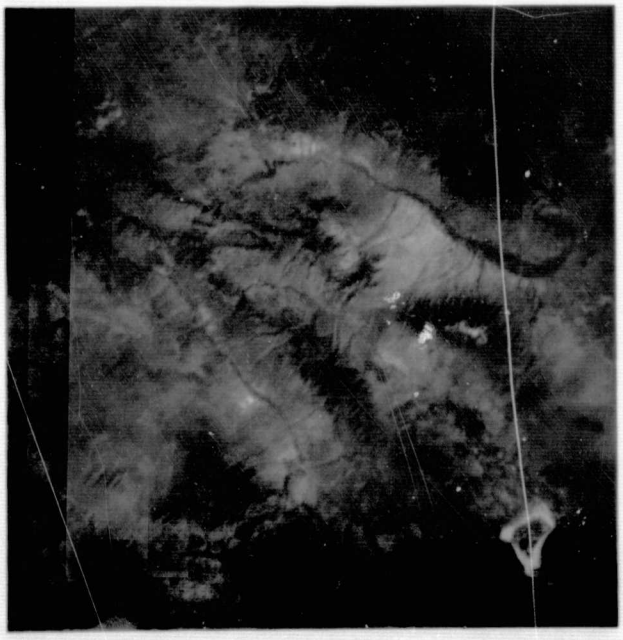


Figure 10. Additive color rendition of 2 November 1972 ERTS-1 imagery in which the (500-600 nm) band is projected as blue, the (600-700 nm) band as green, and the (700-800 nm) band as red.

Additive Color Analysis of ERTS MSS Imagery

ERTS photographic data products were analyzed using additive color viewing analysis techniques. The procudures used, with appropriate instrumentation and significant theories, are described in the subsequent paragraphs.

Spectral Data Model 64 viewer, shown in Figure 11, was an essential instrument for use in the interpretation and analysis of ERTS MSS imagery. The device produces a single color presentation for the spatially calibrated photos by projecting the image of one photo on top of the other using different color light sources. This technique of analysis permits a scientist to select a set of bands and to interpret within results from a single color presentation. In addition, a multispectral viewer provides the scientist with the capability of altering the color of the presentation in order to enhance the particular relationships he may be seeking. Fundamentally, the multispectral technique allows one to create a color presentation specifically for the purpose of his discipline and interests.



Figure 11. Spectral Data Model 64 viewer used for additive color analysis of ERTS-1 multispectral images.

ORIGINAL PAGE IS
OF POOR QUALITY

In order to quantitatively evaluate multispectral color images, color must be colorimetrically defined as that conscious sensation which is exhibited when light of a specific spectral energy distribution enters the eye. It has been experimentally shown that differences in this energy distribution cause variations in the observed response of the eye and may be described in terms of three distinct psychophysical variables. The first is hue which is basically that quality of color which leads to the definition of an object as being red, green, yellow, etc. Saturation, the second quality of color, is described as the amount of white in a given hue. It may be also considered as the concentration of the color. For instance, it is the difference between red and pink. As the amount of saturation in a color decreases, it approaches pure white. Brightness, which is the third variable of color, is described as the amount of visible energy contained in a certain hue which is saturated to a specific value.

DIGITAL IMAGE PROCESSING EQUIPMENT AND TECHNIQUES:

A digital analysis of the ERTS-1 Photographic imagery was performed. The purpose was to make a statistical analysis of ERTS-1 photographic data in order to determine the spectral and temporal variations of the image characteristics, as well as to devise procedures for classification of terrain features.

The equipment used for this purpose was a Spatial Data "System 800". This device, shown in Figure 12, and is described in some detail in Appendix A.

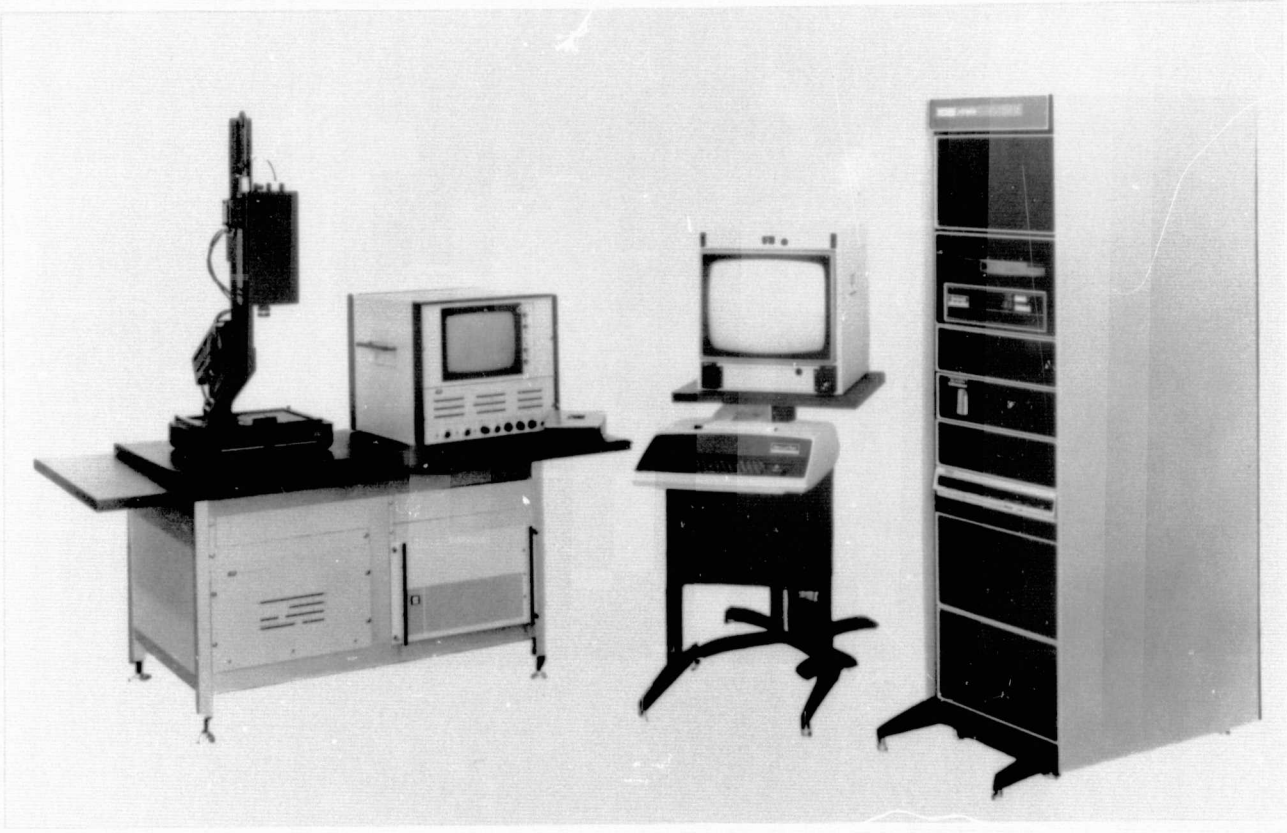


Figure 12. The "System 800" digital processing equipment for multispectral photographs.

This system for digitizing and analyzing multispectral photographs operates as follows:

-- Four multispectral black-and-white transparencies are placed on a light box. These photographs are digitized in registration one at a time by a TV camera. The transmitted brightness (e.g. the density) of each multispectral photograph is digitized into 8 bit binary numbers (256 density levels) in a 512 x 576 point matrix.

-- The 512 x 576 x 8 bit digitized image from each multispectral photograph is stored on the disc of a PDP-11/E-04 computer.

-- A series of programs are used to process the images. For instance addition, subtraction, multiplication and division of any combination of the four multispectral photographs is accomplished by the

ORIGINAL PAGE IS
OF POOR QUALITY

computer and a series of programs. A description of these programs is included in subsequent paragraphs.

-- A digital disc is used to store the processed image and to display it on a color TV monitor. The display is in eight colors. A Decwriter also produces hard copy of statistical results and of operating program sequence.

A description of the "System 800" programs is as follows:

MARKER: Reads, saves, and generates joystick-indicated fiducial marks for multiple picture registration.

DIGIT: Digitizes a video picture into a named computer disc picture file.

HISTOR: Generates a line histogram on a black-and-white monitor displaying the grey scale distribution of a given multispectral picture and accepts joystick inputs to partition the grey scale for DISPLAY.

DISPLAY: Copies a picture from computer disc to the data disc using slice values from HISTOR or a uniform default partition.

AREA: Outputs eight numbers corresponding to the percentages of the full picture of each color on the color TV display.

ADDER: Sets [picture 2] = [(picture 1) + (picture 2)]/2, where pictures 1 and 2 are named computer disc picture files.

NEGATE: Produces the compliment of a given picture.

CONTEX: Performs a contrast expansion of a given picture within variable limits.

SHIFT: Replaces a picture by itself shifted any number of pixels up, down left or right.

ORIGINAL PAGE IS
OF POOR QUALITY

GRID: Generates a variable spaced white-on-black grid on the color TV display.

DIAGON: Performs various exercising, diagnostic and display functions under keyboard control.

Eight bit digitization was selected in order to divide the density range of the photographs into 256 levels. The scanner used for digitization used a special vidicon-type television camera tube and special circuits to accurately sense the light emitted by the image to be digitized. A light image of the object is produced on the photosensitive face of the camera tube by an optical system containing an ordinary camera lens. Brightness at any point on the image is a function of an X and Y coordinate position on the tube face. Image brightness is then defined as a third dimension, Z.

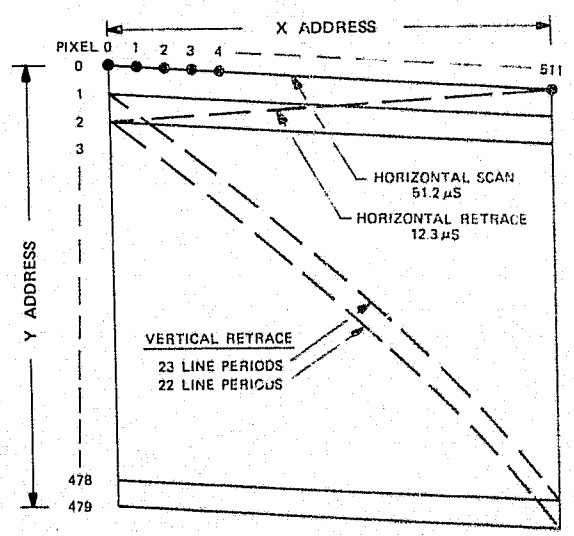
The brightness, or Z-value, is converted into an electrical voltage (video signal) by repeatedly scanning the image with an exploring spot formed by the electron beam of the camera tube. This spot generates an electrical video signal which indicates the brightness at its instantaneous position. The video signal is transmitted through a video amplifier to the TV display, where it controls the brightness of a reproducing spot formed by the CRT electron beam. The reproducing spot moves over the viewing screen in a path similar to, and synchronous with, the exploring spot. The reproducing spot reconstructs the brightness distribution in the image area, both in magnitude (Z) and position (X-Y) and thus generates a television picture of the object.

The scanner path covering the image area consists of a series of straight parallel lines. The spot moves from left to right across each line at a constant speed and then returns to traverse the next line. The

ORIGINAL PAGE IS
OF POOR QUALITY

spot returns back to the top upon completion of the bottom line. During the horizontal and vertical retrace periods the exploring and reproducing spots are disabled, or blanked, so that the image itself is scanned only during the forward, left to right motion of the spots.

In order to reduce flicker in the reproduced picture, the scanning lines are interlaced. That is, instead of moving across the horizontal lines in the sequence 0, 1, 2, 3, 4, ..., the spot first covers the even-numbered lines (0, 2, 4, ..., 478) and then the odd-numbered lines (1, 3, 5, ..., 479). The scanning beam completes two interlacing scanning patterns (fields) to cover the entire image or frame. Each field takes 1/60 second to complete; the entire image is scanned 30 times a second.



Television Scan Pattern

A sync generator provides the signals for synchronizing the exploring spot on the scanner and the reproducing spot on the display. Digital counting circuits divide each line into 512 parts while counting the lines through each frame. The instantaneous digital values represent X and Y positions of the scanning spot. The X-Y addresses select 245,760 points

ORIGINAL PAGE IS
OF POOR QUALITY

"Page missing from available version"

Section 3

In Situ Spectral Reflectance Measurements and Ground Truth Data

Spectral Reflectance measurements were made in situ at the Willcox Playa, Arizona and at Copper Basin and Copper Creek south of Prescott, Arizona. The equipment, techniques used and the significant data obtained are described herein. Also described is the soil moisture data obtained at Willcox Playa and the location of homogeneous kinds of trees in Copper Basin.

Pre ERTS-1 Spectral Reflectance measurements of the Willcox Playa

Willcox Playa, located in the southeastern part of Arizona, is a large dry lake which is clearly resolved on ERTS-1 imagery. It is bounded on the southeast and northeast by cultivated fields and coarser alluvial slopes to the west. The Playa surface is flat and periodic flooding serves as a leveling agent. Variations in sediment size and composition, as well as the availability of surface and ground water, produce a variety of landforms. The central region of the Playa is hard, compact crust which has no microrelief, except that created by mud shrinkage. The dry surface consists of mud polygons which are a light grey buff color. Soft, dry, and porous surfaces are often salt-stained and lead to the sticky-wet areas found where the water table is near the surface. The soft puffy soils are usually a light brown color depending on the salt and moisture content. The Playa is dynamic and it changes in response to the surrounding terrain. The surface drainage on and adjacent to the dry lake changes as a function of the rainfall and a technique is necessary to monitor the dynamics of the

ORIGINAL PAGE IS
OF POOR QUALITY

area. Spectral reflectance measurements of the dry Playa surface indicate a surprising degree of uniformity.

Prior to the launch of ERTS-1 measurements were made of the incident solar irradiance spectra at the Willcox Playa, Arizona. Simultaneous spectroradiometric radiance measurements were obtained of the Playa and large plowed and grass fields adjacent thereto. These data were computer processed to provide relative percent directional reflectance data of homogeneous terrain objects large enough to be well resolved on the space imagery.

The quantitative spectral analysis of soils, vegetation, and rocks requires that simultaneous and accurate measurements of incident and reflected radiation be made. Since the spectral energy reflected by an object varies with that which is incident upon it, the spectroradiometric measurement must be made at the same instant of time. The arrangement of the instrumentation used to obtain simultaneous measurements of incident and reflected radiation is shown in Figure 13. Two instruments were required to obtain reflected radiance measurements due to photomultiplier sensitivity limitations.

A spectroradiometer using a wedge interference filter system enabling the spectrum from 380-1250 nm to be continuously scanned was used to measure the spectral distribution of incident solar irradiance. The instrument was equipped with a diffusing screen so that its directional response was proportional to Lambert's cosine law. This technique of measuring incident irradiance was used since solar energy falls upon the earth's surface and is reflected into an entire hemisphere regardless of its original direction of propagation. True cosine response also eliminates

ORIGINAL PAGE IS
OF POOR QUALITY

ORIGINAL PAGE IS
OF POOR QUALITY



Figure 13. Arrangement of instruments for measuring the spectral distribution of incident and reflected solar radiation in the 380-1250 nm region of the spectrum.

the need for precise aiming to the instrument.

Whereas a radiometer measures in units of energy rate intensity such as microwatts per centimeter square, a spectroradiometer measures in units of energy rate intensity per bandwidth, such as microwatts per centimeter square per nanometer. This latter system of units is most meaningful for measurements of radiation since a graph of the spectral distribution of radiant intensity versus wavelength can be obtained. The area under such a curve can be made numerically and dimensionally equal to energy available in the spectral bands of the ERTS-1 multispectral scanner. The spectroradiometer used was capable of measuring from 0.01 to 1000 microwatts per centimeter square per nanometer. These

values correspond roughly to illumination levels of 0.03 to 30,000 foot candles.

The calibration of the spectroradiometer was verified before and after the experiment. A spectral standard lamp, serially numbered and calibrated against the National Bureau of Standards reference, was used. The lamp was of the ribbon filament tungsten type and had a nominal accuracy of plus or minus five percent relative to the NBS standard.

The half bandwidth of the spectroradiometer used to measure the incident illumination is approximately 15 nanometers in the 380-750 nm range and 30 nanometers in the 750-1250 nm range. Stray light response to unwanted wavelengths of 15 nm bandwidth and far from the wavelength of interest is usually in the order of 0.01 percent.

The periodic calibration of the spectroradiometer used for measuring incident sunlight allowed an accuracy of plus or minus seven percent in the long wavelengths and plus or minus ten percent in the short wavelengths of the spectrum. Most of this error, of course, comes from uncertainty in the secondary standard used. The relative accuracy of all points with respect to each other throughout the wavelength range measured is approximately plus or minus three percent.

The reflectance radiometer system allowed measurements of the average power of the solar radiation reflected by soils and vegetation in the Willcox Playa area. By means of a grating monochromator, these readings can be made at selected wavelengths over a bandwidth determined by the grating and slits. This instrument basically consists of an optical system which limits the entrance of energy to a twelve degree field, a monochromator grating to spectrally isolate the visible energy to a

ORIGINAL PAGE IS
OF POOR QUALITY

five nanometer halfband pass, and the infrared energy to a ten nanometer halfband, as well as detector heads to sense the magnitude of the incident energy.

The reflectance spectroradiometer is designed so that light reflected from an object passes through a diffuser system and is directed by the collective lens into the monochromator housing via the entrance slit. Calibration accuracy is obtained when the light incident on the diffuser is imaged on the entrance slit, completely filling the slit area with light. A collective lens in the beam input optics in front of the monochromator entrance slit, collects the incident light which is properly matched with the diffuser to create a uniform illuminating bundle inside the monochromator housing. This bundle of light is then incident on a plane diffraction grating where it is angularly dispersed according to wavelength. Each wavelength present in the source bundle reflects off the diffraction grating at a different angle. The grating can be rotated to direct any selected wavelength bundle onto the center of a concave mirror. The mirror collects the light and, with the help of a quartz corrector lens, forms an image of the entrance slit on the exit slit.

The visible range grating is a 1350 groove per millimeter grating covering from 350-800 nanometers in the first order and is blazed at 500 nanometers. The reciprocal linear dispersion is 6.4 nanometers per millimeter. The combination of grating and slits determines the dispersion of the system. The effective widths of the visible grating was 20 nanometers as determined by the entrance and exit slit widths are 2.68 and 1.5 millimeters respectively. These particular grating widths

ORIGINAL PAGE IS
OF POOR QUALITY

were selected in order to obtain sufficient photomultiplier response when measuring targets of low reflected brightness.

The visible spectroradiometer utilized a photo diode detector to produce a signal proportional to the intensity of the light which strikes it. However, in order to obtain sufficient sensitivity in the infrared, a cooled photomultiplier detector must be used to produce an output signal which is of sufficient amplitude to allow significant results to be obtained.

Readout was accomplished using a self-ranging picoammeter. This device has the advantage of displaying digitally the detector current output of the spectroradiometers. Thus calibration and dark current values can be readily obtained and monitored. In addition, no scale switching is required and readings can be obtained rapidly.

In order to obtain accurate data, the spectroradiometers were calibrated before and after the experiment. The calibration of the instrument can shift due to such factors as the collection of dust on the optical surfaces or a variety of other random factors. The electronic circuitry of the instrument is very stable and maintains uniform response but, nevertheless, the accuracy of the instrument was verified.

Data Analysis Techniques:

If a sufficient number of sets of independent measurements of incident and reflected radiation (at 27 points in the spectrum from 350-1100 nm) are made and the readings averaged at each wavelength, it is possible to make the Central Limit Theorem apply to the distribution of average reflectance values. Thus,

$$Z_{ij} \equiv \left[\frac{X_{ij1}}{Y_{ij1}} + \frac{X_{ij2}}{Y_{ij2}} + \frac{X_{ij3}}{Y_{ij3}} \right] \frac{100}{n}$$

where: x_{ijk} = the k th measurement of reflected radiation at wavelength i, object j.

y_{ijk} = the k th measurement of incident solar radiation at wavelength i, object j.

z_{ij} = the average percent directional reflectance at wavelength i, object j.

n = number of readings.

By the Central Limit Theorem, the distribution of z_{ij} will be approximately normal regardless of the distribution of the individual values of x_{ijk} and y_{ijk}. This, of course, assumes that measurement errors are independent and randomly distributed.

At each wavelength, for each object, the density spectra is also computed:

$$d_{ij} = \log \frac{100}{z_{ij}}$$

The power which would be reflected if the object had incident upon it radiation emitted by a standard sun is also calculated as follows:

$$s_{ij} = z_{ij} \quad x \text{ (standard value for each i)}$$

Both d_{ij} and s_{ij} have been developed to estimate the density of the image on multispectral photography. These estimates are currently in the process of refinement and are auxiliary to the spectral analysis which is contained herein.

A flow diagram of this computer program is shown in Figure 14.

Note: Computed for (1) each wavelength

(2) each object

ORIGINAL PAGE IS
OF POOR QUALITY

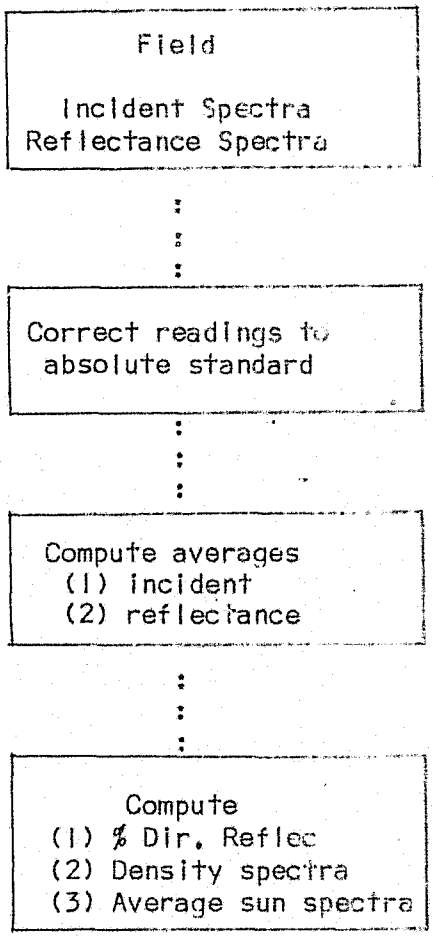


Figure 14. Flow diagram of percent directional reflectance readings.

Computer Output:

The computer output format of the computations performed on the incidence and reflectance spectra is shown in Figure 15. Associated with each wavelength (first column) is the instrument reading (second column) and corrected value of incident sunlight (third column) in microwatts per square centimeter. The reflectance measurements and associated corrected readings (which are determined by the standard lamp calibration) are shown in the fourth and fifth columns.

The percent directional reflectance value shown in the sixth column is the ratio of the value in the fifth column divided by that in the third column. The last column is the value of a standard

ORIGINAL PAGE IS
OF POOR QUALITY

DATE:3/6/69
TIME:1140-1210 MST
WEATHER + LOCATION:CLR. WILL ARI
TARGET:GRASS

WAVE LENGTH (NM)	SUN READING (UW)	ACT. SUN SPECTRA (UW)	REFLECT READING (W*E-10)	ACT. REF SPECTRA (UW*E-2)	PERCENT DIR. REF. (E-1)	DENSITY SPECTRA	STD. SUN REFLECT (UW)
380	15.5	72.912	1.633	6.225	.853768	3.06866	1.40872
400	66	105.336	3.69	11.929	1.13247	2.94597	9.51278
425	127	131.699	6.27	19.1724	1.45577	2.8369	21.8366
450	179	151.255	10.41	27.0316	1.78716	2.74783	37.5303
475	205	160.105	12.08	30.4029	1.89894	2.72149	44.625
500	204	153	13.3	30.7696	2.01108	2.69657	43.266
525	195	139.815	21.7	47.2322	3.37819	2.47131	79.3876
550	160	133.92	23.1	57.1494	4.26743	2.36933	85.3486
575	160	132	16.89	47.5724	3.60397	2.44322	72.0794
600	178	124.778	12.2	40.4064	3.23826	2.48969	72.3609
625	169	117.793	7.88	33.6515	2.85684	2.54411	61.422
650	167	111.222	4.43	27.715	2.49186	2.60347	52.3291
675	176	113.344	2.09	22.3045	1.96786	2.706	44.2763
700	145	97.73	1.677	35.5271	3.63523	2.43947	67.2517
725	147	88.641	1.648	77.3462	8.72579	2.05919	161.427
750	125	81.75	.917	115.791	14.1641	1.84831	226.625
750	* 93	88.9735	5145.46	119.481	13.4841	1.87073	167.09
750	61	96.197	10290.	123.171	12.8041	1.89265	107.554
800	58	79.228	12650.	121.946	15.3918	1.81271	123.134
850	53	71.338	12670.	111.876	15.6825	1.80458	109.773
900	44	58.872	9490.	81.7039	13.8791	1.85764	77.7223
950	32	41.824	4550.	47.6385	11.3932	1.94347	43.2329
1000	36.5	45.8075	3230.	55.879	12.1987	1.91369	59.7734
1050	34.5	39.675	1150.	54.2915	13.6841	1.86378	64.3151
1100	30	29.91	218.	42.51	14.2126	1.84732	55.4293
1150	16.5	15.9225	28.8	24.9955	15.6982	1.80415	29.0417
1200	19	15.435	10.7	34.4487	22.2465	1.65274	36.7067

* = AVERAGE OF TWO INSTRUMENT READINGS

Figure 15. Computer output format of incident and reflectance spectra.

illuminant times the percent reflectance. Thus, the actual power reflected by an object can be computed by knowing the incident radiation and the data in the sixth column of this output.

Figure 16 shows the associated computer plot of percent directional reflectance as a function of wavelength. This is an example of the percent directional reflectance of grass obtained in situ. The chlorophyll reflection band at 550 nm and chlorophyll absorption band at 675 nm are clearly evident as is the mesophyll reflection above 725 nm.

Incident Solar Radiation:

The intensity and spectral distribution of solar radiation falling upon the earth's surface varies with solar angle and atmospheric conditions. Measurement of the absolute amount of solar energy which strikes the terrain is important since all ground objects reflect different amounts of radiation in each spectral band which is in direct proportion to that which is incident.

Theoretical analysis of solar illumination based upon air mass calculations and Raleigh scattering are of little practical value in predicting the spectral distribution of solar energy which actually reaches the ground. This is primarily due to the existence of unknown amounts of Mie scattering and absorption in the atmosphere due to particles which are large compared to the wavelength of the radiation.

Figure 17 demonstrates this condition. Spectroradiometric readings of solar energy (both sunlight and diffuse skylight) using a lambertian detector were measured during a four day interval at Willcox, Arizona. Spectral intensity in microwatts per centimeter squared per nanometer from 380-1200 nanometers is shown for four of these measurements between 1104 and 1515 MST on March 6.

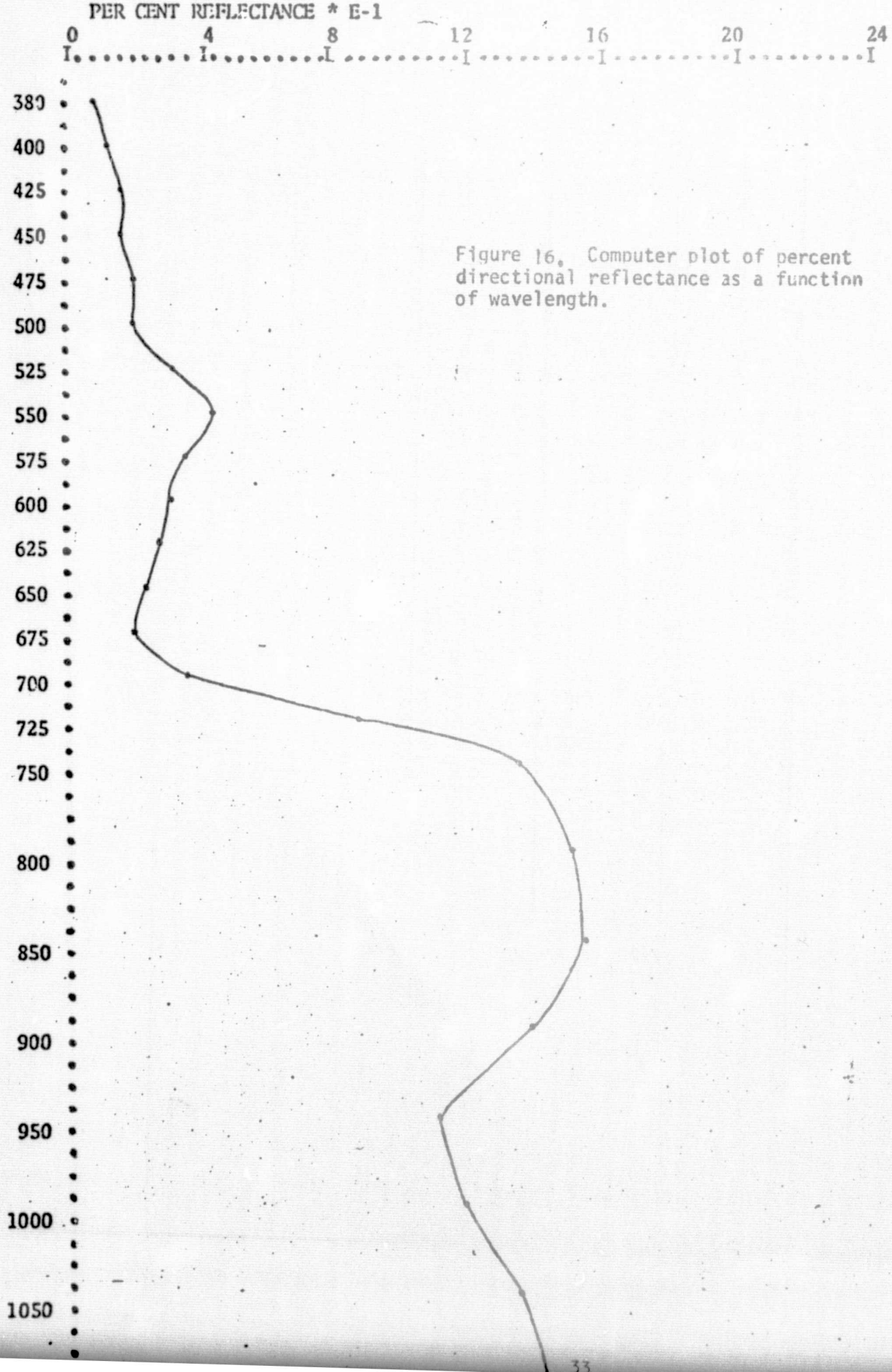


Figure 16. Computer plot of percent directional reflectance as a function of wavelength.

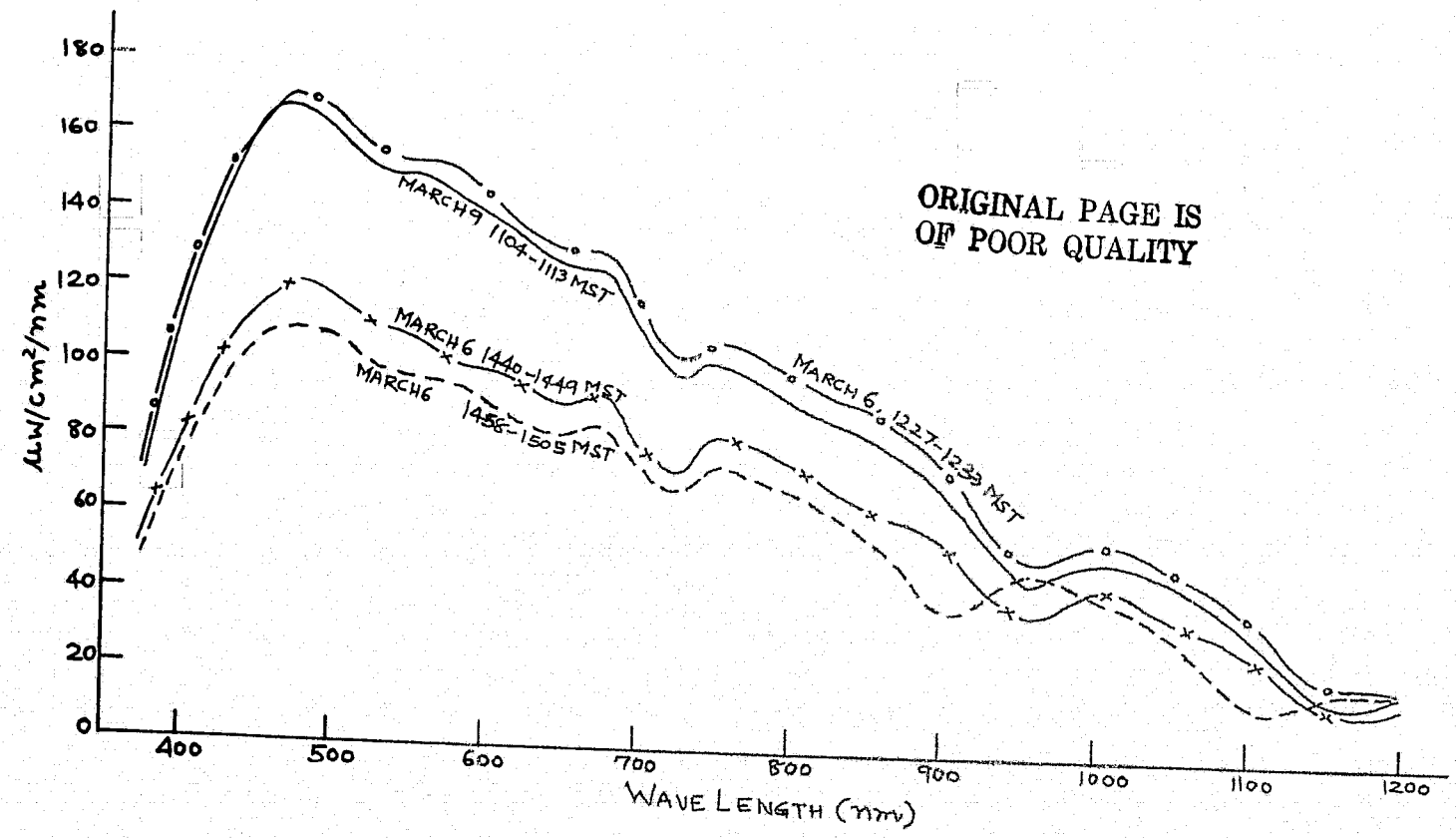


Figure 17. Spectral distribution of solar radiation incident at the Willcox Playa test site at different times during the day.

The first feature clearly evident from this data is the large variation in intensity with wavelength as a function of time (solar angle). The characteristic absorption band below 380 nanometers at 725 and 950 nanometers is also clearly evident.

The percent directional reflectance of the Willcox Playa, Arizona, was obtained for two adjacent areas at the location shown in Figure 18. Simultaneous spectroradiometric measurements of incident global solar radiation were made along with measurements of the radiation reflected by the Playa.

The reflectance spectroradiometers were oriented so as to prevent any specular reflection from the Playa surface from entering the input

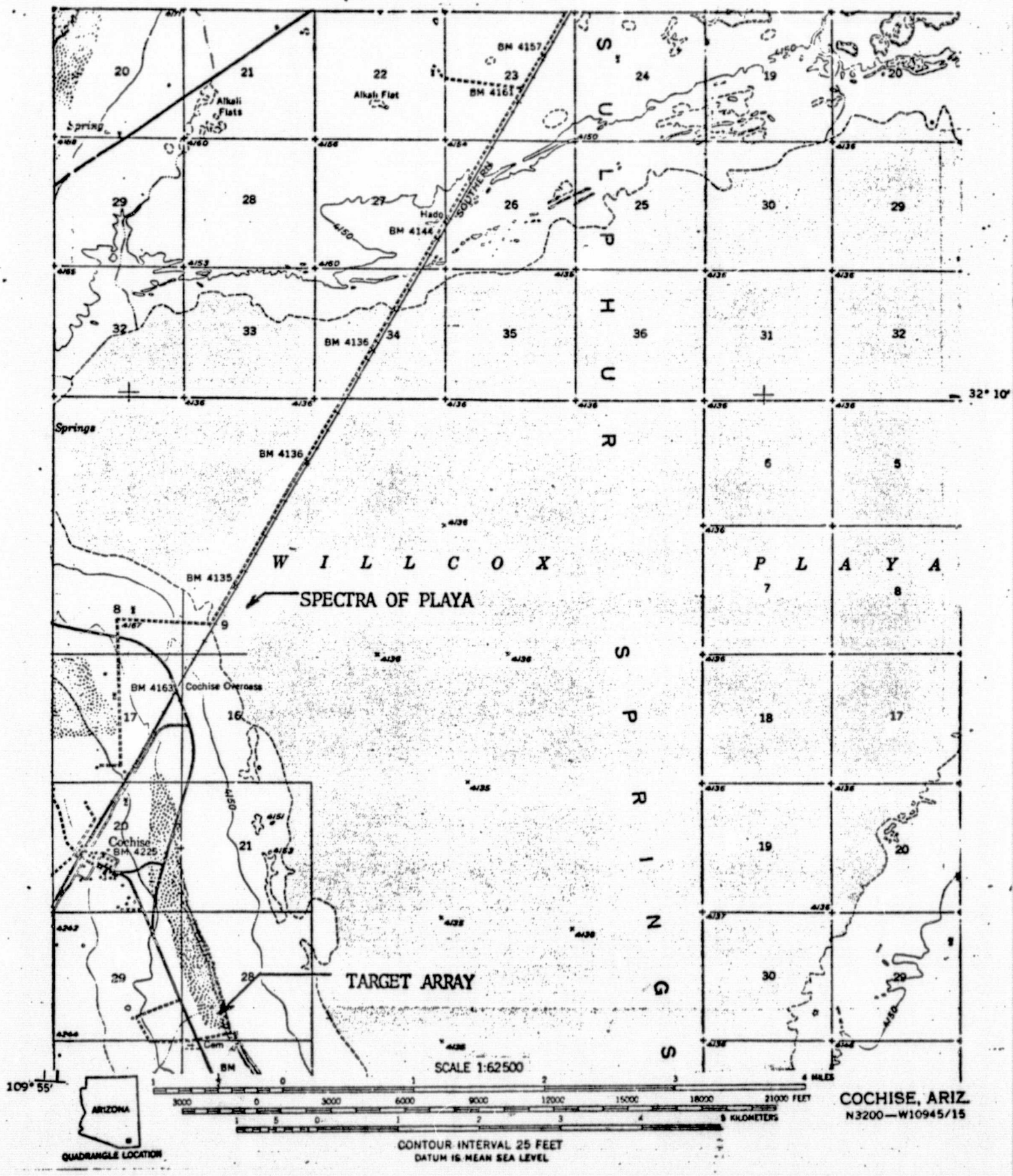
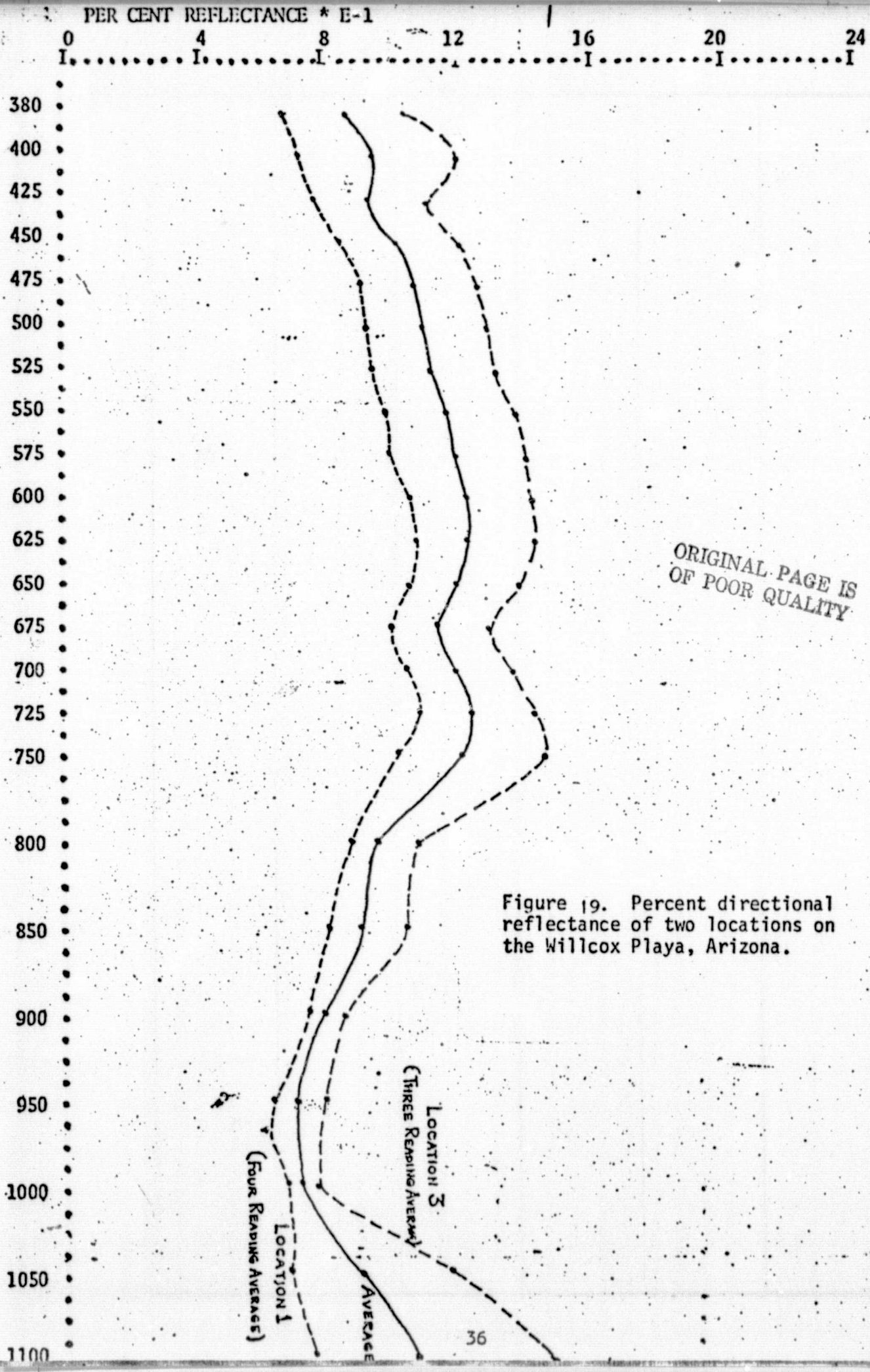


Figure 18. Location at which incident and reflectance spectra were measured.



ORIGINAL PAGE IS
OF POOR QUALITY

Figure 19. Percent directional reflectance of two locations on the Willcox Playa, Arizona.

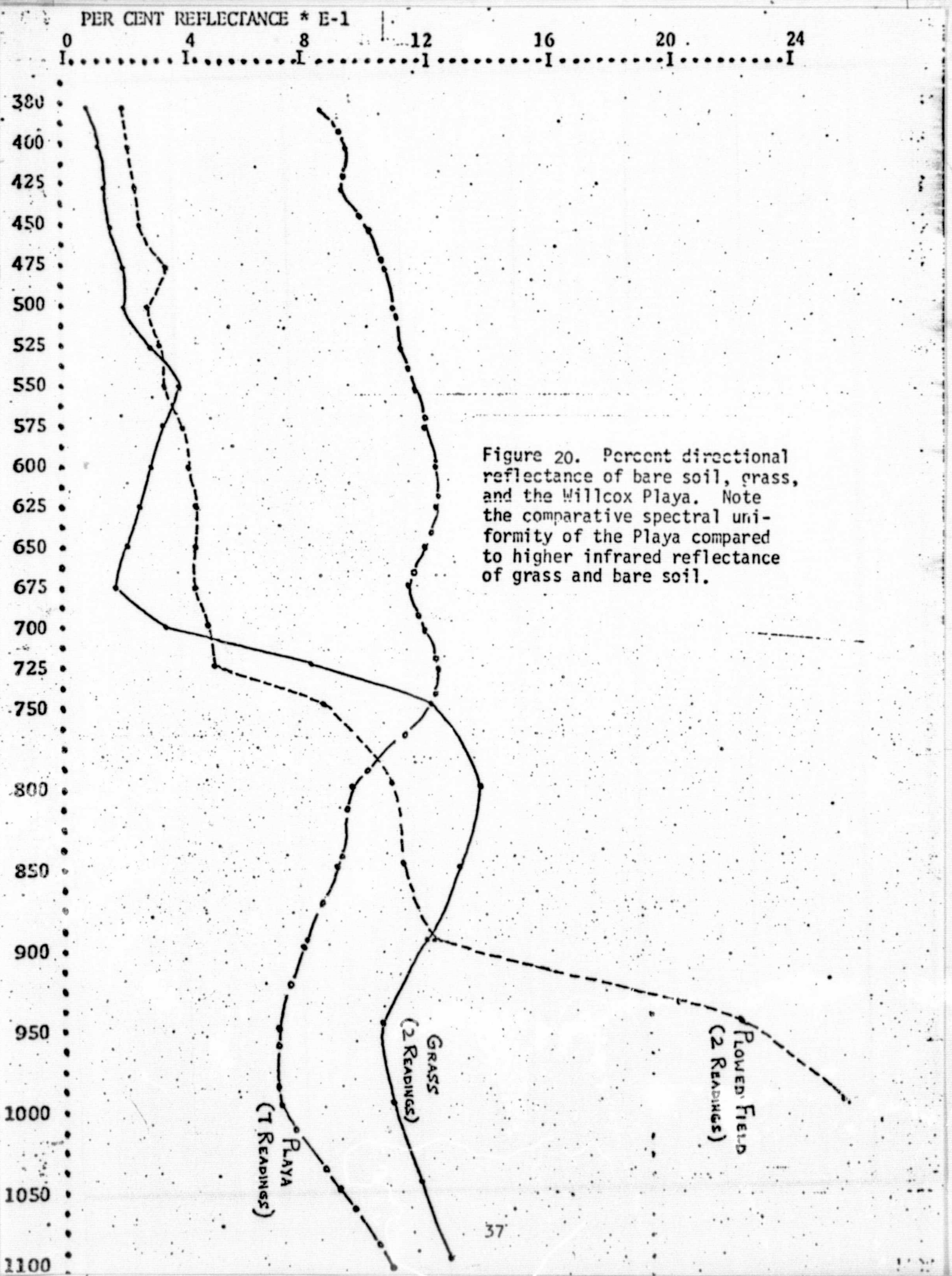


Figure 20. Percent directional reflectance of bare soil, grass, and the Willcox Playa. Note the comparative spectral uniformity of the Playa compared to higher infrared reflectance of grass and bare soil.

optics of the instrument. The partly cloudy atmospheric conditions that existed required that extreme care and patience be used in making these measurements. The incident and reflected spectroradiometric data were corrected and the percent directional reflectance calculated using the computer program discussed previously.

The percent directional reflectance data presented in Figure 19 indicated a surprising degree of uniformity in the reflectivity of the Playa surface. Although there appears to be slight brightness differences between the two areas, the shape of the reflectance curves is quite similar.

A comparison of the spectra of plowed fields and grass with the Playa is shown in Figure 20. The area from which these readings were obtained was adjacent to the target array at the locations shown in Figure 18. The characteristic chlorophyll absorption band (675 nm), chlorophyll reflection band (550 nm), and mesophyll reflection band (above 700 nm) are shown in the spectra of the grass.

Additional Reflectance Spectra of Willcox Playa

The reflectance spectra of twelve locations in the Willcox Playa was obtained in the Fall of 1973. The precise locations recorded on two separate occasions are shown in Figure 22. The appearance of the Playa from the roadway is shown in Figure 23; Figure 21 is a photograph of the Playa also looking eastward.

The incident solar radiation falling on the Playa measured in micro watts per square centimeter per nanometer at 10:22 PDT on 4 September 1973 is shown in Figure 27.

ORIGINAL PAGE IS
OF POOR QUALITY

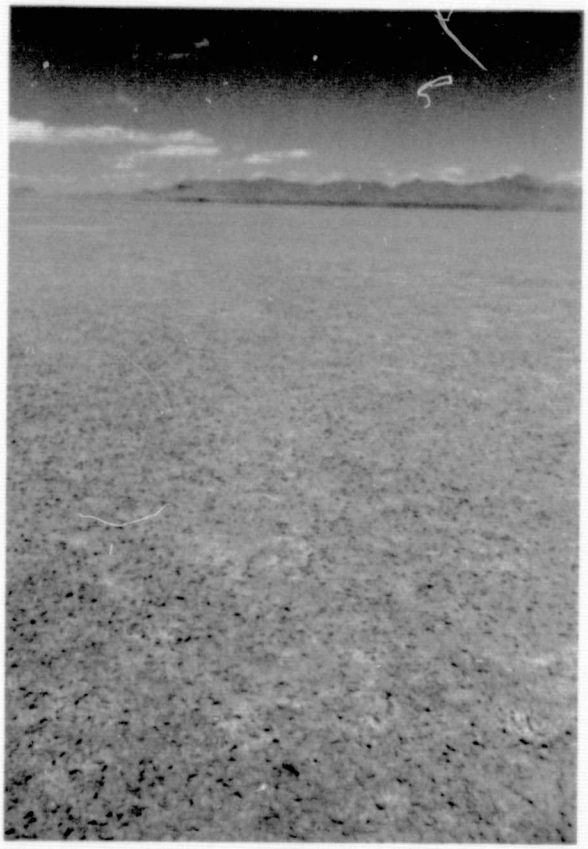


Figure 21. Willcox Playa, looking east.

The percent directional reflectance of the twelve locations on the Playa is shown in Figures 28 and 29. Considerable small local differences were found to exist about site I due to soil moisture variations and hence three sets of reflectance spectra were taken at this location. These variations in the apparent condition of the Playa are shown in the photographs in Figures 24 through 26.

Table I, lists the percent soil moisture at each location. The soil samples were taken at the same time as was the reflectance spectra.

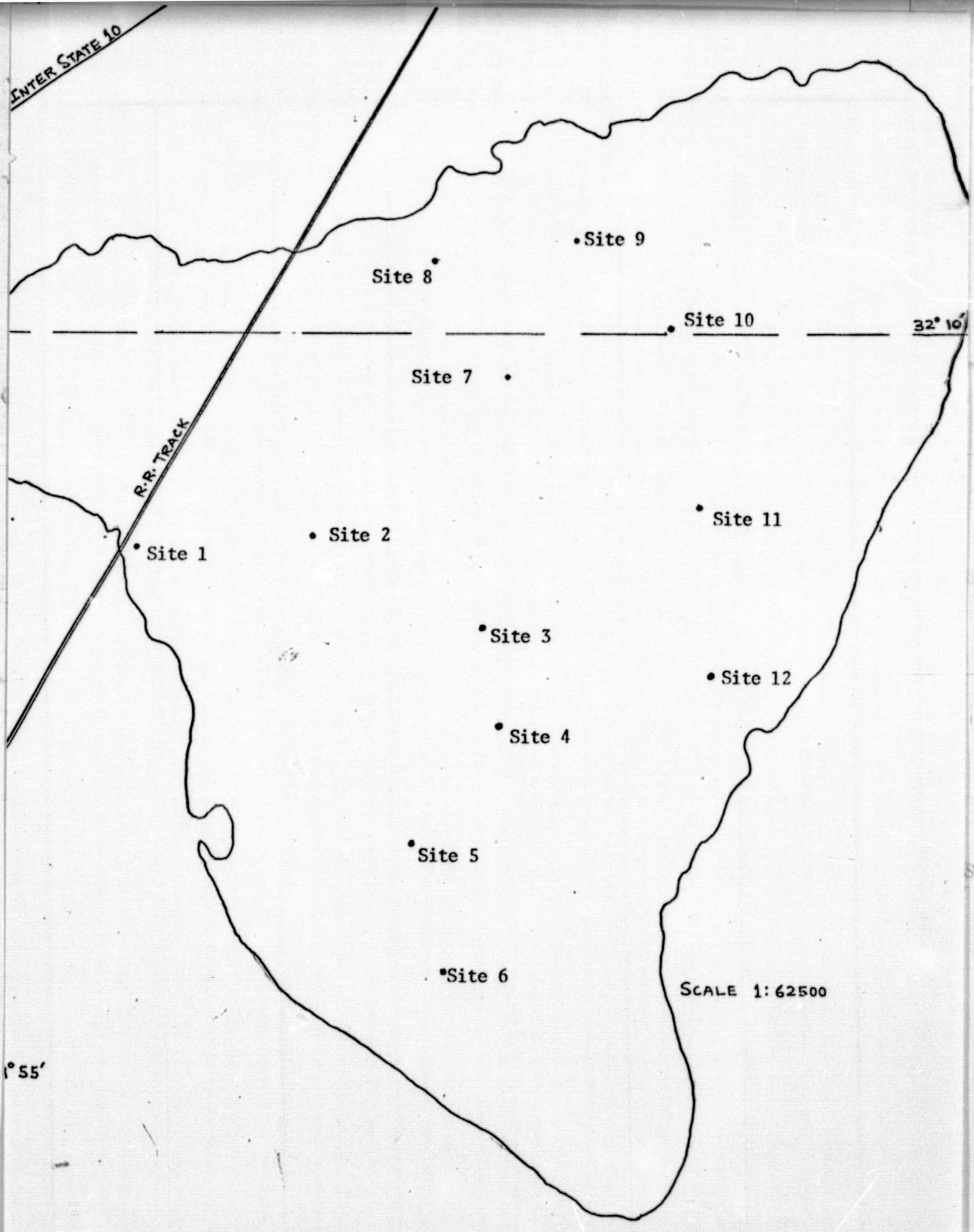


Figure 22. Locations in Willcox Playa, Arizona, where Spectra was taken during Fall 1973.

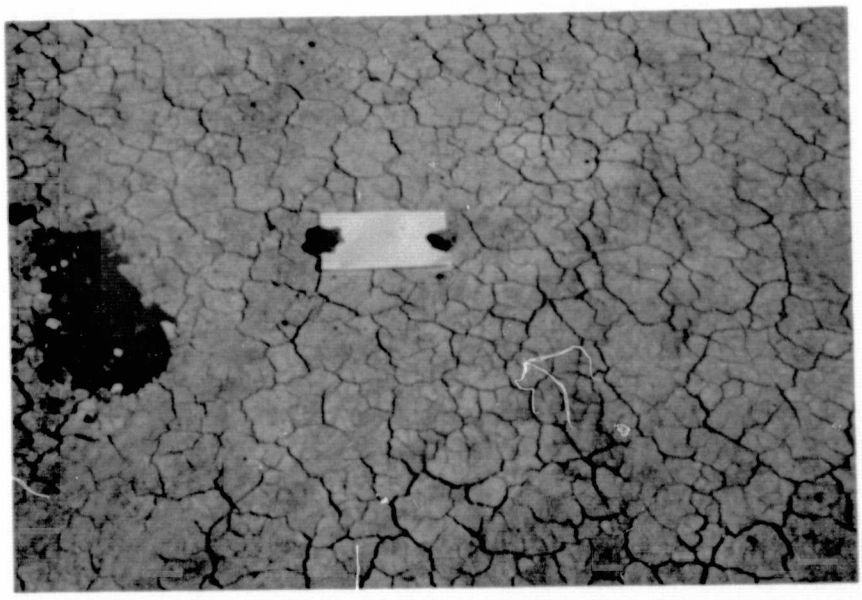
ORIGINAL PAGE IS
OF POOR QUALITY



Figure 23. Willcox Playa, viewed from road looking east.

Site	Weight of Sample (grams)	Percent Soil Moisture
1A	8.7710	5.851
1B	9.5476	5.486
1C	10.6016	67.672
2	8.6695	4.191
3	8.2077	3.708
4	7.0687	3.851
5	7.7994	4.417
6	8.9289	4.288
7	8.1270	3.559
8	11.4335	3.428
9	8.8666	3.068
10	9.9244	4.590
11	8.7659	3.392
12	9.0585	3.663

Table 1. Soil Moisture at different locations in Willcox Playa, Arizona.



ORIGINAL PAGE IS
OF POOR QUALITY

Figure 24. Willcox Playa location 1A, soil moisture 5.9 percent.

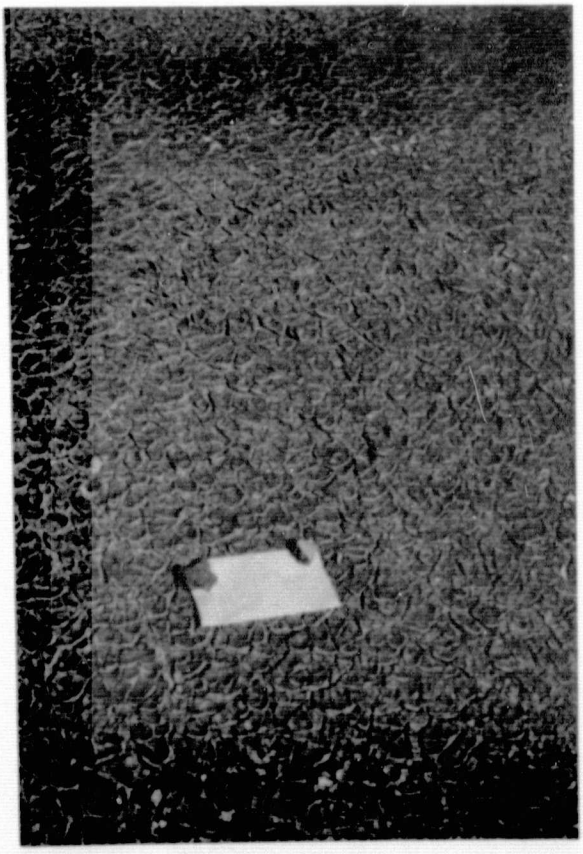


Figure 25. Willcox Playa location 1B, soil moisture 5.5 percent

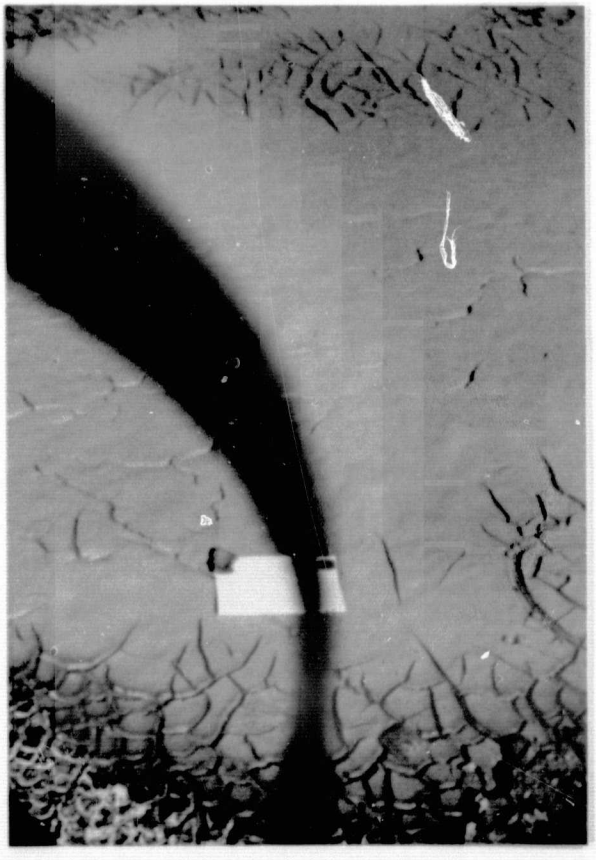


Figure 26. Willcox Playa location 1C, soil moisture 67.7 percent

ORIGINAL PAGE IS
OF POOR QUALITY

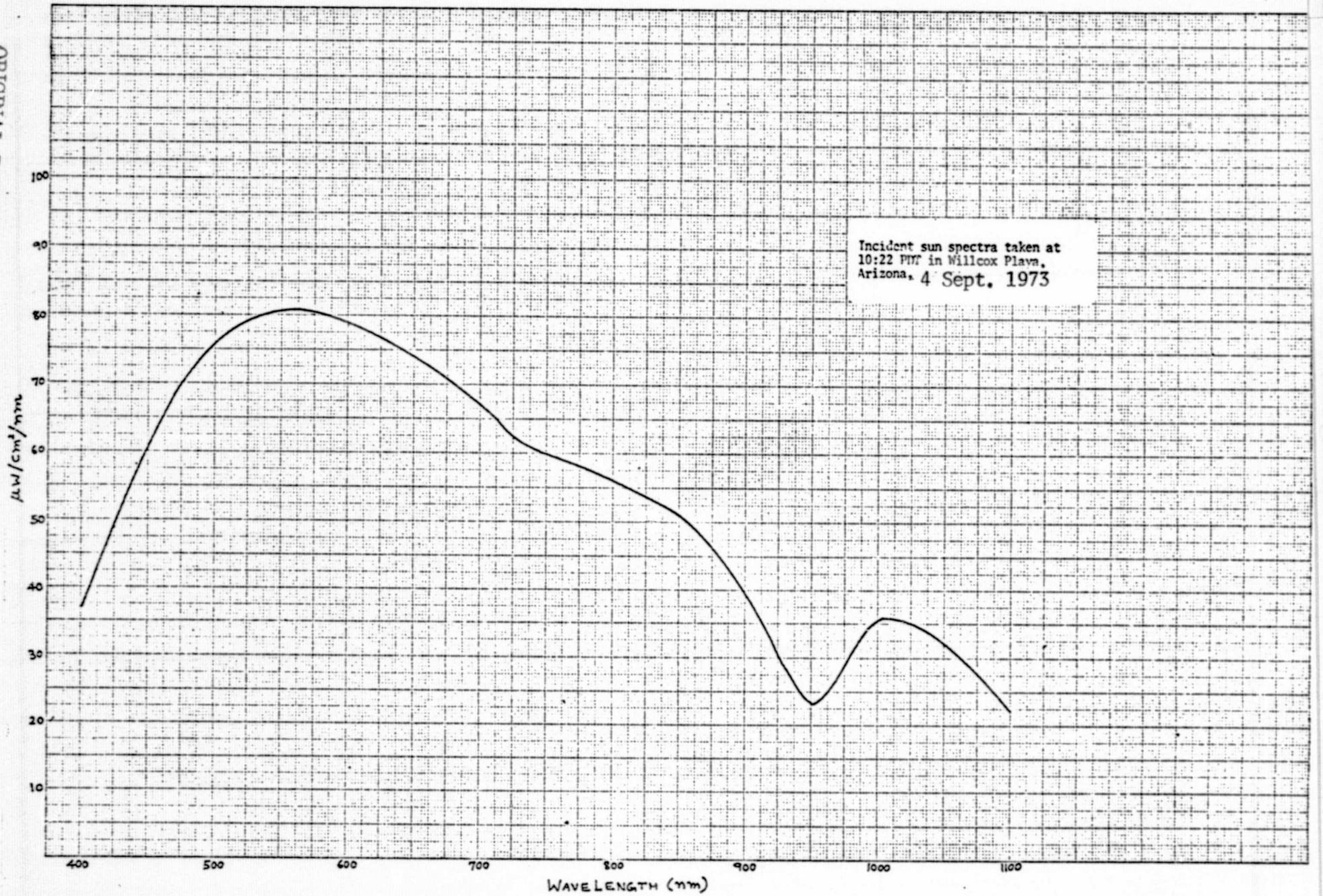


Figure 27. Incident Sun Spectra taken in Willcox Playa on 4 September 1973.

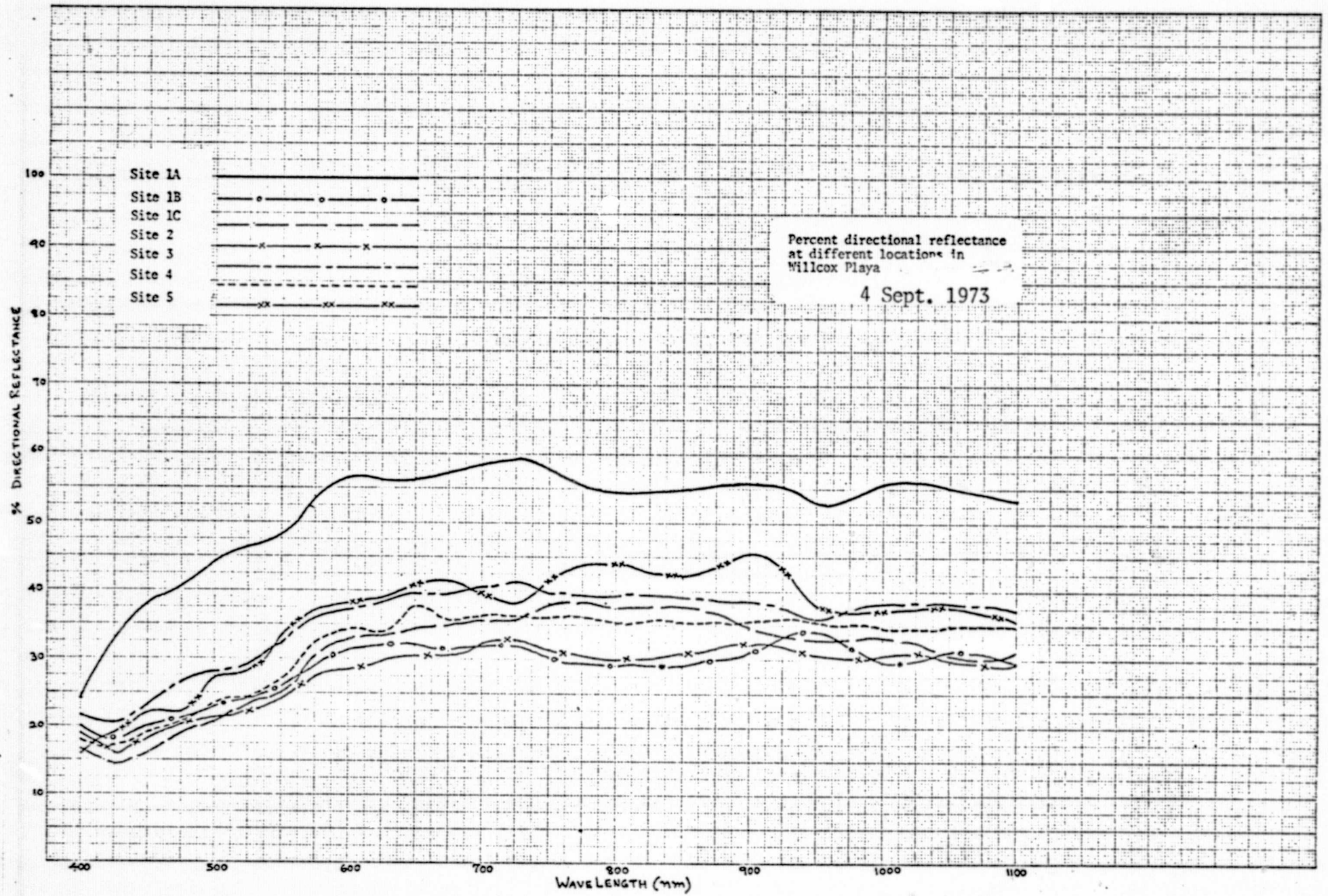


Figure 28. Percent directional reflectance at different locations in Willcox Playa on 4 Sept. 1973.

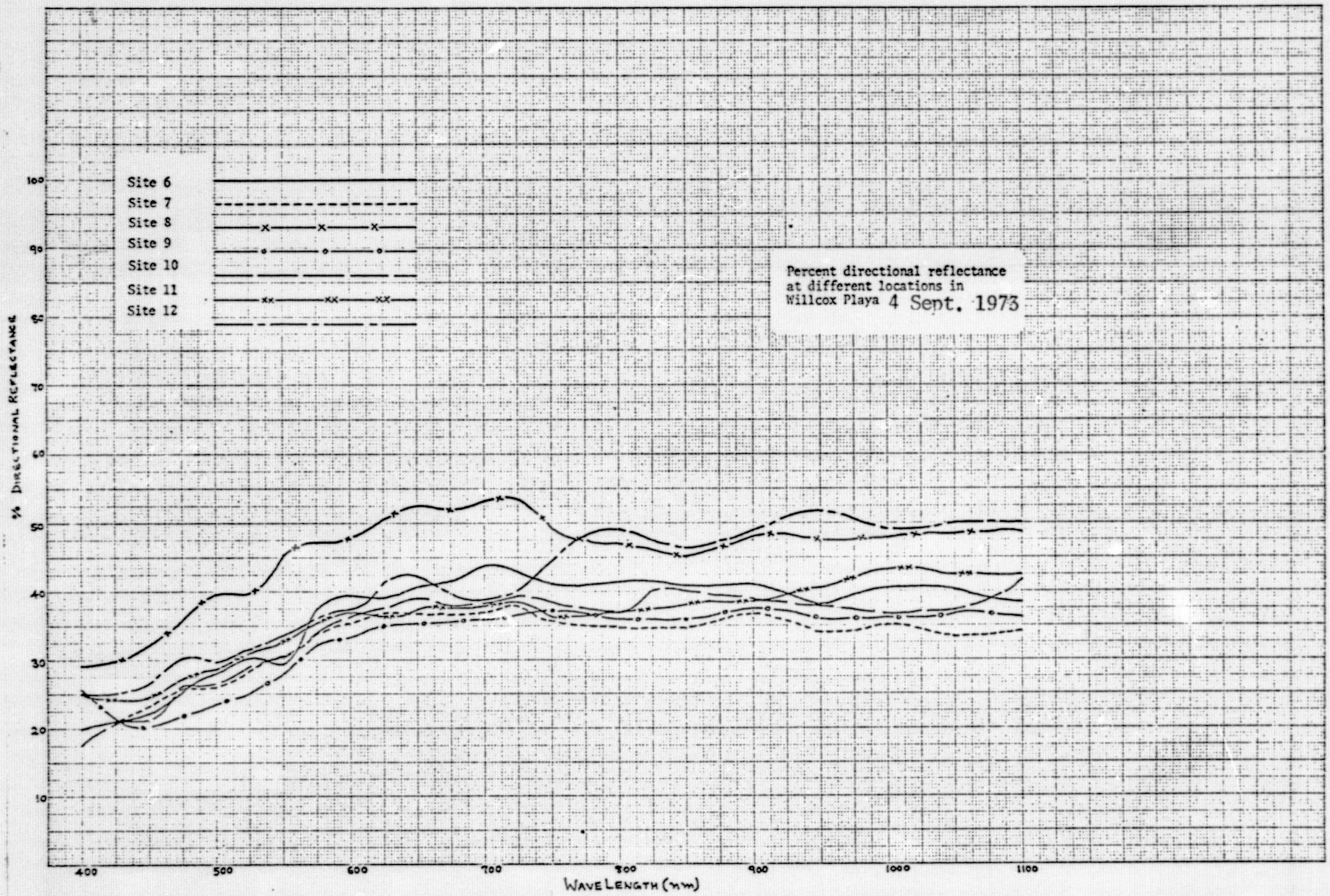


Figure 29. Percent directional reflectance at different locations in Willcox Playa on 4 Sept. 1973.

The percent soil moisture data obtained were plotted against the percent reflectance at 650 nm and 950 nm shown below.

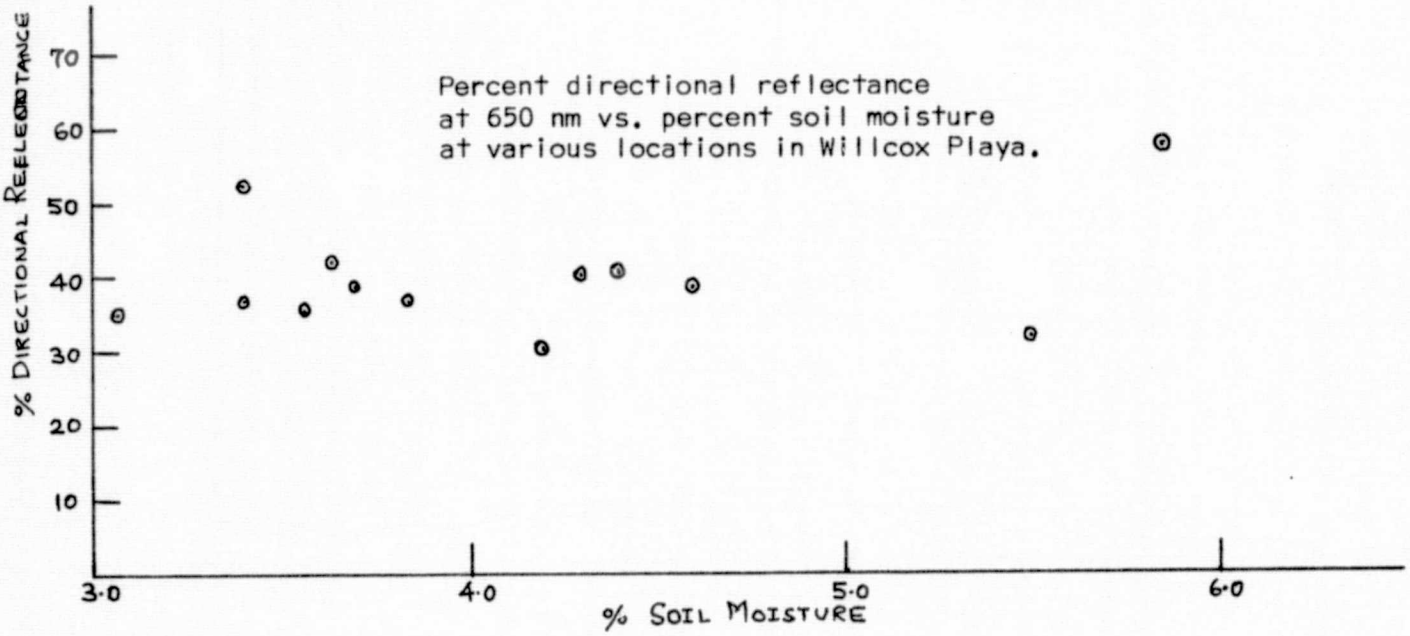


Figure 30. Percent reflectance at 650 nm vs. percent soil moisture.

ORIGINAL PAGE IS
OF POOR QUALITY

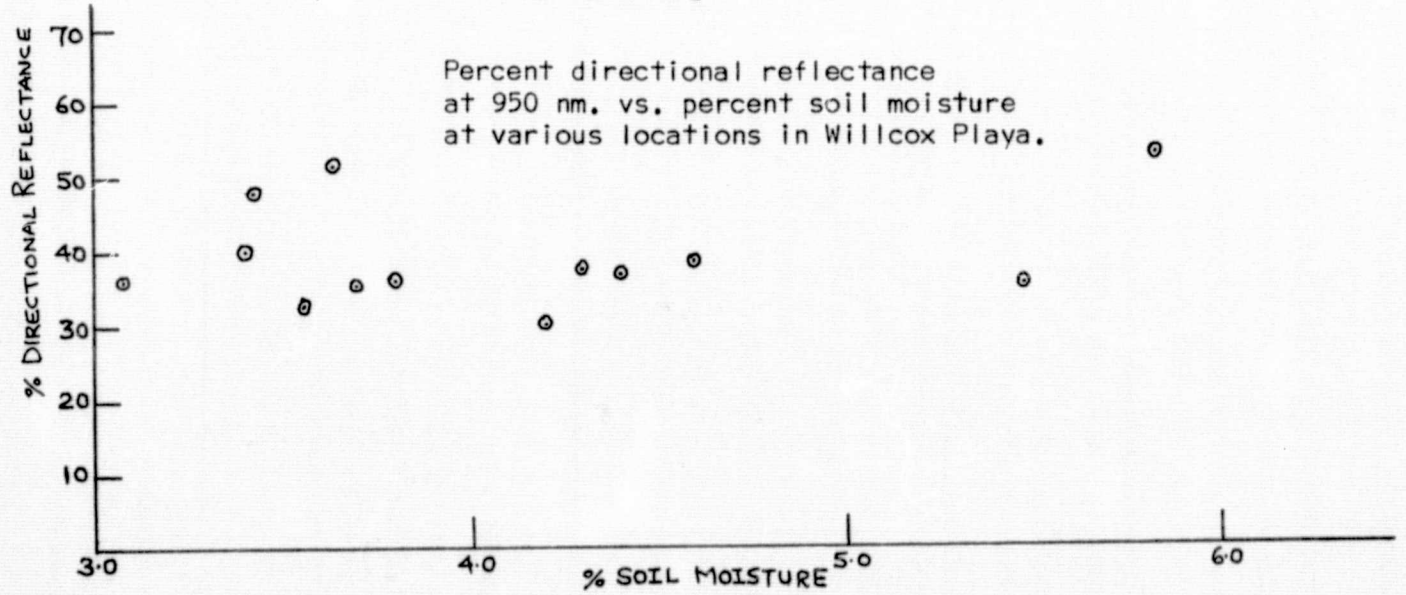


Figure 31. Percent reflectance at 950 nm vs. percent soil moisture.

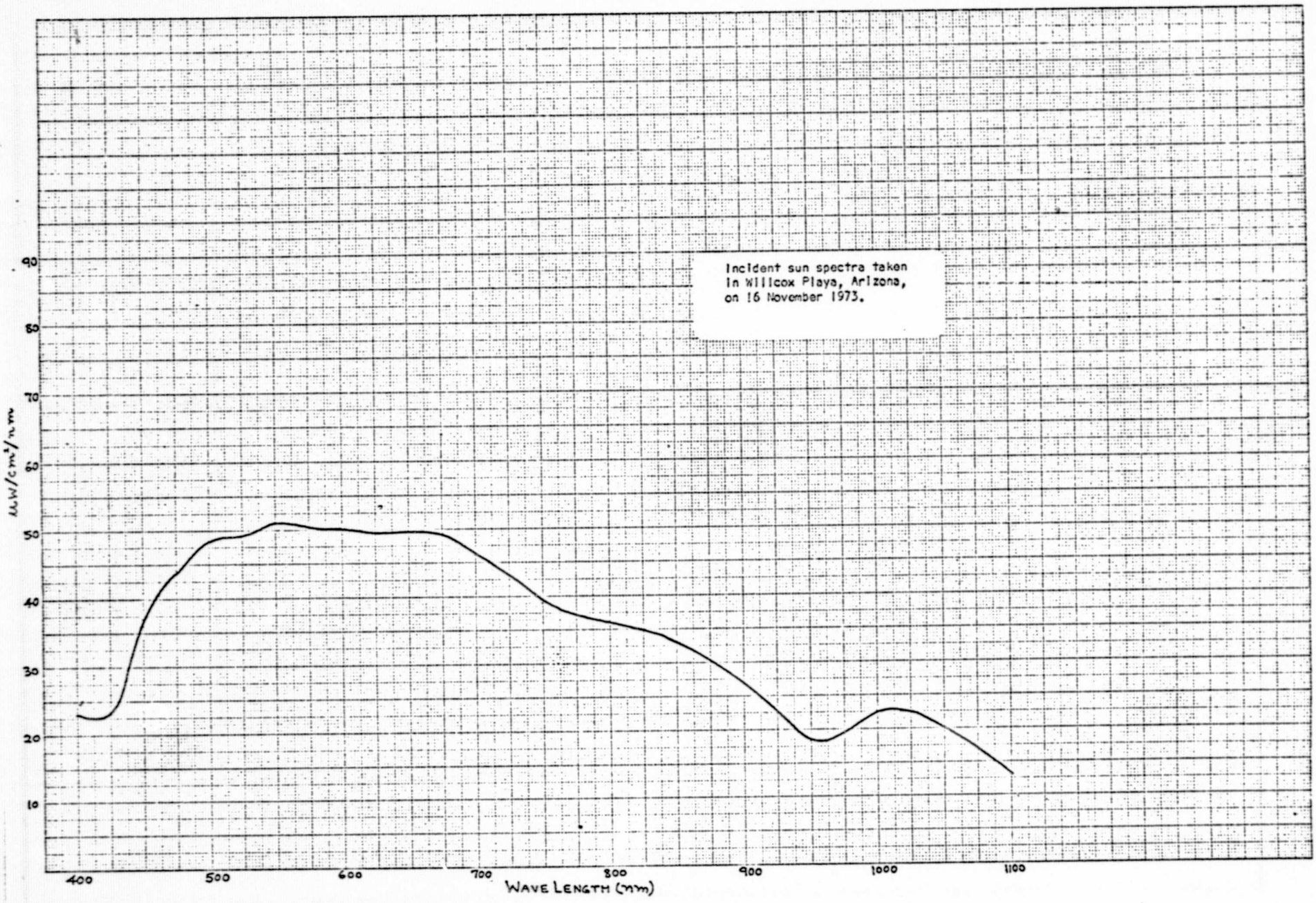


Figure 32. Incident Sun Spectra taken in Willcox Playa on 16 November 1973.

ORIGINAL PAGE IS
OF POOR QUALITY

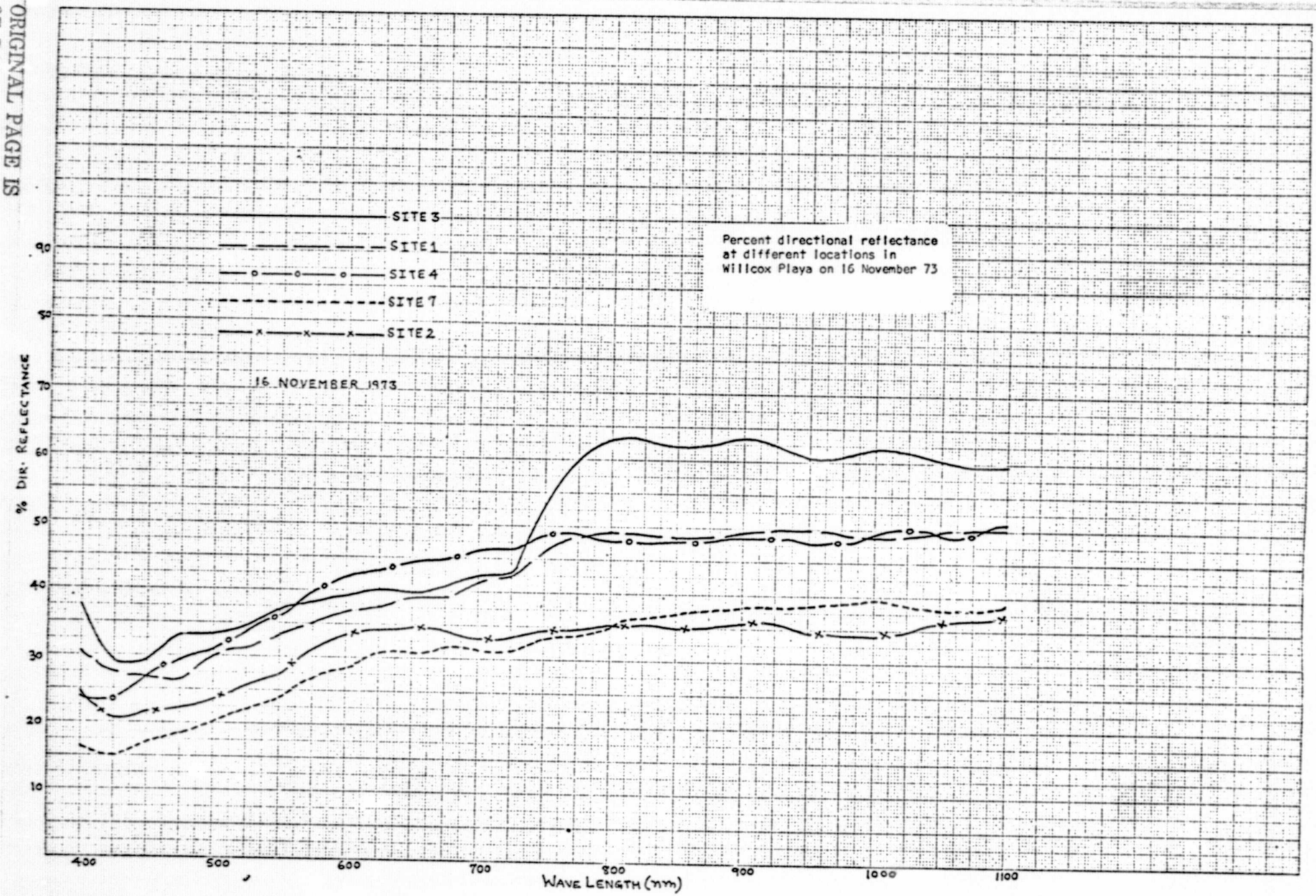


Figure 33. Percent directional reflectance at different locations in Willcox Playa on 16 November 1973.

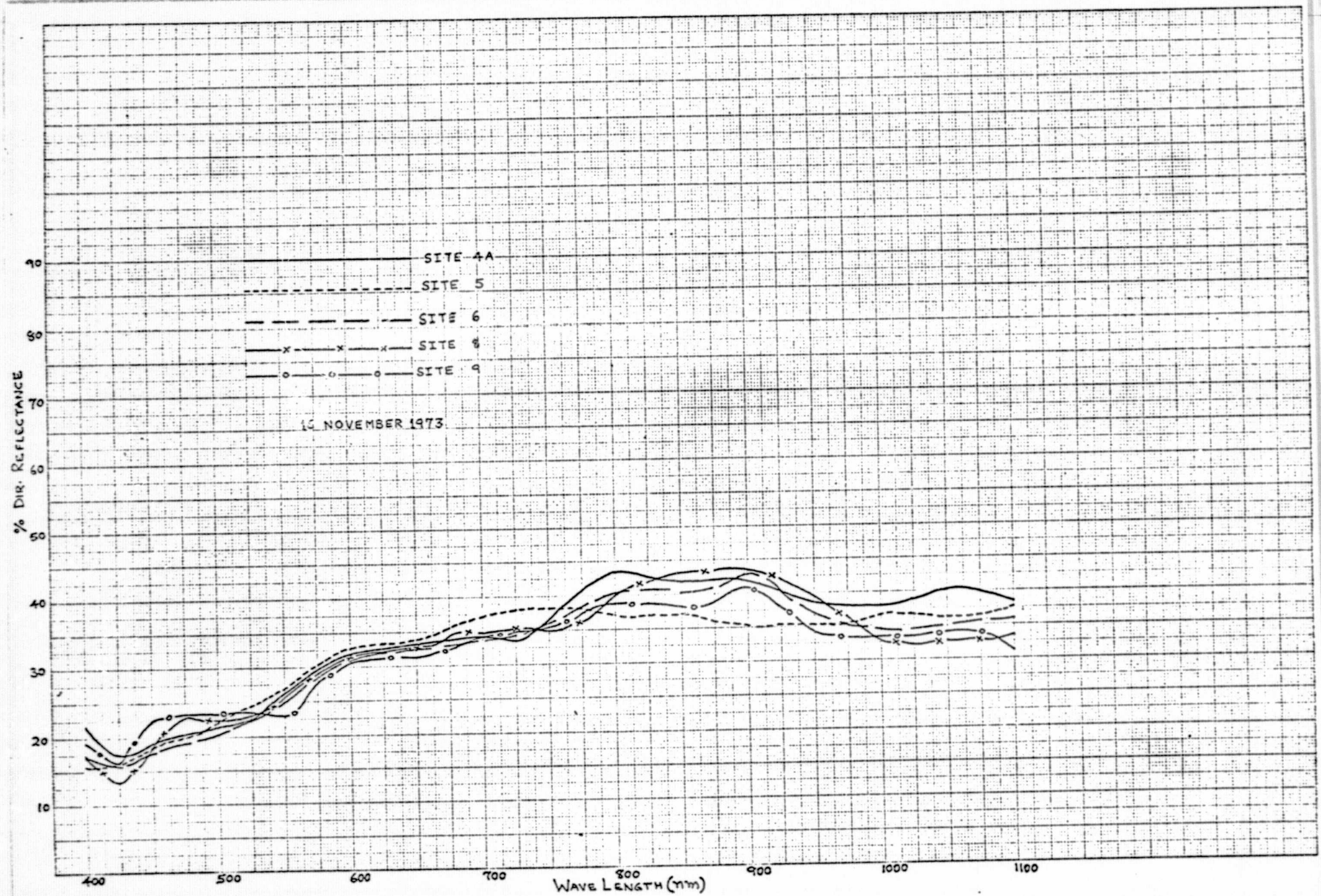


Figure 34. Percent directional reflectance at different locations in Willcox Playa on 16 November 1973.

As can be seen from the two graphs in Figures 30, and 31, soil moisture and percent reflectance at these two wavelengths are uncorrelated on the Willcox Playa. Since water absorbs infrared radiation, the effect of trace amounts of water moisture on reflectance was to be analyzed spectrally.

Figure 32 is a graph of the incident solar irradiance at the Willcox Playa measured in micro watts per square centimeter per nanometer. The data was taken on 16 November 1973, at 1020 PDT. Nine of the twelve locations shown in Figure 22 were recorded and the percent directional reflectance measured. These data are shown in Figures 33 and 34.

Reflectance Spectra of Predominant Vegetation in the Prescott National Forest

In situ spectral reflectance measurements were taken of three prevalent vegetation types in the Prescott National Forest. These species are Pinion Pine, Juniper, and Manzanita. Typical reflectance spectra are shown in Figure 35.

Reflectance spectra in Figure 35 were obtained between 23 October and 28 October 1972.

A computerized telespectroradiometer was utilized to collect the in situ reflectance spectra. This truck-mounted instrument is positioned adjacent to the target to be measured (e.g., a Pinion Pine) and the detector head extended in the air to obtain the similar downward perspective as the ERTS multispectral scanner. The instrument measures and stores in the computer memory the reflectance of a standard white plate which is placed in the field of view of the spectroradiometer. The reference plate is then removed and the spectra of the target is obtained. The computer enters all the necessary instrument corrections, divides the standard white plate reference readings into the target readings at

ORIGINAL PAGE IS
OF POOR QUALITY

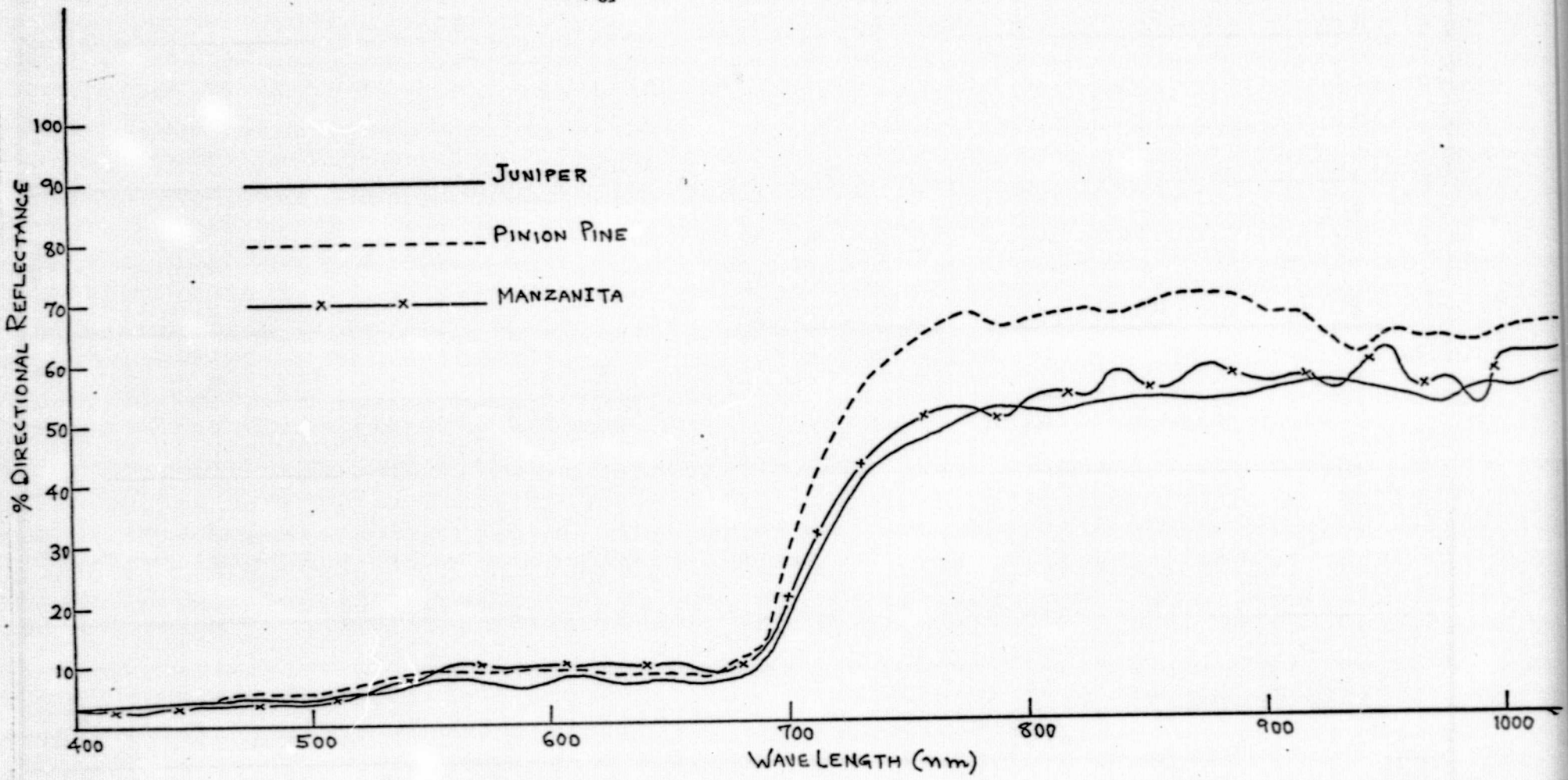


Figure 35. Percent directional reflectance of predominant vegetation species in the Prescott National Forest.

ORIGINAL PAGE IS
OF POOR QUALITY



Figure 36. Truck-mounted telespectroradiometer.

each discrete wavelength measured and prints out the result on a teletypewriter. Figure 36 shows this truck-mounted instrument in operation at the Prescott test site.

The detector head mounted atop the extended ladder is comprised of an imagery optical system, a circular interference filter monochromator, visible and infrared photomultiplier detectors, and an electronic amplifier. The circular filter is indexed into position in the optical system in front of the detector which selects the particular wavelength to be measured. Usually 80 discrete wavelengths are measured between 400 nm and 1100 nm.

The ratio of target reflectivity to standard reflectance reference is automatically calculated by the instrument and displayed under computer

control. The computer is programmed with a list of spectral ranges (visible and infrared), data points (discrete wavelengths of interest), and the number of scans per data point. The computer incorporated in the spectroradiometer is a 16-bit word length general purpose computer having a 4096 work (8K byte) memory. Four hardware accumulators are used in addition to a PC register. The basic control program resides in 3000 core locations and includes a floating point interpretive package. The 1000 remaining locations are used for temporary data storage during target data acquisition. The basic control program takes radiometric measurements at pre-determined wavelengths, stored in a look-up table. For reflectance measurements a white standard reflector is compared to the target and the relative reflectance of the target is computed as a ratio of the target to the standard. The computer then uses this responsivity data to calculate the radiance of a target.

The telespectroradiometer used to collect the data contains two spectral channels - one covering from 400 to 700 nm (visible), the other from 675 to 1350 nm (infrared). The system is comprised of an optical head which contains the telescope optics, a sensing head containing the photomultiplier detectors, and input-output control console which contains the computer, motor drives, analog-to-digital converter, and teletypewriter.

The system is designed to have flexibility in the spectral region of operation and in its mode of operation. The primary filter assembly of the system utilizes a circular variable interference filter which allows continuous variance of the spectral region transmitted to the detector as a function of the angular position of the filter. The spectral response typically covers a two-octave range of wavelengths with an average spectral resolution of 2 1/2%. The system operates in

an incrementally stepped mode which provides the ability to take precise measurements at each wavelength. Time is allowed for gain ranging, amplifier settling, and multiple readings for computer averaging.

The automatic telespectroradiometer used to collect the data consists of four basic units: the optical head, the sensing head, the control cabinet, and the output unit.

The telespectroradiometer contains a 300mm focal length refractive optical system with a 50mm diameter entrance aperture. The mechanical configuration of the optical head of the system is shown in Figure 37. The incoming radiation is focused by the objective lens on an intermediate focal plane where an adjustable field stop is located to define the system's field of view.

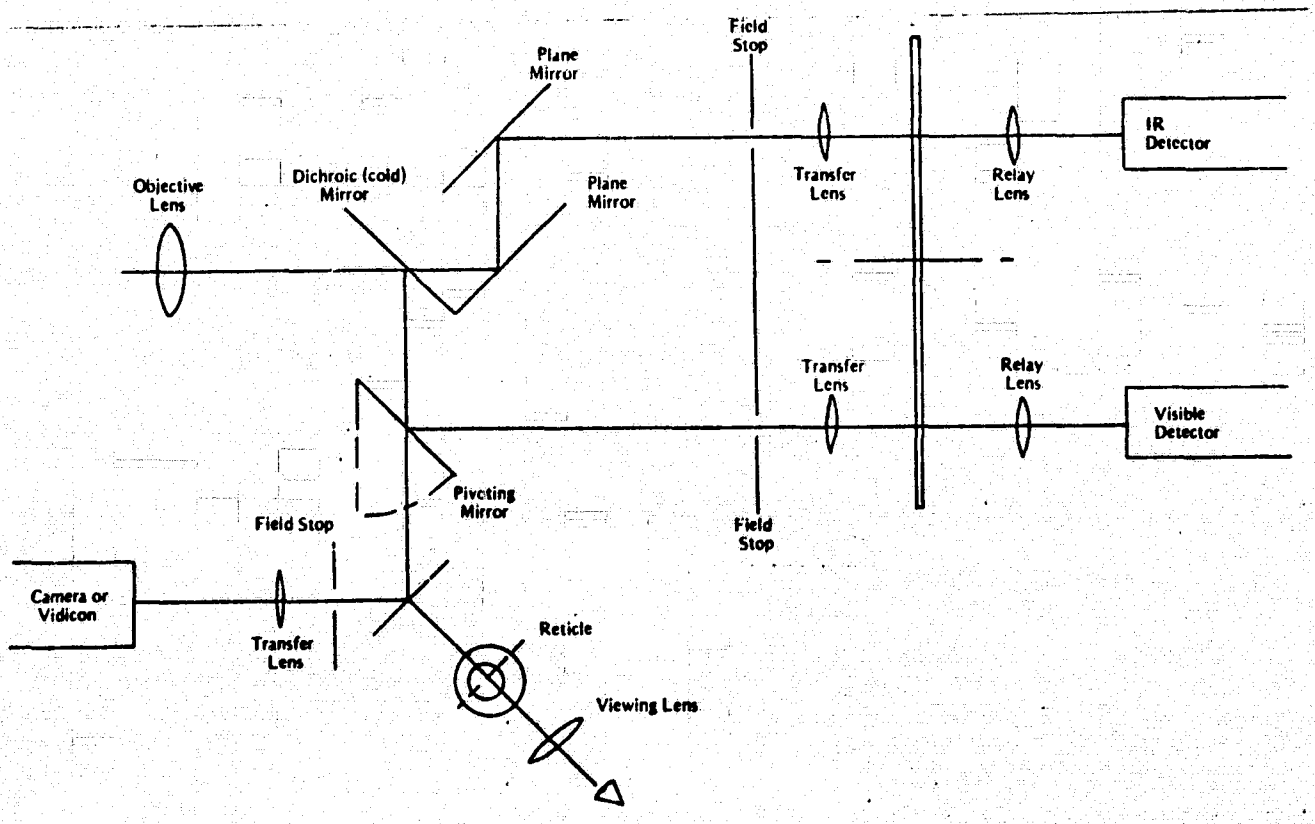


Figure 37. Telespectroradiometer optical schematic.

The radiation passing through the field stop is refocused by the transfer optics onto the front surface of the circular variable filter. The radiation traversing the filter is refocused by a relay lens onto the detector.

The circular variable filter is motor-driven under computer control. The direct coupled angular encoder provides a feedback signal to the computer of the instantaneous position of the circular variable filter. The computer program specifies the angular position at which measurements will be made and monitors the optical encoder output until the correct angular orientation is achieved.

The electrical signals generated by the detector(s) are amplified by a picoammeter amplifier with remote gain-ranging controlled by the computer program. The high-level, low-impedance analog output of the amplifier may be transmitted up to a distance of 250 feet to the computer, allowing completely remote operation. Also located in the optics package are the shutter and viewing mirror solenoids, optical encoder buffer amplifiers, and line drivers.

The picoammeter is a two-stage, solid-state amplifier using compact metal-film feedback resistors and solid-state switching for range selection. The program-controlled or manually-controlled shutter allows dark current measurement and corrections to be made under program control without operator intervention. A block diagram of the electronic circuitry is given in Figure 38.

The analog signal from the optical detector is fed to the analog multiplexer of the analog-to-digital input channel. The multiplexer selects the picoammeter output for conversion or other accessory functions, such as internal self-check functions. The multiplexer output drives the sample-and-hold and the eleven-bit analog-to-digital converter.

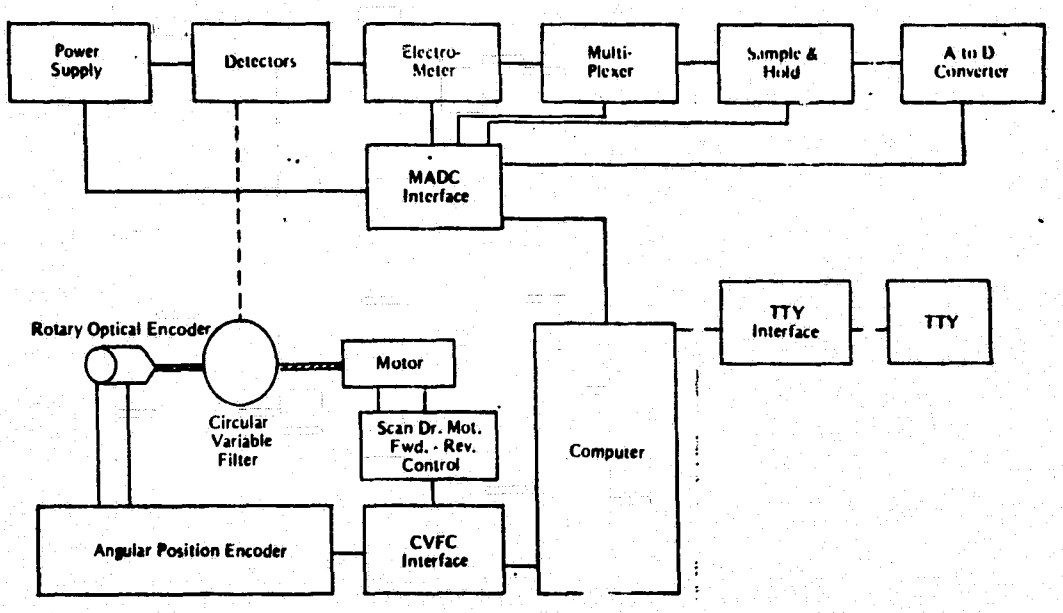


Figure 38. Telespectroradiometer electronics block diagram.

The multiplexer, sample-and-hold and analog-to-digital converter are controlled by the MADC interface which also contains the picoammeter gain control registers, shutter and viewing mirror solenoid buffer registers.

The encoder outputs drive the decoder module which, in turn, drives the present position register in the CVFC interface. The present position register supplies the computer program with the current angular rotational position of the circular interference filter. The CVFC interface contains auxiliary buffer registers for operating the motor drives and synchronization control modules.

SECTION 4

DIGITAL IMAGE PROCESSING OF ERTS-1 PHOTOGRAPHIC DATA

A digital analysis of ERTS-1 Photographic data products was performed using the computerized "System 800". This system digitizes multispectral photographic transparencies on to the disc of a PDP-11 computer; processes the data using a series of image analysis programs; displays the resultant data on a color TV monitor and prints out the associated hard copy on a Decwriter. The description of the "System 800" is contained in Section 2 and in Appendix A.

Analysis of ERTS-1 imagery were performed using the "System 800" of the following:

-- Willcox Playa Arizona, Spectral image analysis

-- Willcox Playa Arizona, Temporal image analysis

-- Phoenix Arizona, Spectral image analysis

-- Prescott Arizona, Spectral image analysis

-- Analysis of atmospheric effects on ERTS-1 image characteristics

Willcox Playa Spectral Image Analysis

A spectral image analysis was performed of NASA ERTS-1 release negatives dated 5 June 1973, of the Willcox Playa using the "System 800". The purpose was to investigate the spectral uniformity of the playa surface on that date.

Bands 4, 5, 6 and 7 and a reference grey scale were placed on the digitizer light table at the same time. The digitizer maximum and minimum video signals using a linear digitization were adjusted so that the playa and surrounding area in Band 5 fall within the 256 level digitization capabilities of the instrument. This maximum digitization

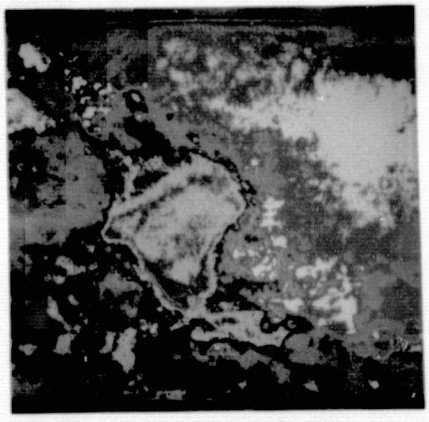
level corresponded to grey step number 4 and the minimum level to grey step number 15. A histogram of the 256 levels of the 250,000 pixels digitized from band 4 were examined and bands 4, 5 and 6 were digitized as followes:

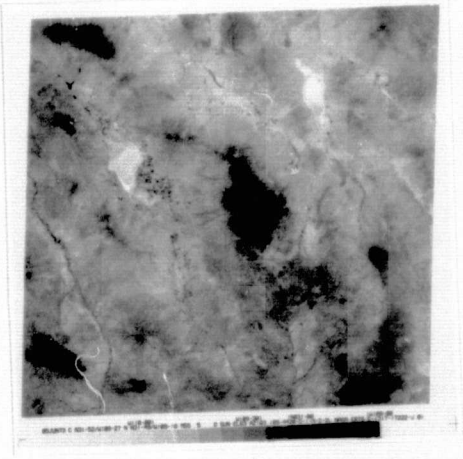
0-28	=	Black
29-43	=	Red
44-58	=	Green
59-73	=	Yellow
74-88	=	Blue
89-93	=	Magenta
94-108	=	Cyan
109-255	=	White

Band 7 was found to be off scale so the digitization levels were adjusted as follows:

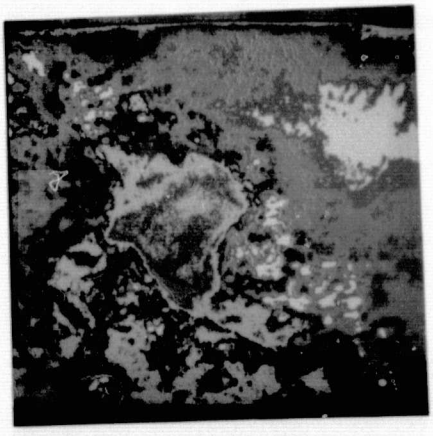
0-30	=	Black
31-50	=	Red
51-70	=	Green
71-90	=	Yellow
91-110	=	Blue
111-130	=	Magenta
131-150	=	Cyan
151-255	=	White

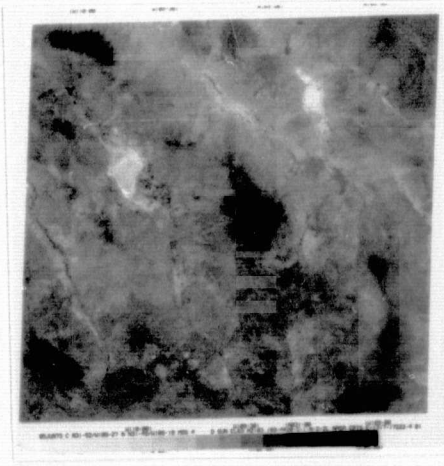
Figures 39 and 40 show a contact positive of each input ERTS negative and the resulting 8 color display of the digitized image produced by the "System 800" of the Willcox Playa portion of each input ERTS chip. Since negatives were inputed into the "System 800"





Band 4 (500-600 nm)

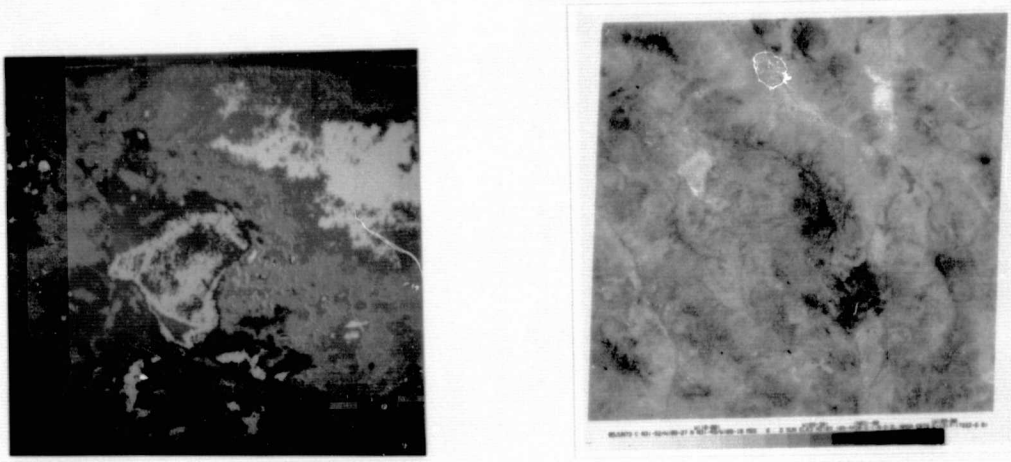




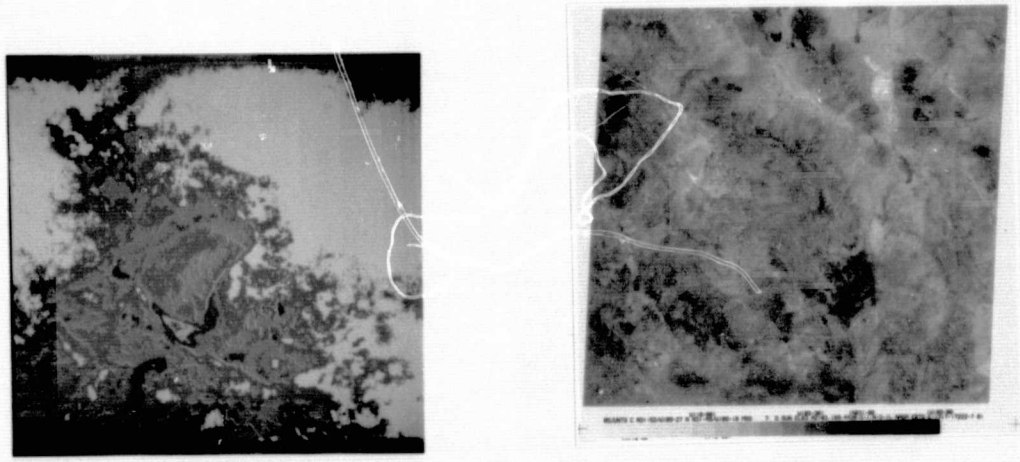
Band 5 (600-700 nm)

Figure 39. WILLCOX PLAYA "SYSTEM 800" DIGITAL IMAGE ANALYSIS OF ERTS-1 5 JUNE 1973. Band 4 and Band 5 negatives.

ORIGINAL PAGE IS
OF POOR QUALITY



Band 6 (700-800 nm)



Band 7 (800-1100 nm)

Figure 40. Willcox Playa "System 800" Digital Image Analysis of ERTS-1 5 June 1973. Band 6 and Band 7 negatives.

ORIGINAL PAGE IS
OF POOR QUALITY

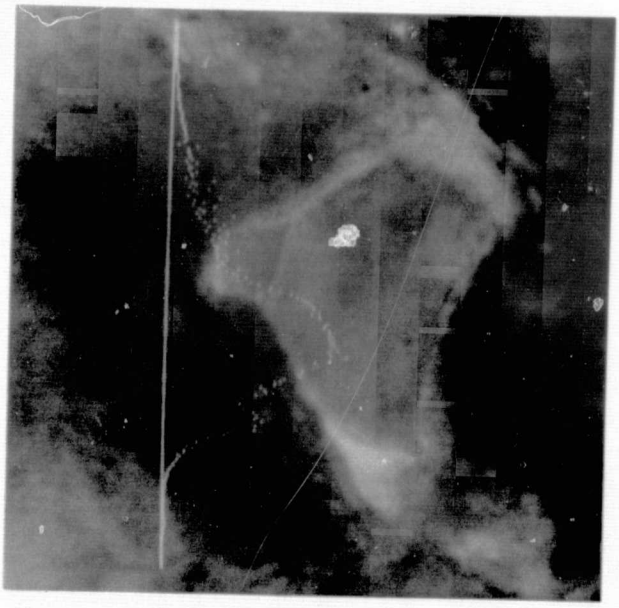
brightness is inversely related to the digitization levels and colors listed above.

The Playa is brightest in Band 4 where the 0 to 73 digitization levels contain all image detail with at least 60 percent of the Playa falling into the 59-73 level. The extreme brightness of the extreme south west portion of the Playa is evident. Band 5 shows lower brightness than does Band 4 with about 50 percent of the Playa image detail falling into the 44-58 brightness catagory without any of the extreme brightness detail in the south west part of the Playa that was evident in Band 4. Band 6 is less bright than Band 5 in all areas of the Playa although the south west area is still brightest. Band 7 contained the least brightness of all the four ERTS-1 chips although the difference in reflectance across the surface of the Playa was similar in all four ERTS-1 bands.

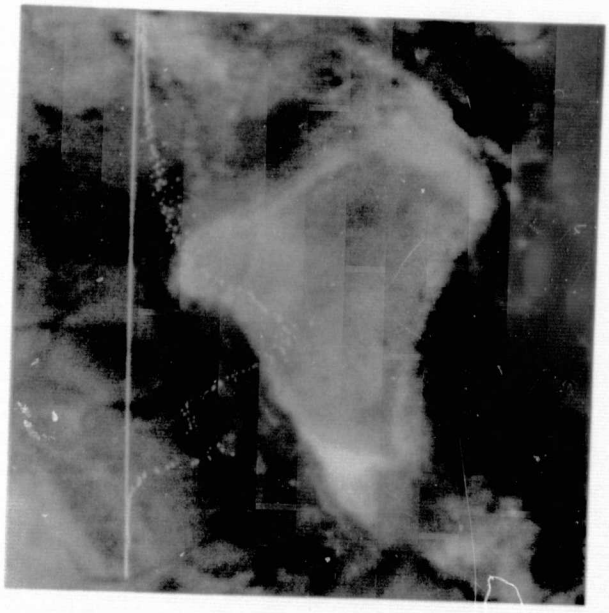
Willcox Playa - Detailed Spectral Image Analysis

Positive transparencies of the four ERTS-1 spectral bands taken on 4 September 1973 were digitized in registration using the "System 800" with MARKER, HISTOGRAM, DIGITIZE and DISPLAY programs. The size of the image digitized was made as large as possible within the limits of the video camera optics.

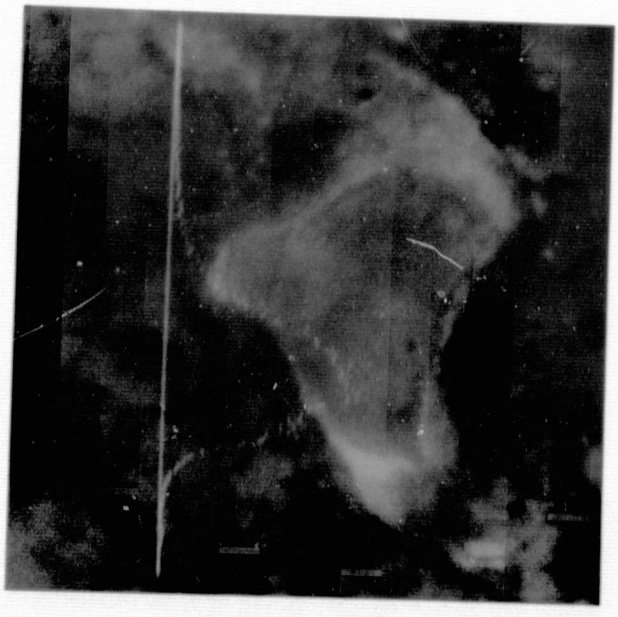
The digitized positives of Willcox Playa for each of the four ERTS-1 spectral bands are shown in Figure 41. Superimposed on the imagery is the frequency distribution of the 294,912 digitized pixels in each band.



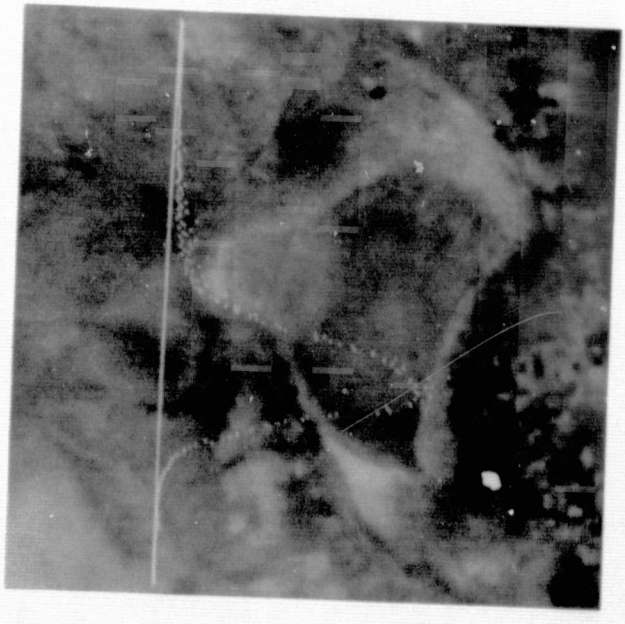
Band 4



Band 5



Band 6



Band 7

Figure 41. Digitized ERTS-1 4 September 1973, images of Willcox Playa from positive film transparancies showing statistical distribution of brightness levels (dark at top of Vertical scale in photos).

ORIGINAL PAGE IS
OF POOR QUALITY

The AREA Program was run on each of the four bands using the digitized grey levels shown in the following table.

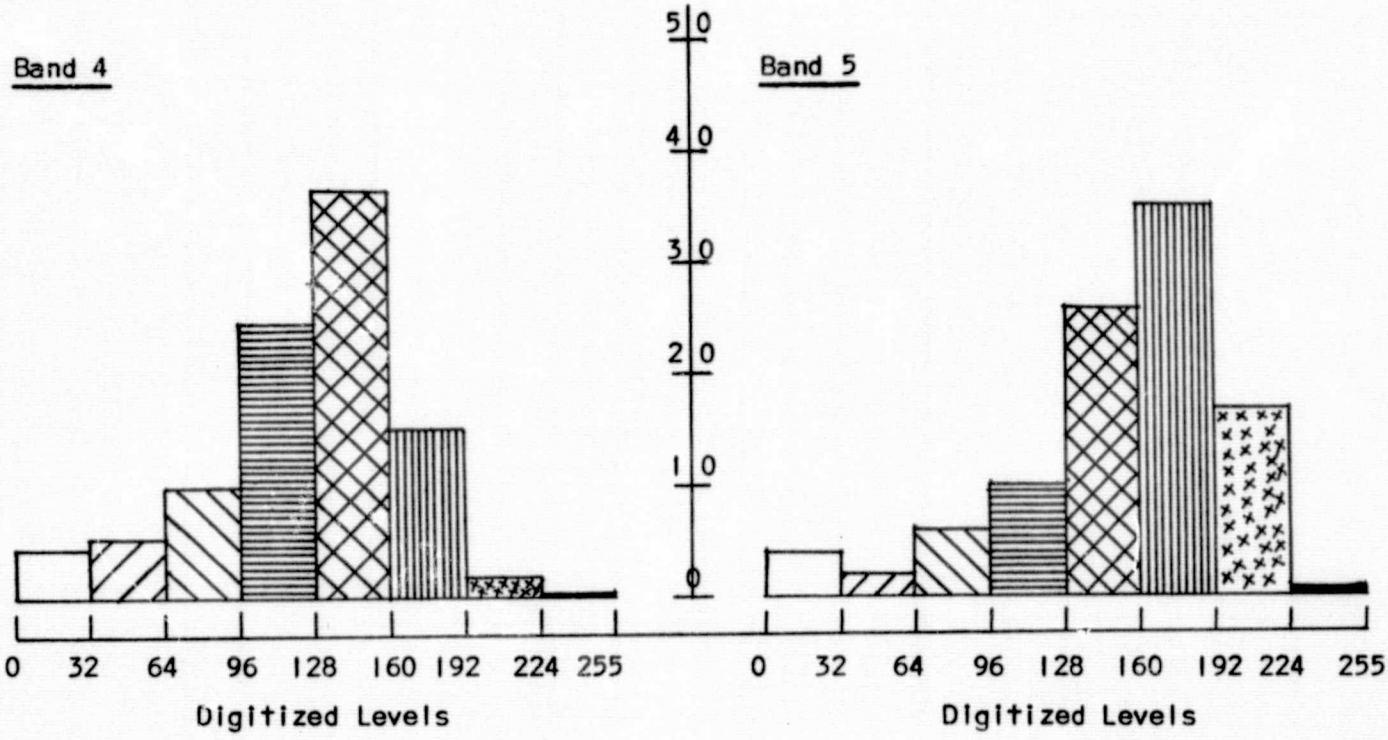
Digitized Grey Levels	4 September, 1973 ERTS-1 Positive			
	Band 4	Band 5	Band 6	Band 7
0-32	4.32	3.12	5.64	2.38
33-64	4.70	1.98	0.62	1.00
65-96	10.02	4.30	1.36	2.24
97-128	26.30	10.04	5.90	5.98
129-160	37.18	26.30	27.62	39.94
161-192	16.26	35.76	46.38	45.90
193-224	1.04	17.62	12.00	2.32
225-255	0.08	0.76	0.36	0.14
Totals	99.9	99.88	99.88	99.9

Table 2. Digital Brightness Classification of ERTS-1 multispectral images of Willcox Playa taken on 4 September, 1973.

A histogram has been plotted of the digitized brightness levels in each of the four ERTS-1 spectral bands and have been plotted in figure 42. Table 3 below shows the expected value and standard deviation of the brightness in each of the four bands.

	4 September 1973 ERTS-1 Positives			
	Band 4	Band 5	Band 6	Band 7
Expected Value, $E(x)$	124.9	155.4	156.1	152.8
Standard Deviation, $\{\sigma(x)\}$	41.2	45.0	44.4	34.0

Table 3. Statistics of the 4 September 1973 ERTS-1 positives of the Willcox Playa, Arizona.

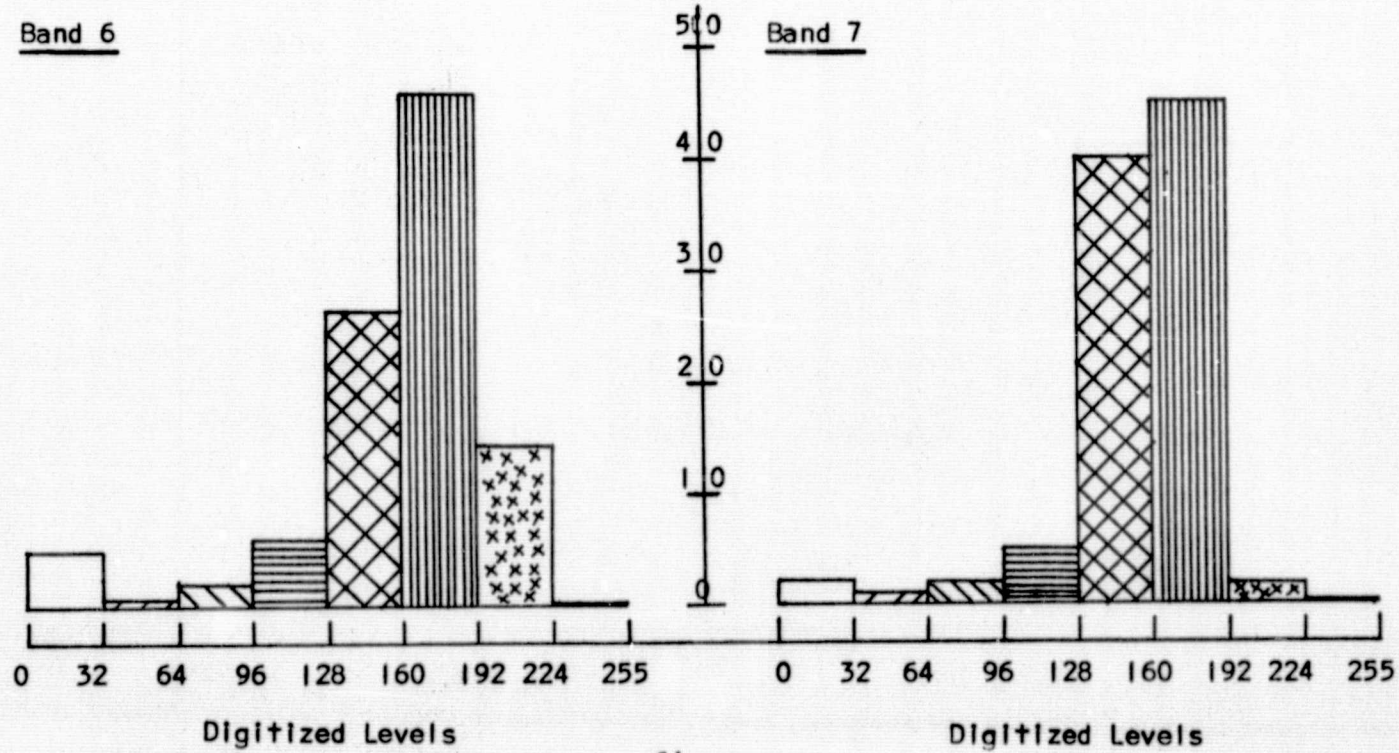


4 September 1973

ERTS-1 Positive Transparencies

of Willcox Playa

Figure 42



From the above statistics, the histograms shown in Figure 42 and the frequency distributions superimposed on the ERTS-I digitized images in Figure 41, the following inferences are made:

-- The Playa is darker in Band 4 than in any of the other ERTS-I Bands.

-- The brightness of the Playa is approximately the same in Bands 5, 6 and 7.

-- The variability of the brightness data is less in Band 7 then in any of the other ERTS-I bands.

-- The frequency distribution of brightness has two modes (peaks) in bands 4 and 5 which are absent from bands 6 and 7.

Willcox Playa - Temporal Image Analysis

In order to investigate the change in reflectance of the Willcox Playa as a function of time, an analysis of four ERTS negatives obtained on four different dates were made.

The following four ERTS-I negatives, all Band 5, were used as inputs to the "System 800" and digitized in the linear mode:

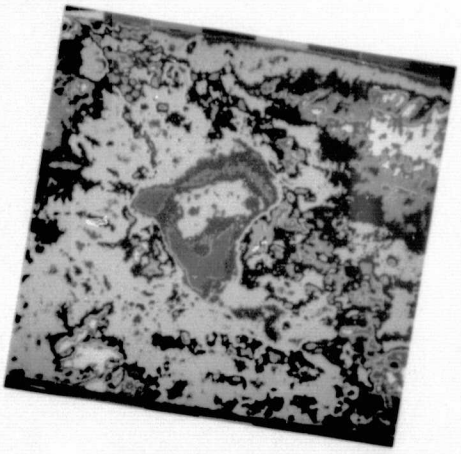
1 November, 1972

18 February, 1973

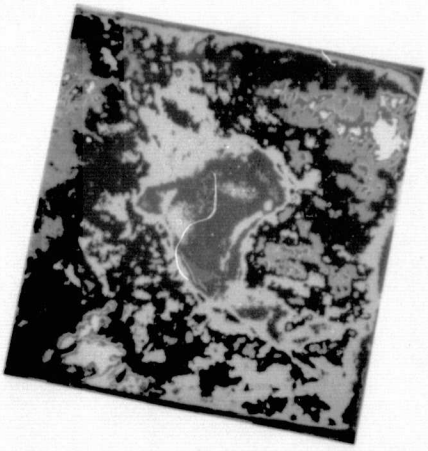
18 May, 1973

5 June, 1973

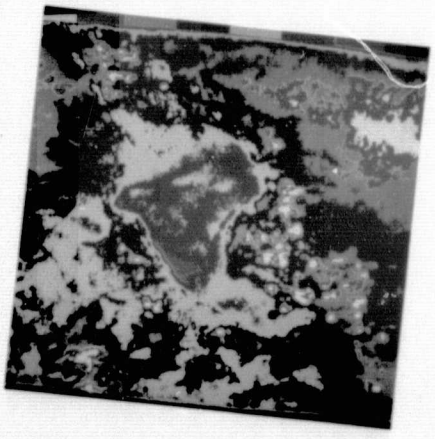
All four bands were digitized in registration using DIGIT and MARKER PROGRAMS. Following this, the HISTOGRAM Program was run classsifying the 256 digital levels into exactly the same light equal levels on all of the multidata imagery. The AREA program was then run and used to compute the percent of the 294,912 picture elements falling into each of the eight classes. The results are shown in the Table 4 on page 65.



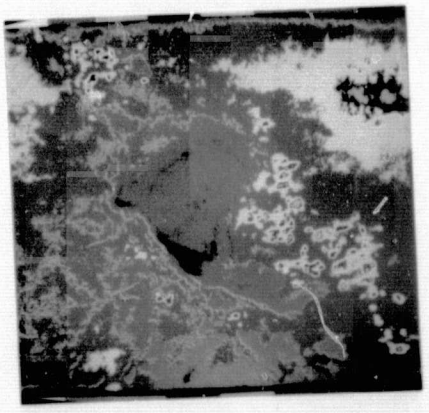
1 November 1972



18 February 1973



18 May 1973



5 June 1973

Figure 43. Willcox Playa Temporal Analysis - Digital Image Analysis of ERTS-1 Photographic Negatives Band 5 (.6 to .7γ) on four different levels.

ORIGINAL PAGE IS
OF POOR QUALITY

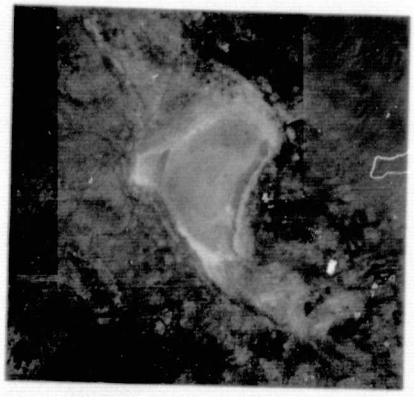
Digitized grey levels	Color code	ERTS-1 Band 5 (.6 to .7μ) on the following dates			
		1 November 1972	18 February 1973	18 May 1973	5 June 1973
0-32	Black	1.18	14.48	1.00	3.28
33-64	Red	2.72	1.98	0.58	31.26
65-96	Green	8.40	8.70	6.90	48.46
97-128	Yellow	37.90	19.92	20.32	14.06
129-160	Blue	29.24	35.06	42.92	2.52
161-192	Magenta	11.76	13.26	18.88	0.32
193-224	Cyan	5.10	3.76	6.68	0
225-255	White	3.62	2.72	2.62	0
	Totals	99.92	99.88	99.90	99.90

Table 4. Digital brightness classification of multidate imagery of Willcox Playa.

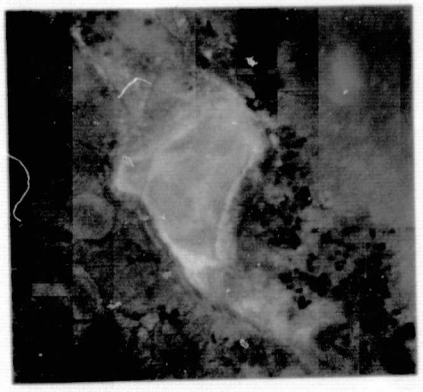
The display program was run and each brightness classified band was photographed and is reproduced in Figure 43. In addition, the 18 February 1973 and the 18 May 1973 Band 5 negatives were digitally averaged. A visual comparison of this result shown in Figure 44 with the individual brightness classifications for these dates depicted in Figure 43, shows very little variance between these four dates for the Playa itself.

A histogram was constructed of the digital brightness classification of Band 5 on each of the four dates which is shown in Figure 45. The mean of this data is tabulated below.

Band 5 - Date	Mean ($\bar{x}$)
1 November 1972	126.7
18 February 1973	120.7
18 May 1973	143.9
5 June 1973	74.2

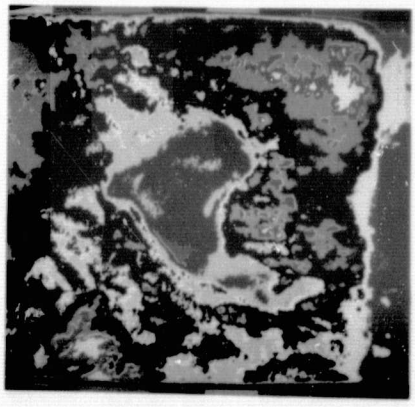


18 February 1973
ERTS-1 Band 5



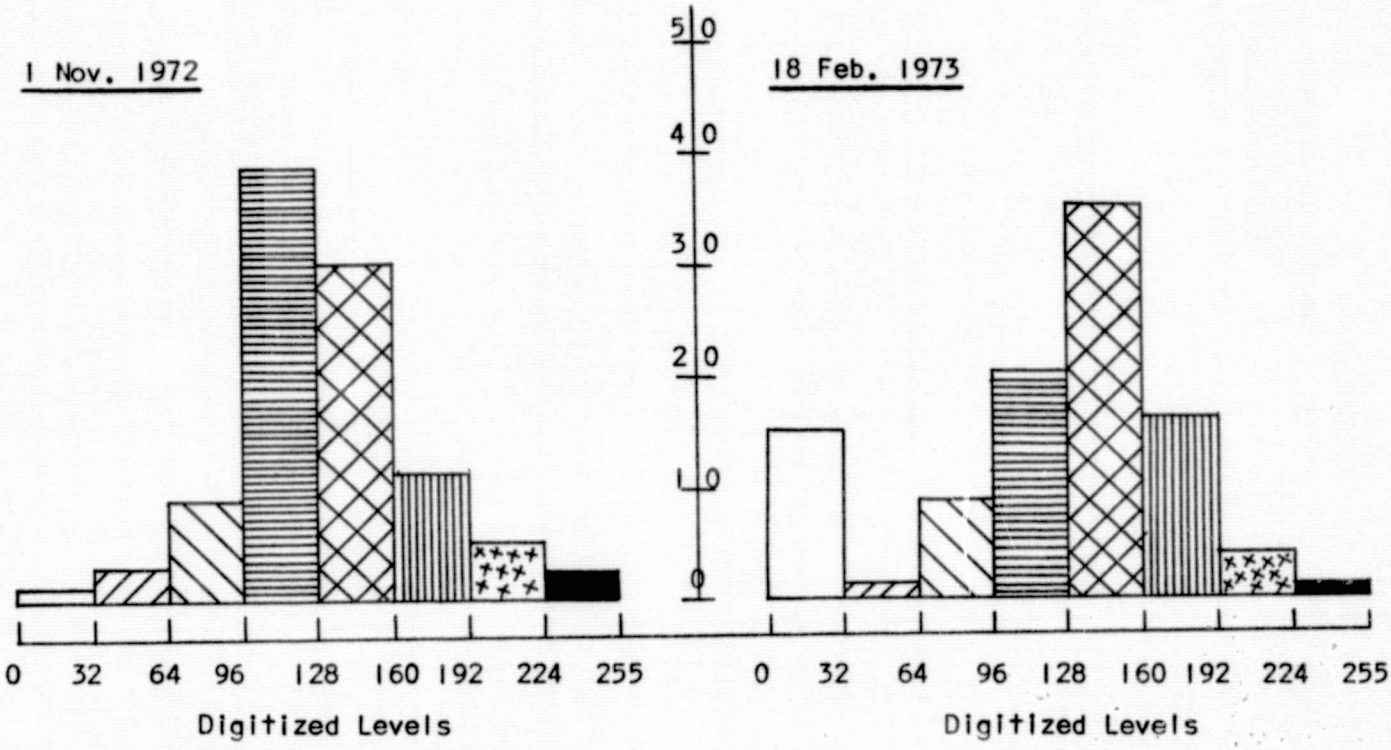
18 May 1973
ERTS-1 Band 5

ORIGINAL PAGE IS
OF POOR QUALITY



Average of 18 February and 18 May 1973
ERTS-1 Band 5

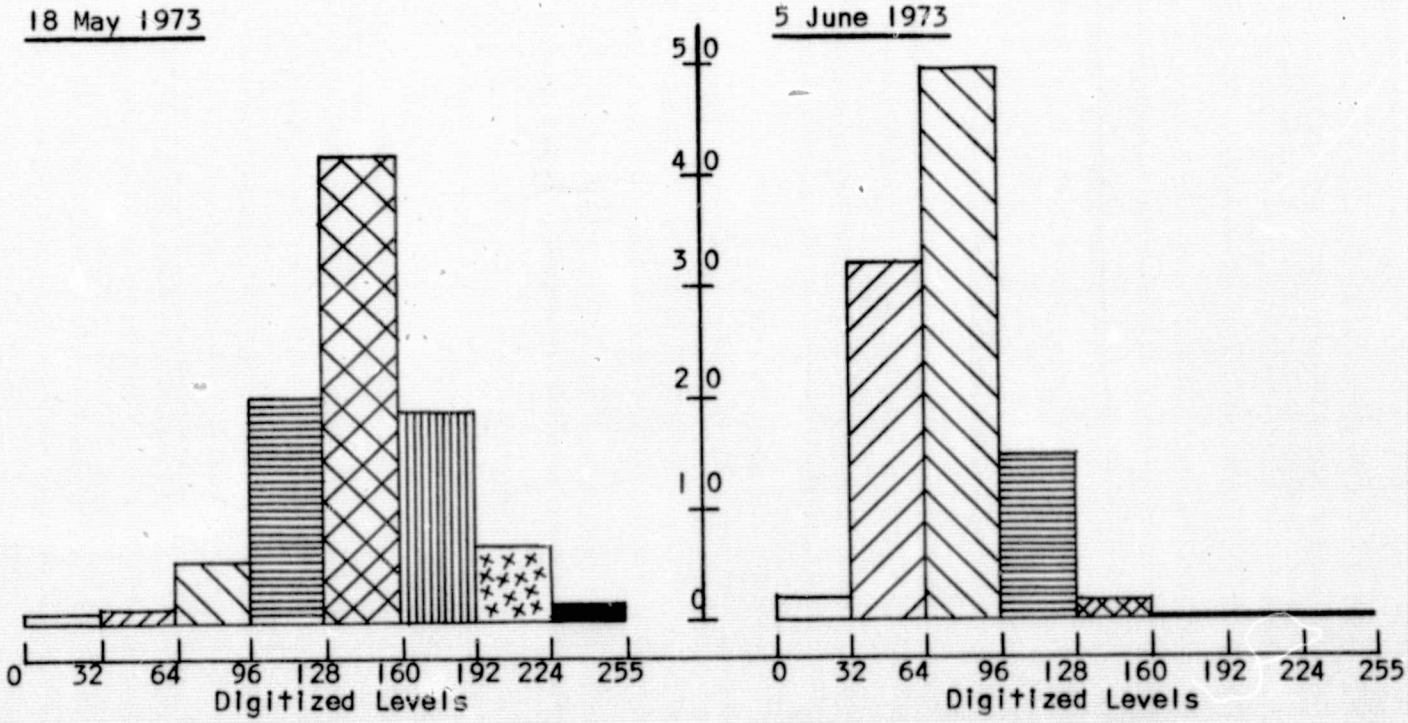
Figure 44. Digitally averaged brightness values of the Willcox Playa, Arizona on two dates.



Total Picture Elements 294, 912

Willcox Playa Temporal ERTS Band 5

Figure 45



Willcox Playa Temporal ERTS Band 5

1 Nov. 72, 18 Feb. 73, 18 May 73, 5 June 73

Figure 46

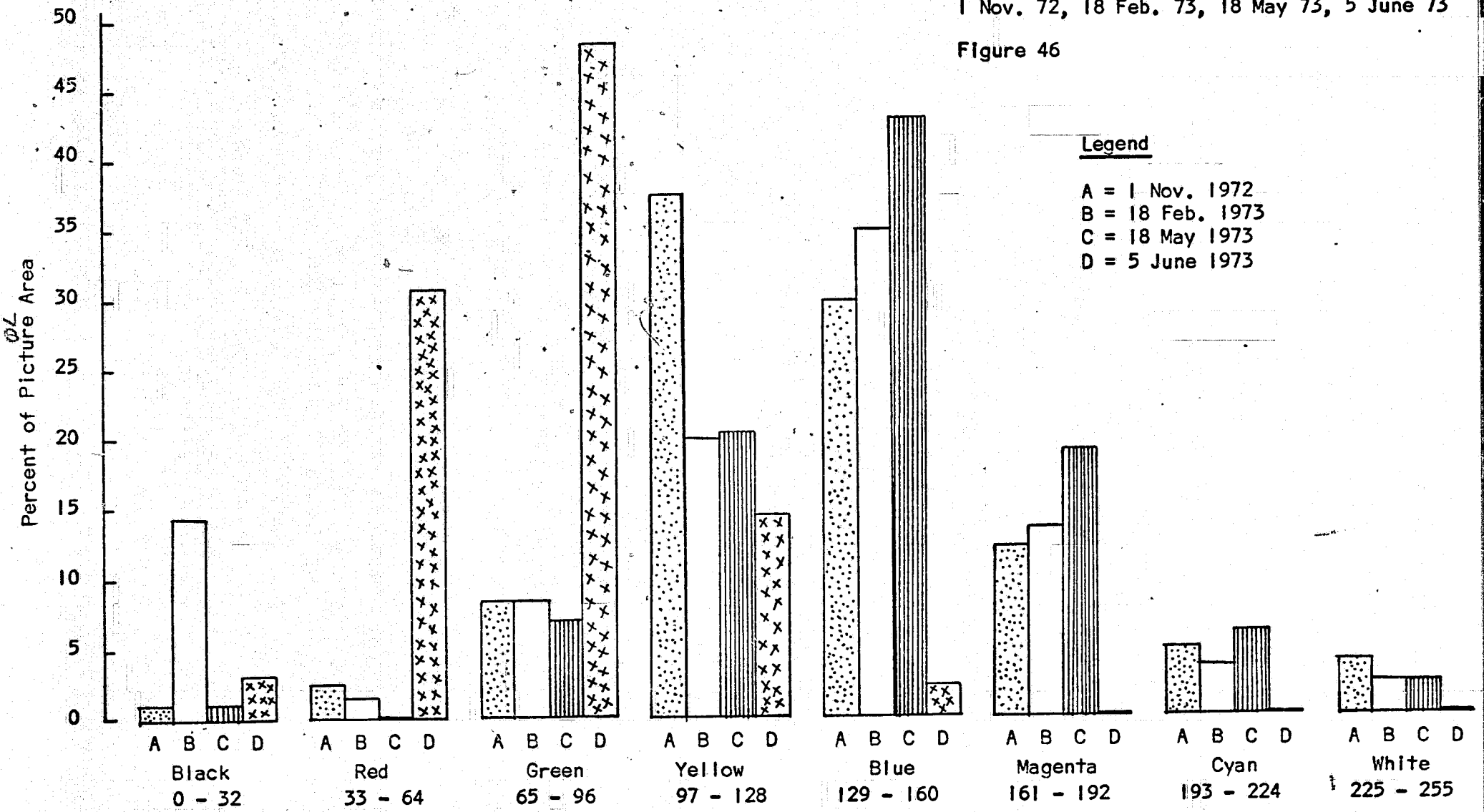


Figure 46 shows the percent of each of the brightness levels on the four multidate negatives in each of the eight digital classes. Clearly the 5 June 1973 imagery is anomalous in each class to the other dates.

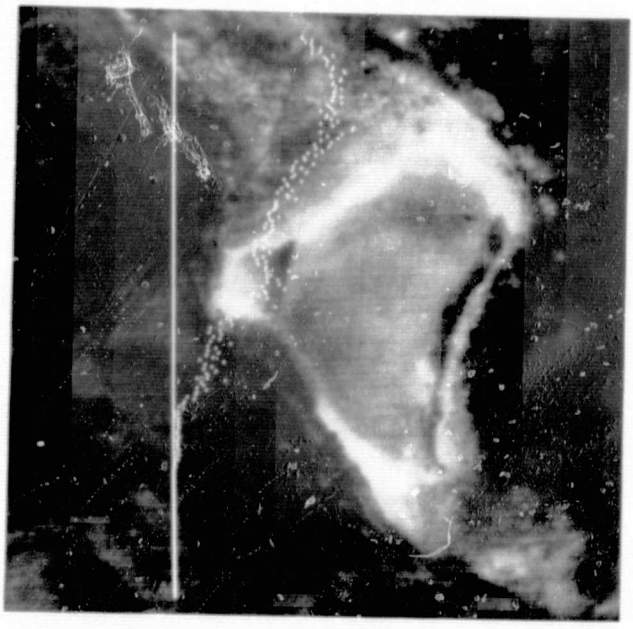
Band 4 of four ERTS-1 positives of Willcox Playa obtained on the four different dates were digitized in the log mode. These four digitized images with superimposed frequency distributions of brightness levels are shown in Figure 47. The digitized grey levels as computed using the AREA Program as shown in Table 5. A histogram of these brightness levels is plotted in Figure 48.

Digitized grey levels	Band 4 ERTS-1 Imagery of Willcox Playa			
	4 September 1973	18 May 1973	1 November 1972	18 February 1973
0-32	3.12	5.50	0.96	20.92
33-64	1.98	5.92	0.08	24.40
65-96	4.30	21.84	0.36	24.72
97-128	10.04	30.04	1.10	15.26
129-160	26.30	19.70	11.38	10.72
161-192	35.76	14.72	64.70	3.60
193-224	17.62	1.98	18.44	0.28
225-255	0.76	0.22	2.82	0
Totals	99.88	99.92	99.84	99.90

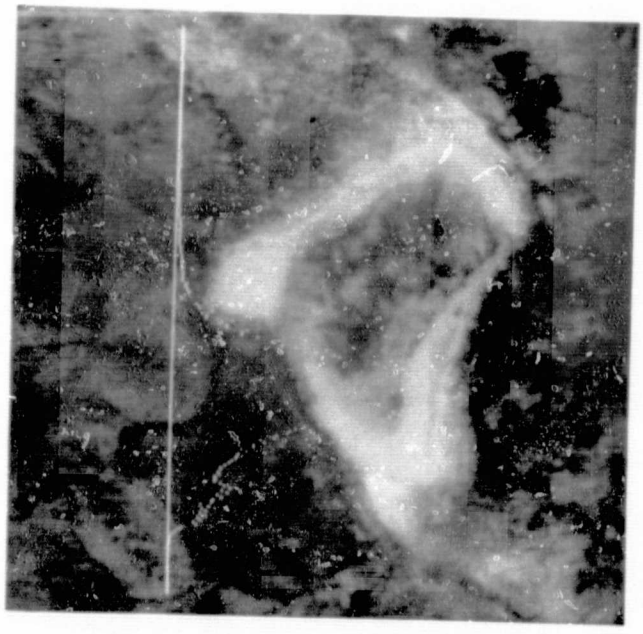
Table 5. Digital brightness classification of multidate imagery of Willcox Playa.

In order to evaluate the change in reflectance of the same areas of the Playa on the four different dates, three areas of the Willcox Playa were measured in each photograph: 1) the bright area at the south end of the Playa, 2) the west area of the Playa adjacent to the railroad track, 3) locations within the body of the Playa chosen randomly. The results are presented in the table on Page 72.

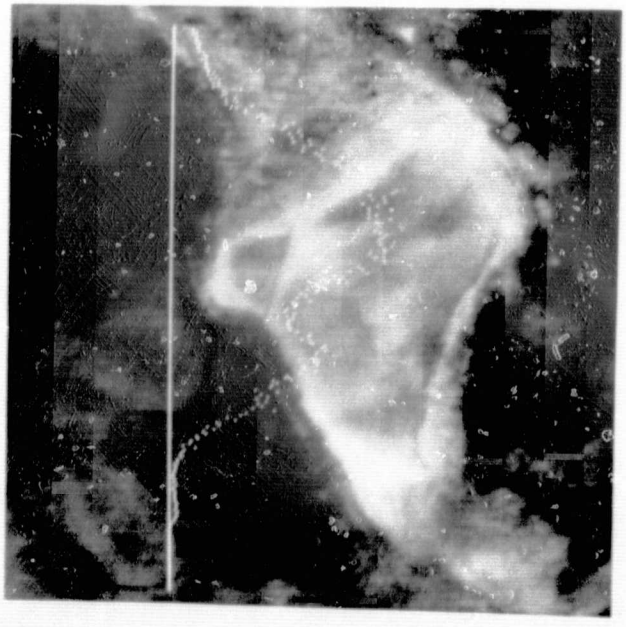
ORIGINAL PAGE IS
OF POOR QUALITY



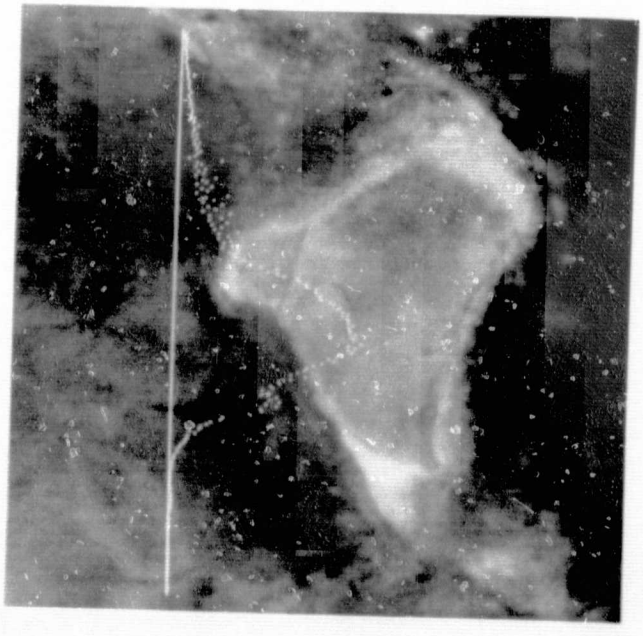
18 February 1973 Band 4



1 November 1972 Band 4

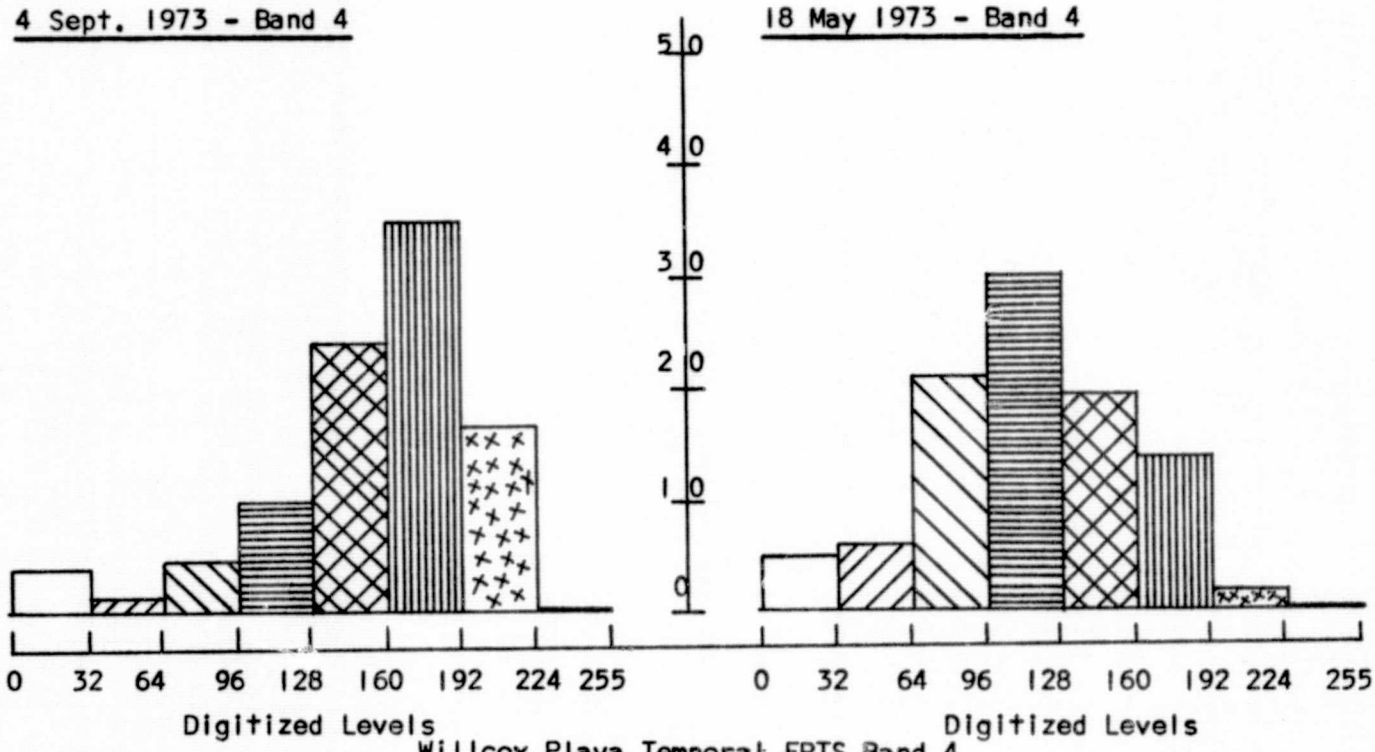


18 May 1973 Band 4

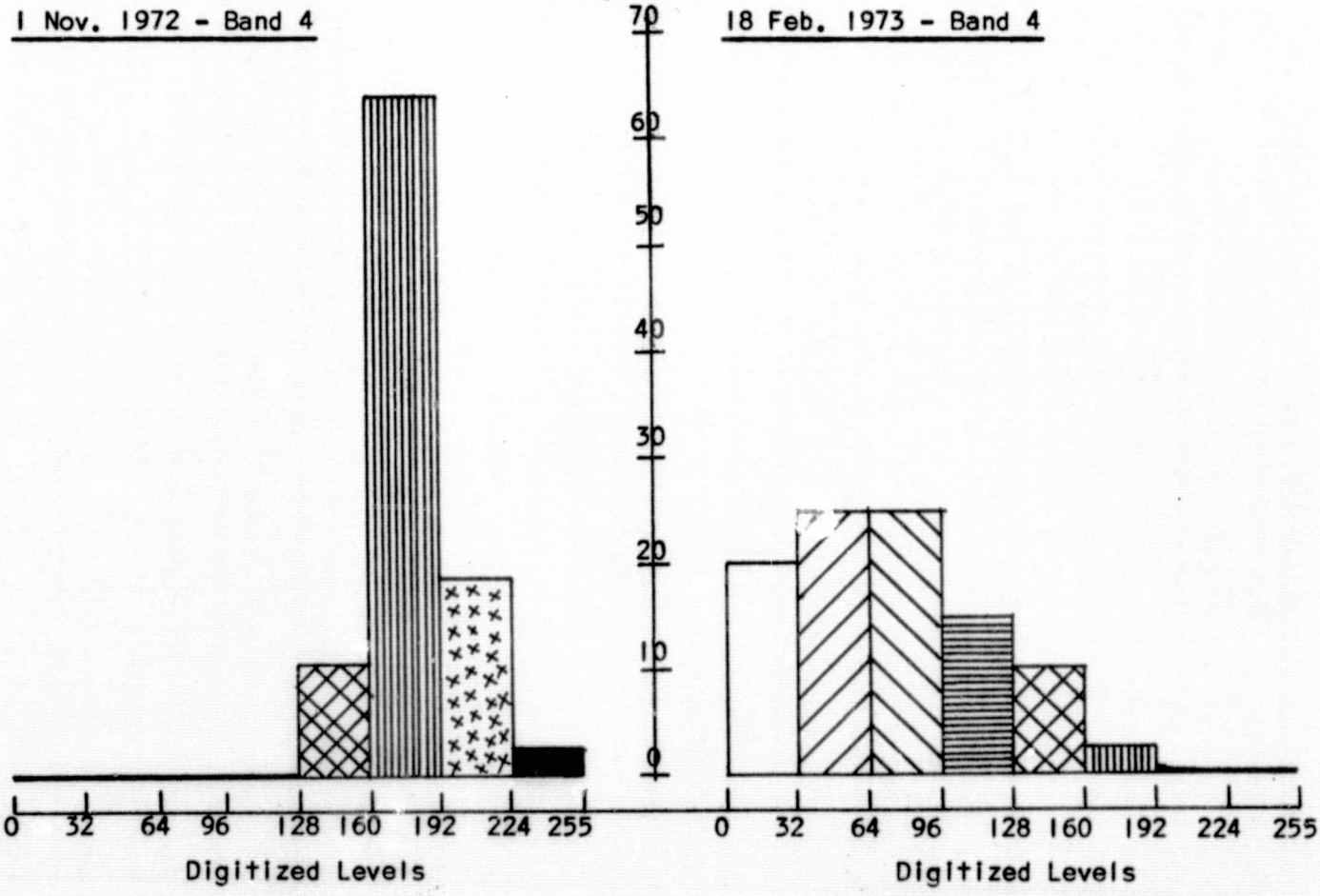


4 September 1973 Band 4

Figure 47. Digitized ERTS-1 Band 4 images from positive film transparencies showing variations (.5 to .6γ) reflectance on four different takes.



Willcox Playa Temporal ERTS Band 4
Figure 48



Location	4 September 1973		18 May 1973		1 November 1972		18 February 1973	
	$\bar{x}$	s	$\bar{x}$	s	$\bar{x}$	s	$\bar{x}$	s
South end of Playa Sample size = 5 (n=5)	224.4	1.5	228.6	3.2	237.2	4.6	199.8	5.8
Playa near Railroad sample size = 5 (n=5)	176.6	2.4	158.0	3.8	219.0	4.5	100.4	23.9
Random locations in Playa sample size = 10 (n=10)	174.6	10.6	168.6	11.8	191.8	10.7	137.7	12.8

Table 6. The mean and standard deviation of the relative brightness of the Willcox Playa on four different dates as recorded in ERTS-1 Band 4 imagery.

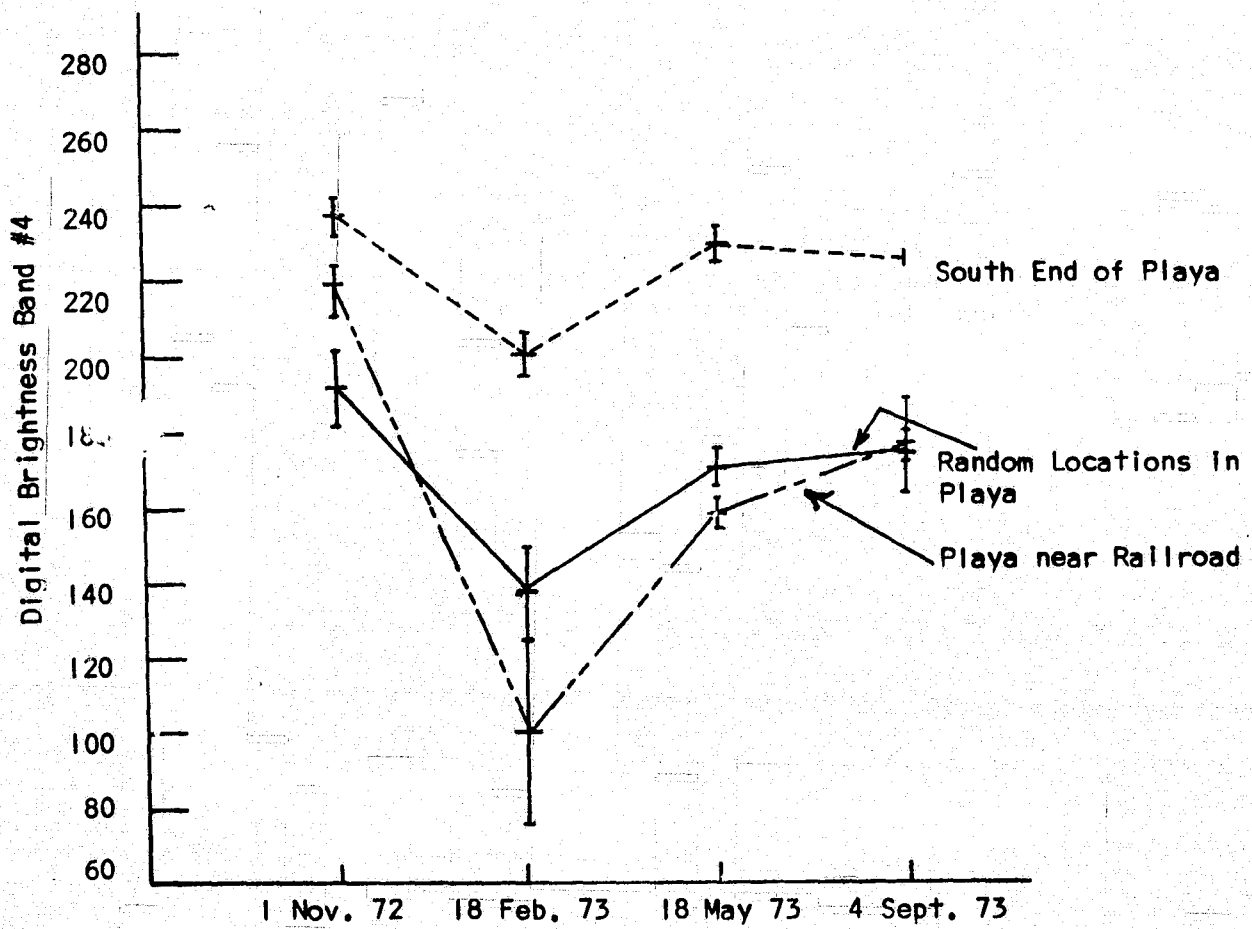


Figure 49. ERTS-1 Band 4 mean and variance of digital brightness measurements of three locations in the Willcox Playa, Arizona on four different dates.

Brightness measurements in the Playa depend on location. The higher south end of the Playa is brighter and shows less deviation from the mean brightness than the main body of the Playa. The area of the Playa north west of the railroad tracks crossing the Playa, where water is known to be impounded, shows the greatest variability on the four dates.

From these dates it is clear that variations in the spectral reflectance of the Willcox Playa as recorded by ERTS-1 vary greatly between spectral bands and in the same spectral band on different dates.

Phoenix, Arizona Spectral Analysis

A spectral analysis of ERTS-1 imagery of an urban area of Phoenix, Arizona taken on 14 April 1973 was digitally analyzed to establish atmospheric effects on the image in urban scenes in semi-arid terrain. Four carefully prepared positive images were made from NASA release ERTS-1 negatives. These were linearly digitized in registration using the MARKER and DIGIT program; following which HISTOGRAM and AREA programs were run using about equal digitization levels as shown in Table 8 on the next page.

Digital brightness measurements were made of bright cloud tops and dark ground shadows which were cast over urban areas of Phoenix. The mean and standard deviation of this data are tabulated in Table 7.

	Cloud Tops		Shadows	
	mean $\bar{x}$	Standard deviation (s)	mean $\bar{x}$	Standard deviation (s)
Band 4	170	20	52	12
Band 5	173	19	46	12
Band 6	210	7	69	12
Band 7	223	22	63	12

Table 7. Digital brightness statistics of clouds and shadows appearing in Phoenix, Arizona 14 April 1973 positives.

Digitized grey level	Color Code	14 April 1973 ERTS-1 Image			
		Band 4	Band 5	Band 6	Band 7
0-32	Black	13.56	15.20	1.96	2.52
33-64	Red	21.70	16.66	4.54	5.62
65-96	Green	26.42	23.86	12.62	15.44
97-128	Yellow	30.92	26.76	24.80	30.68
129-160	Blue	6.64	14.96	31.82	28.76
161-192	Magenta	0.66	2.18	20.60	13.48
193-224	Cyan	0.02	0.30	3.50	2.94
225-255	White	0	0	0.08	0.42
	Totals	99.92	99.92	99.92	99.86

Table 8. Digital brightness classification of urban section of ERTS-1 imagery of Phoenix, Arizona taken on 14 April 1973.

From the above data it is seen that the difference in the means of the brightness of cloud tops and shadows increases as follows:

	mean $(\bar{x}_1 - \bar{x}_2)$	Standard deviation $(s_1^2 + s_2^2)^{1/2}$
Band 4	118	23
Band 5	127	23
Band 6	141	14
Band 7	160	25

Table 9. Brightness difference between cloud tops (x_1) and shadows (x_2) in Phoenix, Arizona 14 April 1973.

Assuming comparatively uniform spectral reflectance for cloud tops and cloud shadows (in an urban area), we see that the contrast in each band as a percent of Band 7 increases with increasing wavelength as follows.

$$\frac{\text{Band 4}}{\text{Band 7}} \times 100 = 74\%$$

$$\frac{\text{Band 5}}{\text{Band 7}} \times 100 = 79\%$$

$$\frac{\text{Band 6}}{\text{Band 7}} \times 100 = 88\%$$

Prescott, Arizona Spectral Analysis

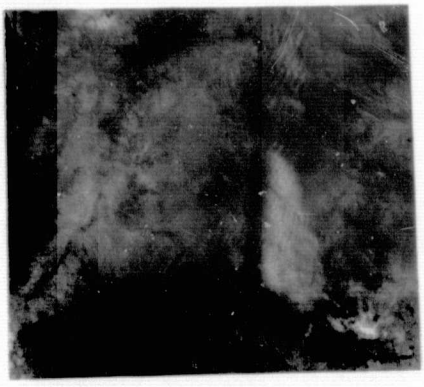
Four ERTS-1 negatives taken on 29 September 1972 were digitally analyzed in order to establish if known communities of Ponderosa Pine could be detected in the Copper Basin Area of the Prescott National Forest. The results of the HISTOGRAM and AREA programs run with the digitization levels (partitions) are as follows:

Digitized grey levels	Color Code	29 September 1972 ERTS-1 Negatives			
		Band 4	Band 5	Band 6	Band 7
0-32	Black	4.34	9.64	9.22	7.00
33-64	Red	11.96	16.80	24.84	23.38
65-96	Green	27.54	25.84	33.16	36.10
97-128	Yellow	29.34	19.28	18.86	20.06
129-160	Blue	15.50	11.82	9.30	8.56
161-192	Magenta	7.18	6.92	2.90	2.52
193-224	Cyan	3.16	4.00	0.78	0.84
225-255	White	0.90	5.60	0.86	1.44
	Totals	99.92	99.90	99.92	99.90

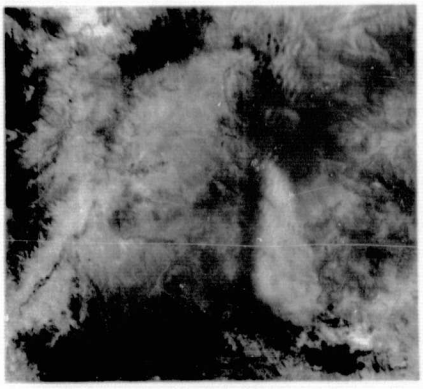
Table 10. Digital brightness classification of Prescott National Forest on ERTS-1 negatives taken 29 September 1972.

Positive prints of portions of each of the ERTS-1 bands are reproduced in Figure 50. Textural patterns in Copper Basin Area are evident in this imagery principally in Band 7. The results of the "System 800" are shown in Figure 51. These data are analyzed with respect to ground reflectance spectra in Section 3 of this report.

ORIGINAL PAGE IS
OF POOR QUALITY



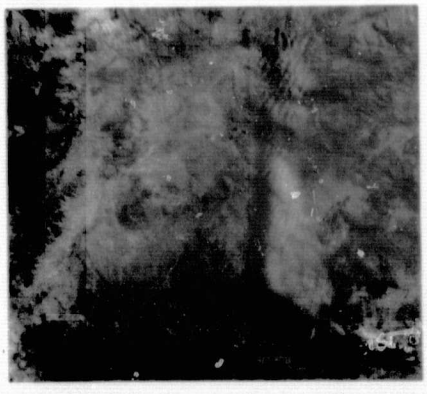
Band 4



Band 5

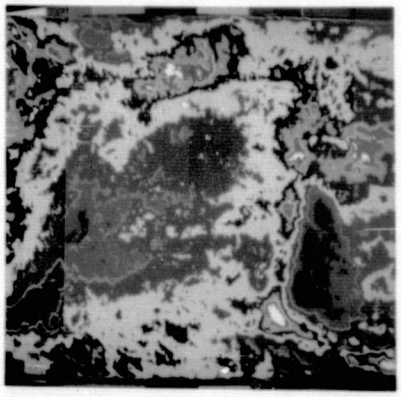


Band 6



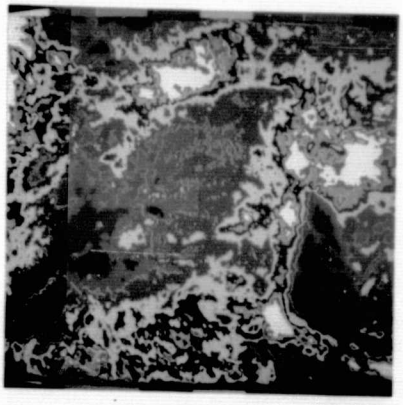
Band 7

Figure 50. Prescott, Arizona - Positive ERTS-1 images acquired on 29 September 1972.

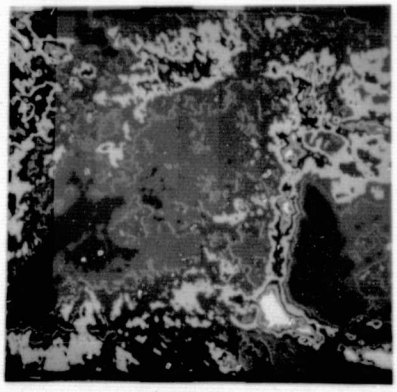


Band 4

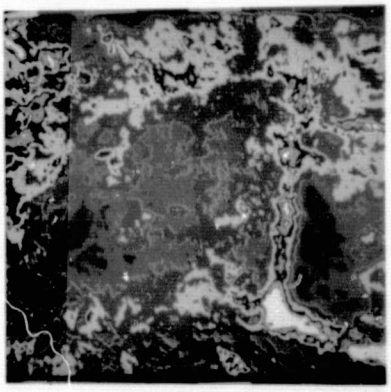
ORIGINAL PAGE IS
OF POOR QUALITY



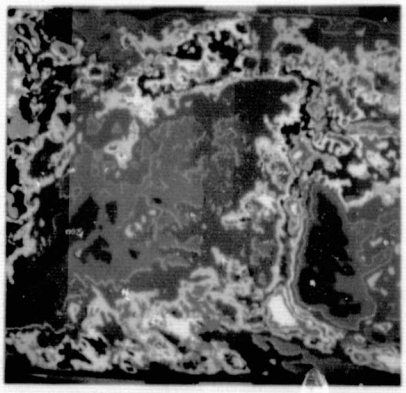
Band 5



Band 6



Band 7



Average of Bands 4, 5, 6 and 7

Figure 51. Prescott, Arizona - digitized brightness presentation for photographic negatives acquired by ERTS-1 on 29 September 1972.

Atmospheric Effects in Desert Areas

The relative effect of the atmosphere in each of the four spectral bands was analized using ERTS-1 imagery of the Willcox, Arizona, area acquired on 4 September 1973. Positive photographic images of a desert area containing clouds were log digitized. The digitization range was adjusted to give it the same range for all four photos in order to maintain a constant relative relationship of the eight digitization levels between the four spectral bands.

By use of the MARKER, DIGIT, HISTOGRAM, AREA and DISPLAY programs the following brightness classifications of each image were made:

Digitized grey levels	4 September 1973 ERTS-1 Positive			
	Band 4	Band 5	Band 6	Band 7
0-32	1.30	1.56	1.02	1.24
33-64	0.46	1.80	0.68	0.58
65-96	1.62	4.80	1.34	1.30
97-128	9.64	9.42	3.74	3.04
129-160	62.80	49.28	38.46	24.78
161-192	20.92	30.34	51.48	65.38
193-224	2.34	2.14	2.62	2.84
225-255	0.92	0.58	0.54	0.74
Totals	99.90	99.92	99.88	99.90

Table 11. Digital brightness of ERTS-1 images of Southern Arizona taken on 4 September 1972.

Ten digital brightness measurements of clouds, cloud shadows and desert terrain immediately adjacent to cloud shadows were made using HISTOR program. The mean ($\bar{x}$) and standard deviation (s) of these measurements are tabulated on the following page in Table 12. The digitization levels were adjusted to make the brightness of cloud approximately the same in all bands.

Image Area measured	4 September 1973 ERTS-1 Positives							
	Band 4		Band 5		Band 6		Band 7	
	$\bar{x}$	s	$\bar{x}$	s	$\bar{x}$	s	$\bar{x}$	s
Bright Cloud	230.7	10.4	230.3	4.3	229.0	1.8	232.9	2.4
Terrain in shadow	99.4	7.7	59.6	12.9	51.7	8.6	20.1	10.8
Terrain not in shadow	145.5	3.6	141.1	3.7	154.1	2.2	156.4	4.6

Table 12. The mean and standard deviation of image brightness measurements of desert terrain in shadow and illuminated by sunlight.

The full printout of all measurements, the statistics of which are shown above is contained in Appendix F . The statistics in this table were computed from a sample of ten (e.g. n=10) random measurements of each of the three areas on each of the four ERTS-1 positive images as follows:

$$\text{sample mean} = \bar{x} = \frac{\sum_{i=1}^{n} x_i}{n}$$

$$\text{sample standard deviation} = s = \left[\frac{\sum_{i=1}^{n} (x_i-\bar{x})^2}{n-1}\right]^{1/2} = \left[\frac{\sum_{i=1}^{n} x_i^2 - n\bar{x}^2}{n-1}\right]^{1/2}$$

A plot of the digital brightness levels of all four ERTS-1 bands compared to band 7 as a standard is shown in Figure 52. The increasing brightness of the terrain in shadow with decreasing brightness and decreasing wavelength is evident from this graph. This data quantifies the effect of atmosphere with brightness and wavelength.

Correction factors were computed to make the digital brightness values in all four bands equal to the same value (e.g. 230). These corrected values are shown in Table 13.

The percent decrease in scene brightness range with decreasing wavelength from the last row in Table 13 has been plotted in Figure 53 .

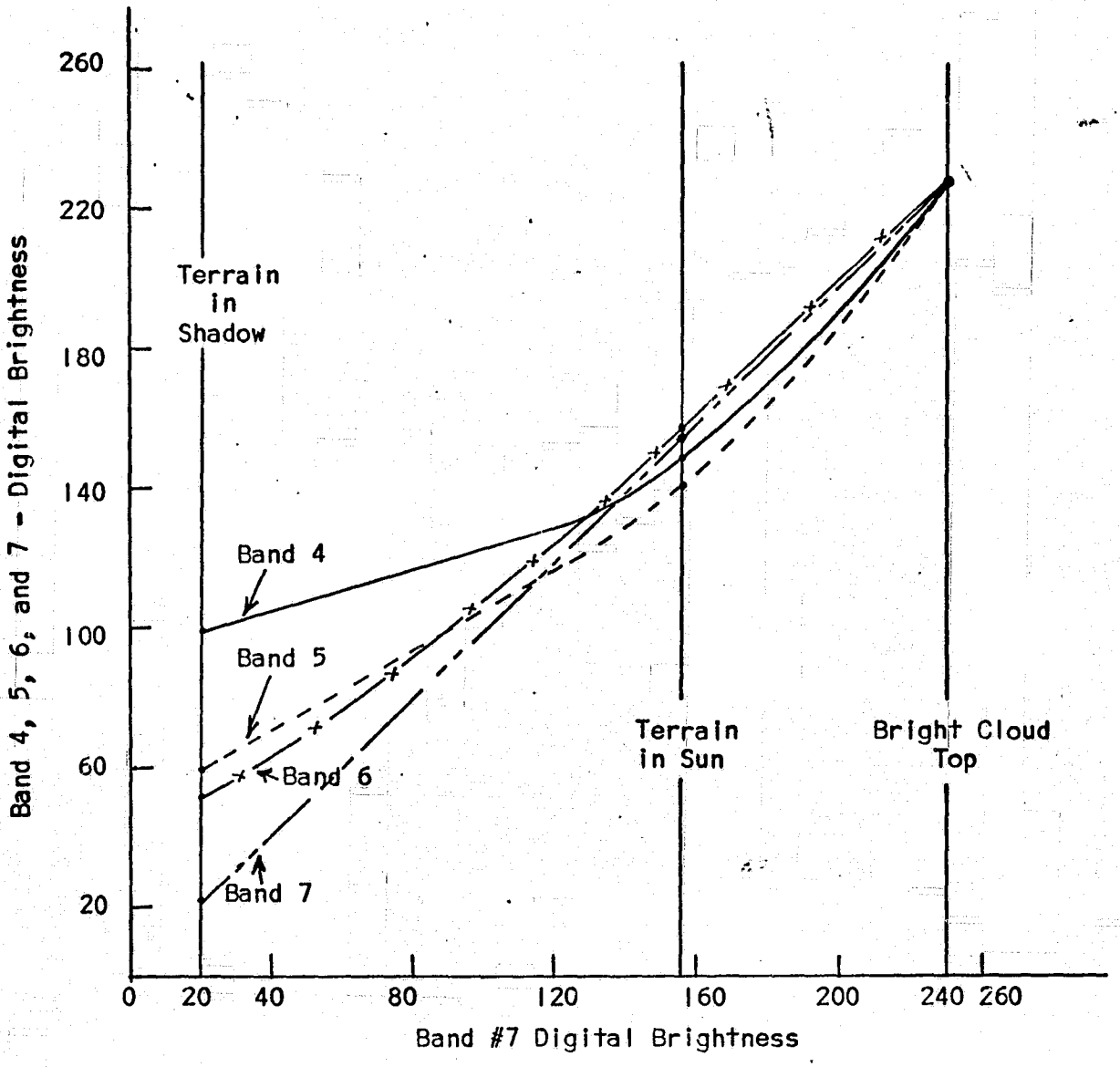


Figure 52. Digital brightness levels of the four ERTS-1 bands compared to Band 7 for cloud tops, terrain in sun, and terrain in shadow.

	4 September 1973 ERTS-1 positives			
	Band 4	Band 5	bBand 6	Band 7
Correction factor	.9969657	.9986973	1.0043668	.9875483
Bright cloud x corr. factor	230	230	230	230
Terrain in shadow x corr. factor	99.1	59.5	51.9	19.8
Sunlight terrain x corr. factor	145.1	140.9	154.8	154.5
Δ = corr. factor x (sunlight-shadow)	46.0	81.4	102.9	134.7
Δ as a percent of Band 7 Δ	34.1	60.4	76.4	100

Table 13. Terrain and shadow measurements normalized to equal cloud brightness measurements.

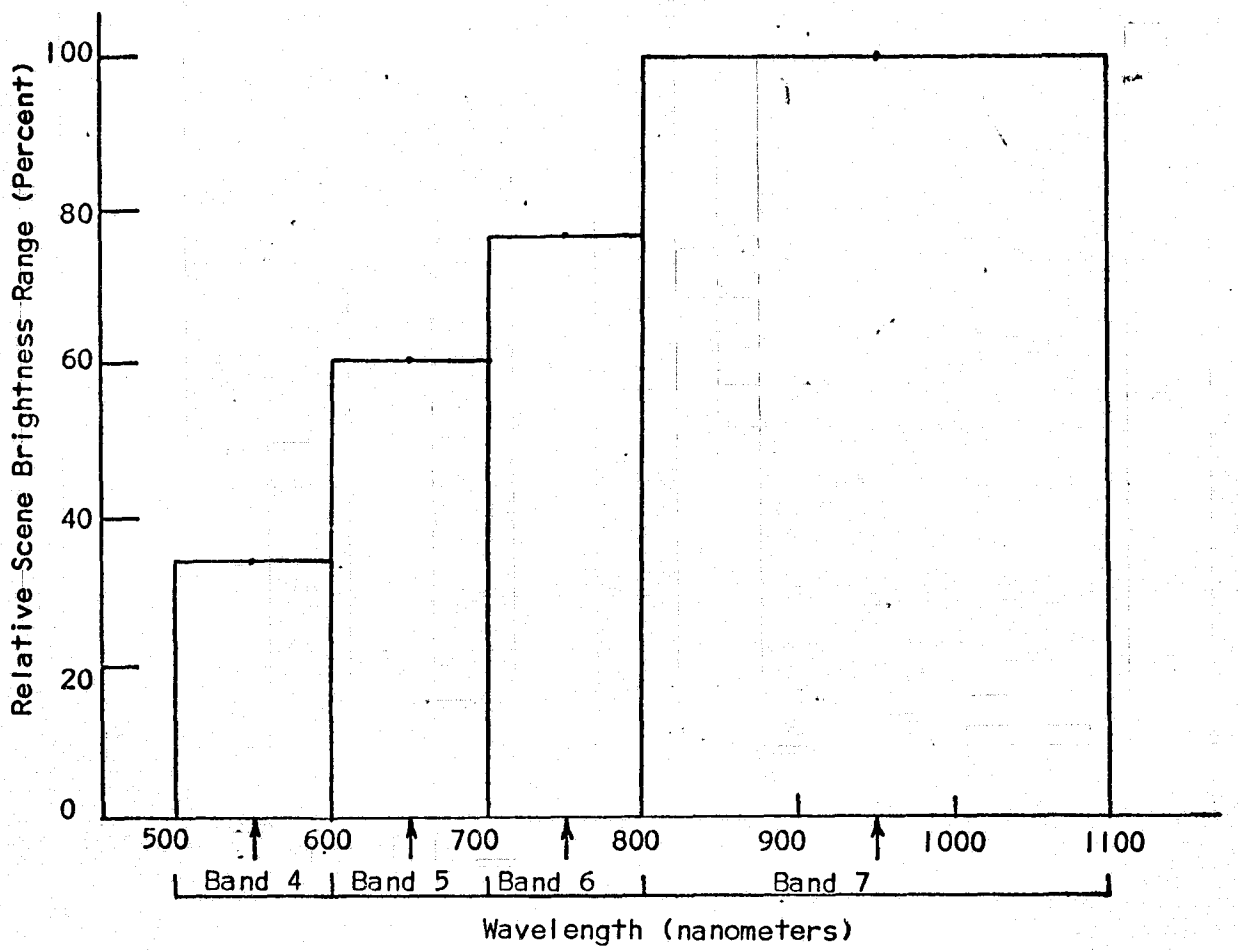


Figure 53. Scene brightness range of sunlit desert terrain minus similar terrain in shadow. The range of Band 7 is used as 100 percent.

		4 September 1973 ERTS-1 positives			
		Band 4	Band 5	Band 6	Band 7
1	(19.8) (corr. factor) ÷ ÷ (terrain in shadow)	.20	.33	.38	1.00
2	(154.5) (corr. factor) ÷ ÷ (terrain in sunlight)	1.06	1.10	1.00	1.00
3	reciprical of row 2 above	.943	.909	1.00	1.00
	row 1 times row 3 = corr.factor to normalize scene brightness	.19	.30	.38	1.00

Table 14. Computational steps to arrive at correction factors to compensate for atmospheric scattering of low brightness desert terrain.

In order to derive correction factors which can be applied to each band to compensate for atmospheric scattering as a function of wavelength, all data were normalized with respect to Band 7 which is used as the standard since it is known that Raleigh scattering is least in the infra-red wavelengths.

The data from Table 14 have been used to construct a graph showing the approximate correction to apply to ERTS-1 positive images of desert areas as a function of brightness in each band. The procedure is:

1 - Adjust digitization so that bright cloud tops have equal brightness values in all four bands.

2 - All image areas in deep shadow should have digitized brightness values greater than zero.

3 - Measure adjacent desert area in shadow and in sunlight in all ERTS-1 bands. The brightest value = 100 and the darkest value = 0.

4 - Apply the correction factor shown in Figure 54.

A summary of the analysis of variability of the digital brightness measurements in each ERTS-1 spectral band is shown in Figure 55. Therein it is seen that the statistical stability of the variability of the measurements of digital brightness of sunlit and shadow desert terrain does not vary with ERTS-1 band. However, the variability in cloud brightness measurements decreases with increasing wavelengths.

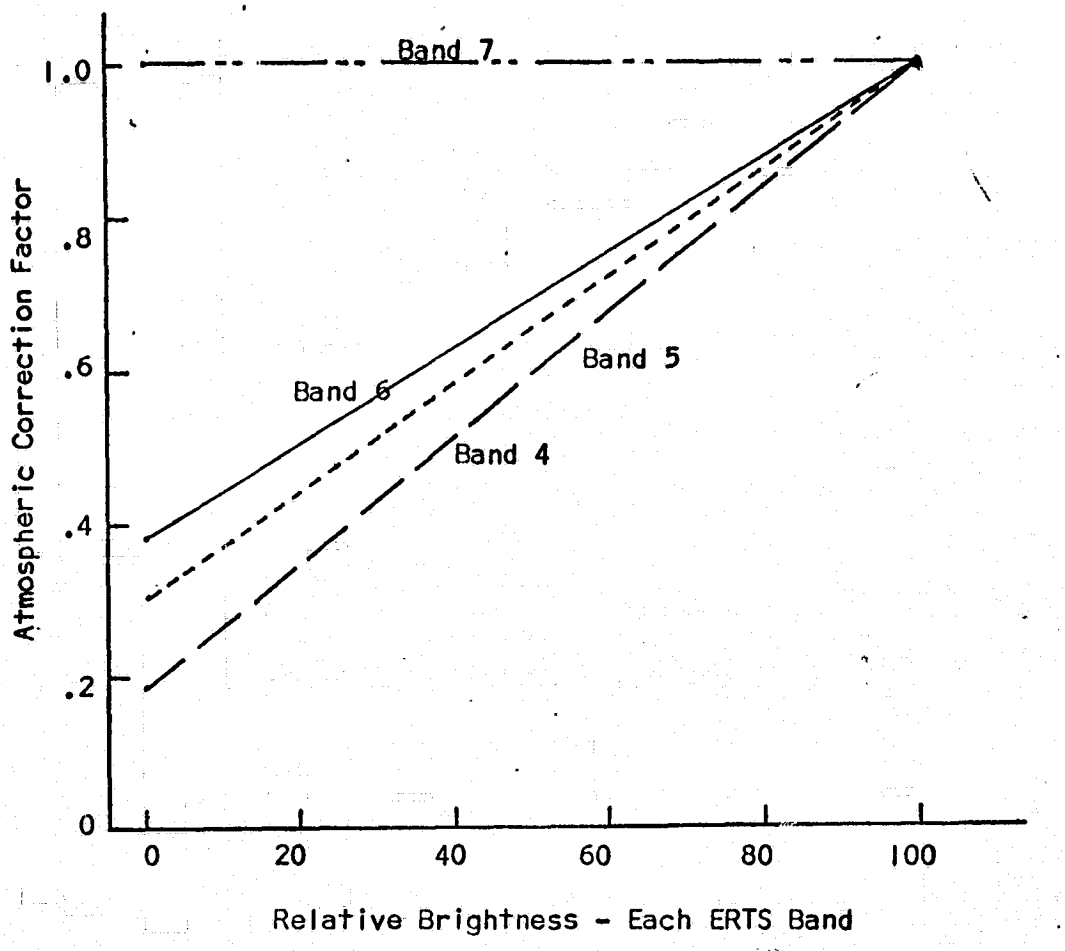


Figure 54. Atmospheric correction factor for ERTS bands.

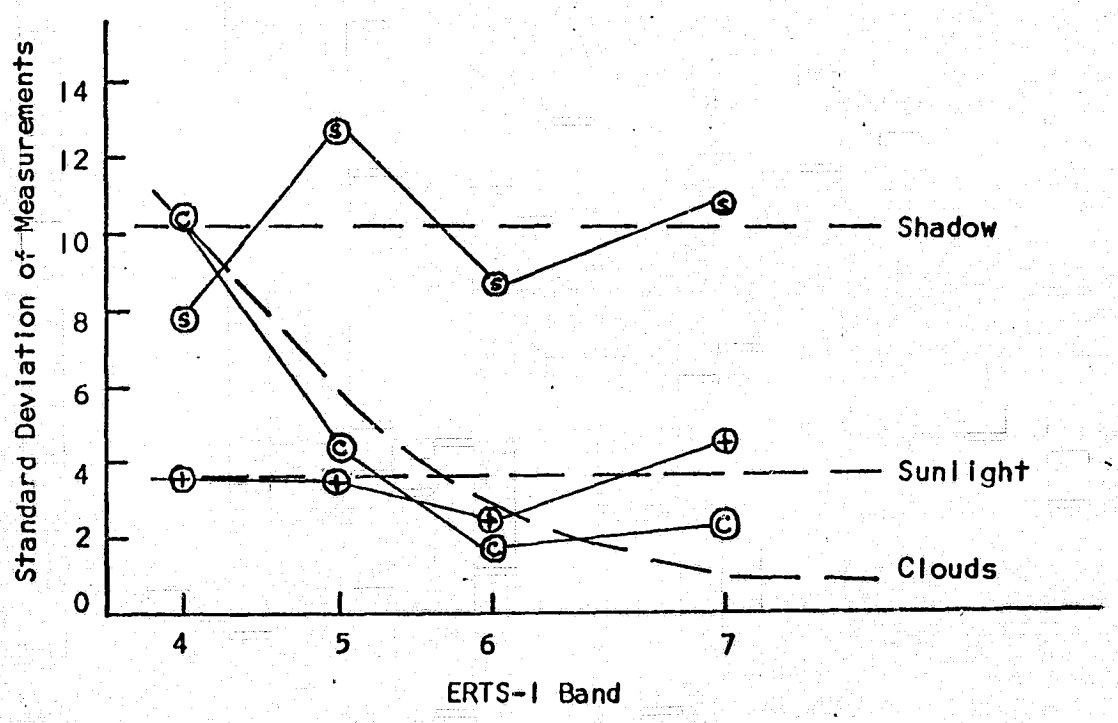


Figure 55. Variability of the digital brightness in each ERTS band.

Section 5

ERTS Geologic Interpretation using Optimum Image Characteristics

An experiment was conducted to establish the best or optimum characteristics of ERTS black-and-white positives making additive color images for geologic interpretation. Described herein are both the techniques used to establish the optimum image characteristics and the subsequent geologic interpretation made therefrom.

Optimum Photographic Characteristics of ERTS for Geology

The best additive color presentation of ERTS images was established by conducting an experiment in which five different exposure vs. density relationships (gamma γ) were evaluated. A 5 June 1973 ERTS MSS of the Willcox Playa area was chosen. Five sets of positives were made from this one set of negatives. The photographic parameters of the positives were varied to produce a set of transparencies in which the ΔD (density range) of the area of geologic interest were expanded to as a great a degree as possible. Photographically, these were steps 4 through 13 on the ERTS grey scale at the bottom of the image. Exposure was carefully controlled in order to keep the geologic detail of the area of interest compatible with the requirements of additive color projection.

Density measurements were made of the negative, release positive (γ1), and the positive with increasing gamma. The results are tabulated in Table 15, in terms of ΔD of the area of interest, and the expansion factor. The expansion factor is defined as the degree of expansion of the density range of the areas of interest.

Image	ΔD Areas of Interest	ΔD Expansion Factor	Total ΔD
Negative	.56	none	1.70
Release Positive (γ=1)	.71	1.26	1.77
γ=1.3 Positive (nominal)	.67	1.19	1.90
γ=1.5 " "	.82	1.46	2.09
γ=1.7 " "	.98	1.75	2.55
γ=3.0 " "	1.39	2.48	3.16

Table 15. Photographic characteristics of ERTS positives reproduced to give optimum additive color picture for geologic interpretation.

It is interesting to note that while the total ΔD follows an orderly progression, the D of the areas of interest, and the expansion factor are lower in the γ=1.3 positive than in the γ=.1 release positive. This is due to a slightly different slope of the two curves. The characteristic curves that is negative grey scale density vs. positive grey scale density is shown in Figure 56.

Screen reproductions of the five additive color images are shown in Figures 57 and 58 . An examination of these images shows an increase in color differentiation with increasing gamma, with the most dramatic improvement being the γ=3.0. This is due to a combination of both the expansion of the ΔD, and the lower ΔD min allowed by this particular film-developer combination. An examination of the step wedge in the grey scale data block shows the decrease in the brightness image that can be accommodated with increasing gamma.

Visual Analysis of ERTS Image for Geologic Information

A study was performed, employing visual analysis only, to investigate the application of ERTS additive color images to geology and related disciplines. The images used were made from optimally processed

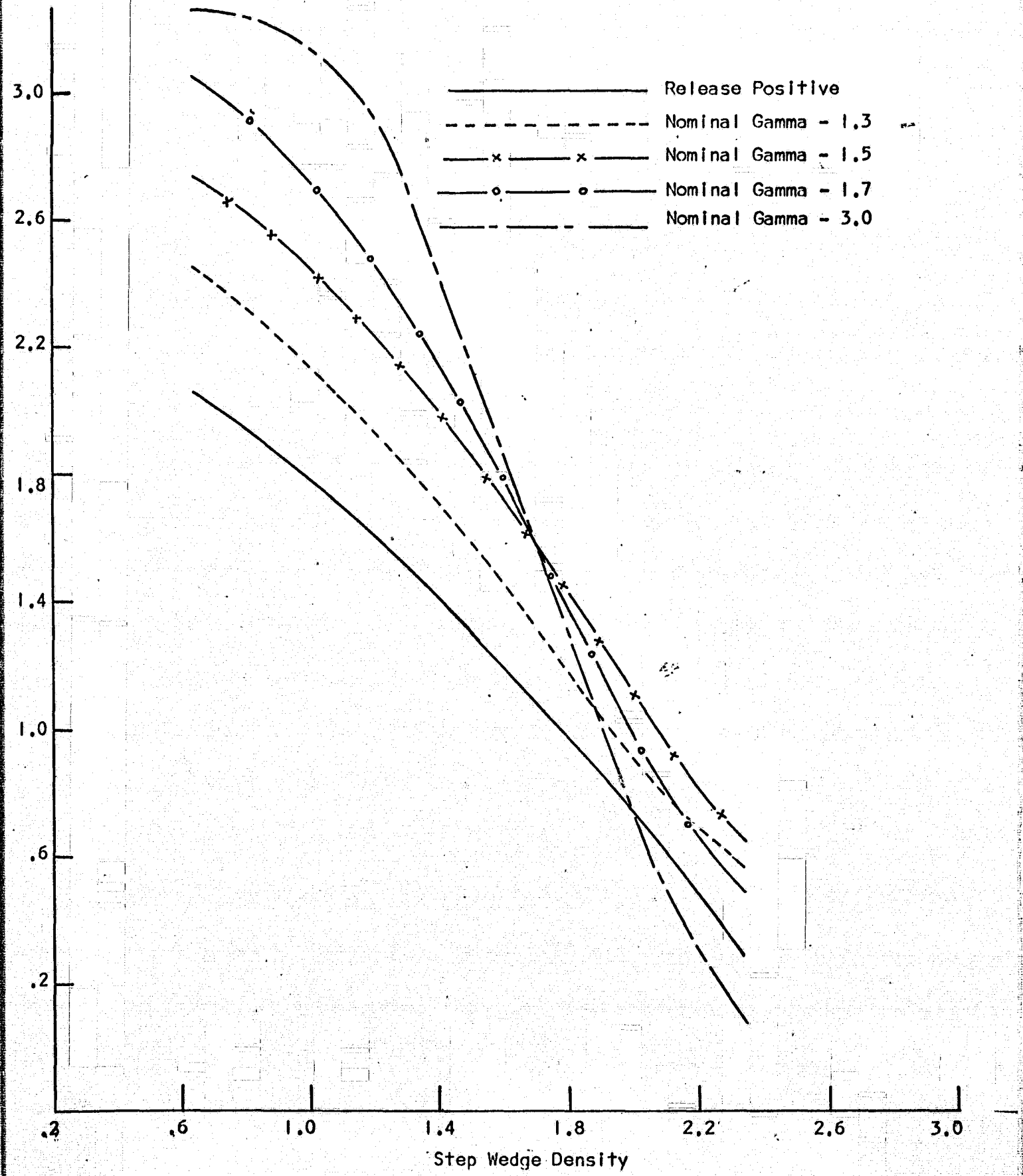
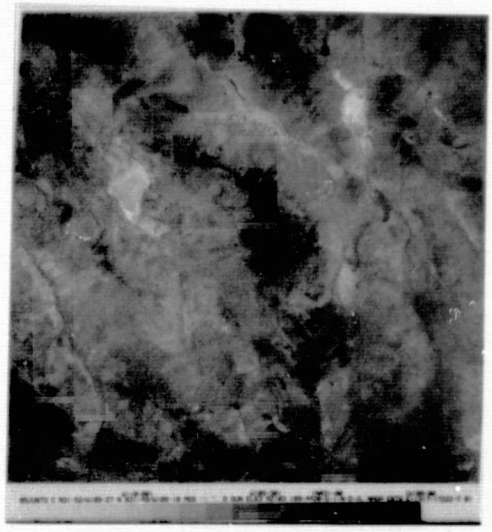


Figure 56. Photographic characteristics of positives made from NASA Release Negatives to produce optimum additive color image for geologic interpretation.

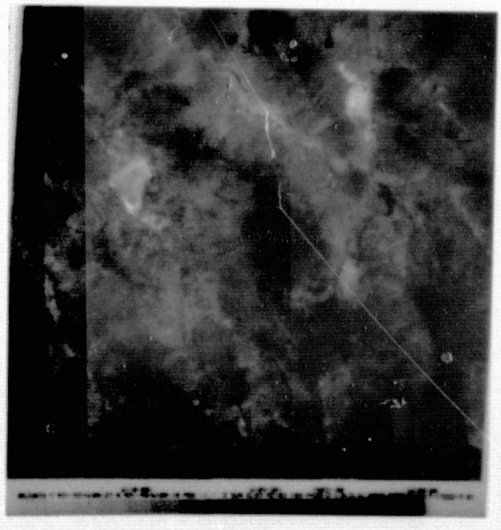


Gamma one (γ=1)

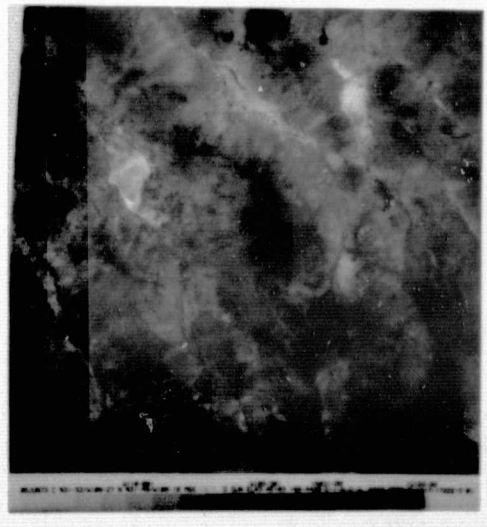


Gamma one point three (γ=1.3)

ORIGINAL PAGE IS
OF POOR QUALITY



Gamma one point five (γ=1.5)



Gamma one point seven (γ=1.7)

Figure 57. Variation of geologic image quality with increasing gamma.

ORIGINAL PAGE IS
OF POOR QUALITY

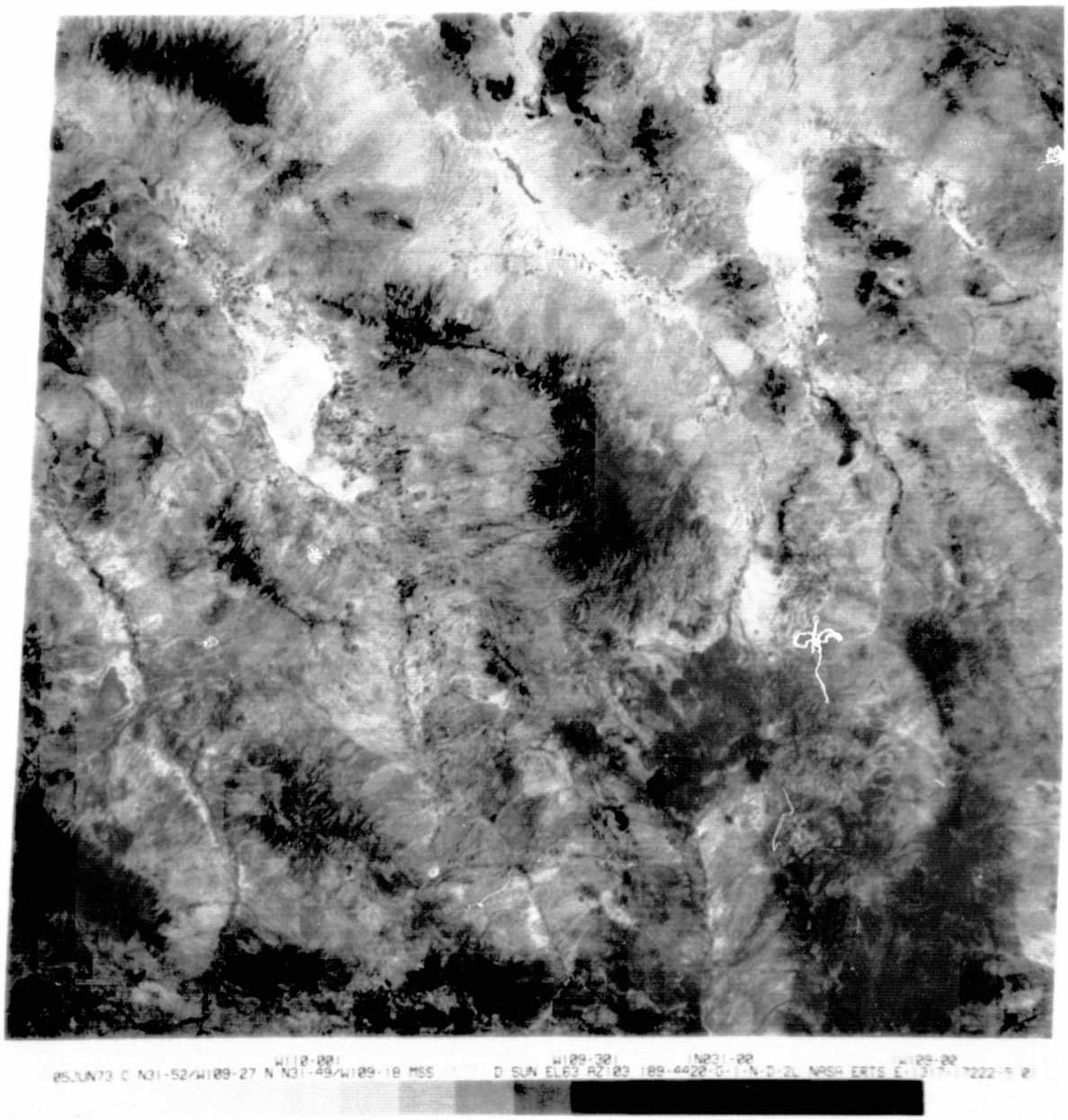


Figure 58 . ERTS image produced using optimum reprocessing of black-and-white positive images.

gamma 3.0 positives. The two basic types of geologic information for which the image was examined were: (1) the detection of structural lineations, and (2) the discrimination of lithologic units.

Geologic, vegetation, and soil maps were visually compared with the ERTS image for any possible correlations. Basaltic rock units which were recorded on the state geologic map of Arizona showed up clearly on ERTS-1 additive color images. The intricate geology in the mountain ranges was not readily detectable. The most recent fluvial deposits which were not recorded on the state geologic map were imaged and easily seen on ERTS-1.

A portion of the ERTS-1 image was enlarged and visually compared with a large scale USGS geologic map. Contacts between general bedrock and alluvium, and between limestone and siltstone formations were observable on this enlargement. No faults and other lithologic contacts, present in the study area, were able to be detected from the enlargement.

Objectives of the Geologic Investigation

The purpose was to determine what useful geological information could be extracted from the additive color rendition of ERTS-1 frame number E-1317-17222. The two basic types of geological information for which the image was examined were: (1) the detection of structural lineations (faults, fractures, etc.), and (2) the discrimination of lithologic units. Due to the scale and resolution inherent in ERTS-1 imagery, lithological discrimination was to be solely based upon color differences on the image and not upon other parameters such as texture, topographic expression, and drainage patterns which commonly are used in aerial photographic interpretation.

This geologic information can be put into two separate categories: first, information which has already been recorded on existing sources, i.e. geologic maps; and second, information which has not been recorded either because this information was undetected, or it came into existence subsequent to the published sources.

Procedure:

To see how much of the previously recorded information could be detected on the image, visual comparison was made between the image and various published maps. If there appeared to be a significant amount of information common to both data, the information contained on the published map was drawn on a clear vinyl overlay which was then placed over the ERTS image for a more detailed visual analysis. The additional information which was on the image but not on the geological maps was drawn on separate overlays. The information on these overlays was then compared to non-geological data, such as, soil and vegetation maps.

Sources Used:

The main source of geological information used in this study was the 1969 state geological map of Arizona published by the Arizona Bureau of Mines and the U.S. Geological Survey. It would have been most desirable to have compared the images with more-detailed geologic maps having a larger scale. Unfortunately, virtually no U.S. Geologic Quadrangle Maps exist for this area. There were a few USGS Miscellaneous Geological Investigation Maps in this area but these were poor quality and contained only geologically monotonous areas. The one exception was a USGS M.G.I. Map of the southern portion of the Mule Mountains. Correlations between this map and ERTS images are discussed in detail.

One coincidental advantage in using the state geologic map was that visual comparison with the ERTS image was facilitated because both items were at the same scale of 1:500,000.

Non-geological sources included a small scale, very generalized vegetation map of the state of Arizona published by the University of Arizona, several soil maps which were included in the Soil Survey of the Sulphur Spring Valley Area, 1954, and the General Soil Map of Cochise County, Arizona, published by the Soil Conservation Service in 1971.

Discussion of Correlations and other findings in ERTS-1 Frame Number E-1317-17222

Since there seemed to be some correlation between the additive color image and the state geologic map, all the lithologic and structural information contained on the map was transferred to an overlay which was then placed over the image; this is shown in Figure 59. The most noticeable of these correlations was the delineation of the two major basaltic occurences in the area. These volcanic rock units can be clearly distinguished as having a darker visual signature than the surrounding areas. Even the small outlines of these units can be easily seen.

It was found that a large percent of the intricate geology in the mountain ranges cannot be detected from the image. The most obvious reason for this is that most areas in the ranges are heavily obscured by vegetation. However, on close examination, some lithologic contacts in the ranges were detectable. For example, the major contact between the granite and the schist (Tkg and PCsc, respectively on the geologic overlay) in the Little Dragoon Mountains, could be observed on the image. No faults could be detected in the ranges.

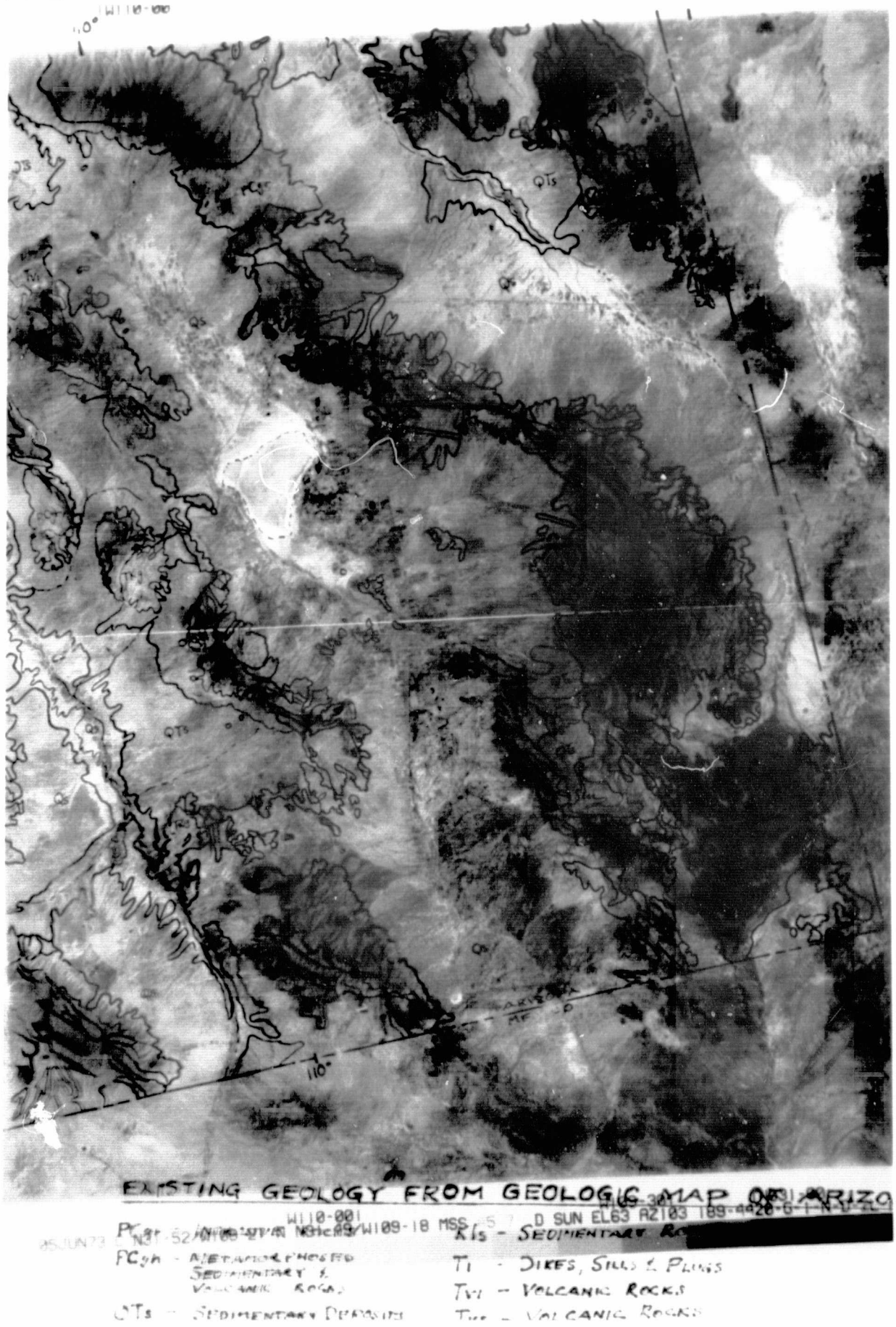


Figure 59. ERTS-1 images of south eastern Arizona on which is superimposed an overlay of known geology from existing geologic maps.

ORIGINAL PAGE IS
OF POOR QUALITY

Among the additional information contained on the image but not on the geologic state map of Arizona were the various color subdivisions of the basins (Figure 60). These different colors could not be checked for the possible correlation with different alluvial types because the alluvial deposits on the state geologic map were so greatly generalized that any such correlation was impossible to make. The vegetation and soil maps were also examined for possible correlations. The vegetation map was too generalized and the soil maps were too-large-scaled and detailed for the resolution of the image to be of any use. No correlations were made with these materials. It is still not known what the different colors in the basins, which appear in the ERTS-1 image, represent.

Other features imaged but not appearing in the state geologic map are the most recent fluvial deposits or alluvium. These recent deposits have a white visual signature on the additive color image. In this ERTS frame, they can be seen along the San Simon River, San Pedro River and around the Willcox Playa in Arizona.

These locations of the most recent fluvial deposits can be easily explained. During pluvial periods (times when the area's climate was more humid than today) stream water was high and deposits were laid down along the major drainage lines. Also, during these wet times, the Willcox Playa was a fresh water lake with several streams flowing into it. As these streams entered the standing lake water, they lost some velocity and had to deposit their load. Thus, fluvial deposits became concentrated around the perimeter of the Willcox Playa. During interfluvial periods, such as the present, the lake water dries up and evaporates (gypsum, rock salt, etc.) are precipitated and deposited in the center of the playa.



Figure 60. Additional geologic information contained in ERTS-1 image but not appearing on state geologic maps.

ORIGINAL PAGE IS
OF POOR QUALITY

Discussion of Correlations and Other Findings in the Mule Mountains:

As previously mentioned, Geologic Quadrangle Maps and Miscellaneous Geologic Investigation Maps were almost totally non-existent for this area. The one exception was the Miscellaneous Geologic Investigation Map No. 418, Geologic Map of the Southern Part of the Mule Mountains, by Hayes and Landis, published in 1964.

Due to the availability of this map, a detailed visual comparison of this map with the ERTS imagery was performed. To aid this analysis: first, the portion of the ERTS image which corresponded to the mapped area was enlarged to the approximate scale of 1:125,000; then, all the lithological information was drawn onto an overlay. (Faults were not included for the purpose of keeping the overlay uncluttered.) This overlay was photographically reduced to the same scale as the enlargement and subsequently placed over the enlargement for comparison.

Again, the two types of geologic information which were intended to be extracted from the images were the discrimination of lithologic units based on color differences in the image and the detection of structural lineations (faults, fractures, etc.).

Lithologic discrimination of this area was greatly limited to the observable contacts between the alluvium and the general bedrocks of the Mule Mountains. This alluvium/bedrock contact is clearly visible along the total eastern side of the Mule Mountains (see (1) on the overlay), and also in the area SE of the major tailings pond, (2) on the overlay. Only in one place is the contact between the valley fill and the pediment gravels (Qts and Qg on the geologic map, respectively) observable. This area is east of the San Pedro River where the Greenbush Draw joins it (3) on the overlay). However, going away from this

ORIGINAL PAGE IS
OF POOR QUALITY

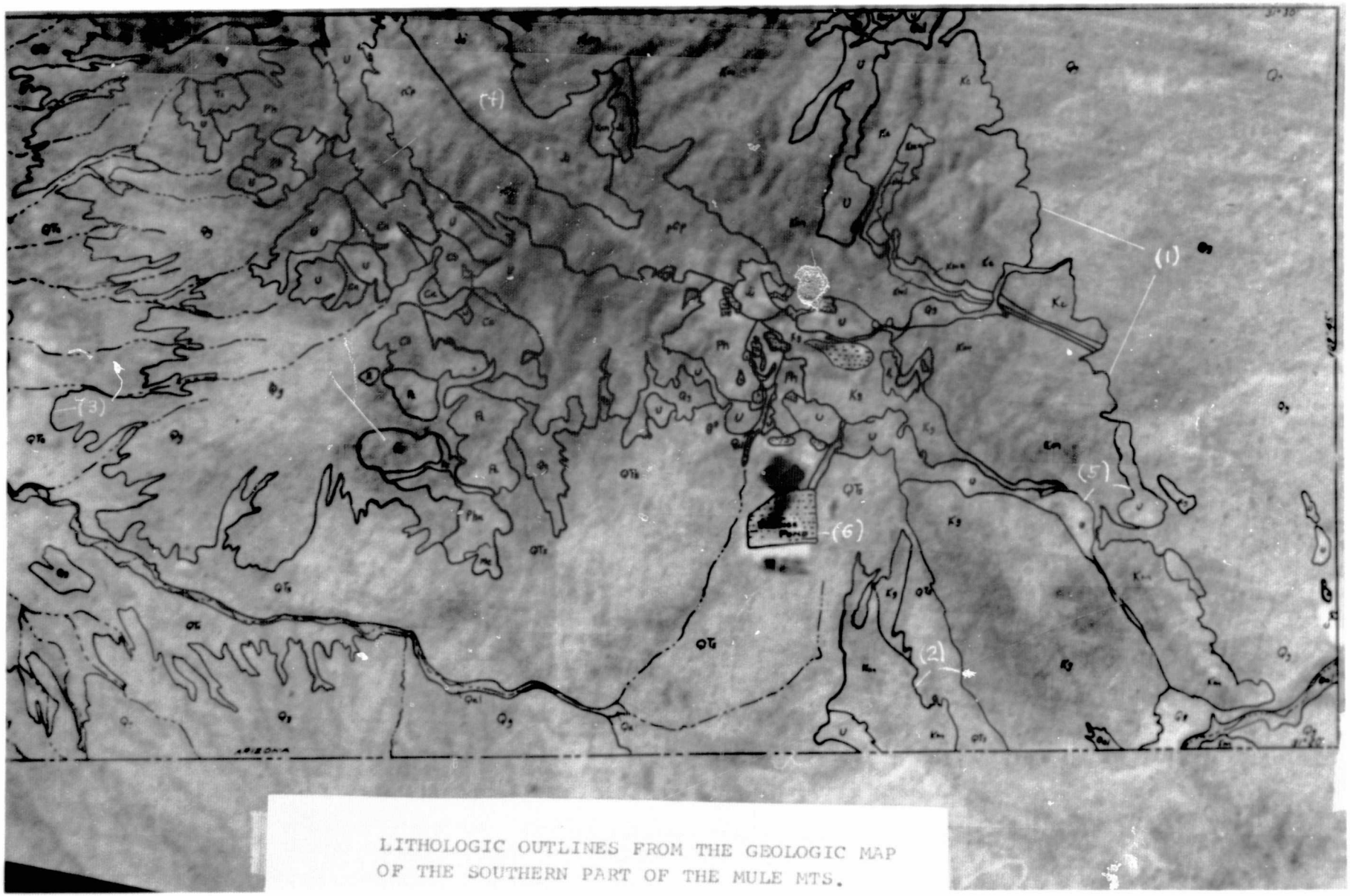


Figure 61. Lithologic outlines for the Geologic map of the Southern Part of the Mule Mountains, Arizona, superimposed on an enlargement of ERTS additive color rendition of that area.

area, the contact becomes completely unobservable.

The Juniper Granite (Ji on the geologic map) can be seen on the enlargement (4) but this is because of the growth of the vegetation around, but not on, this lithologic unit. The outline of the Juniper Granite also can be clearly traced on the 1958 Bisbee 15' topographic quadrangle due to this same preferred growth of the vegetation. At two separate locations in the southeastern portions of the Mule Mountains, contacts between limestone (5) and siltstone formations are visible as color differences on the ERTS imagery, the limestone being whiter than the siltstone.

No other bedrock contact or faults and fractures could be detected on the enlargement. One possible reason for this might be that vegetation covers the areas where most of these contacts and faults occur, i.e. the center of the Mule Mountains.

The most prominent feature seen on the enlargement is the tailing pond (6) and the smaller ore dumps and other mining waste sights, located just southwest of Bisbee. In every case, these waste sights appear to be larger on the image then on the geological map. This discrepancy could have different explanations. These waste sights may have been expanded since the geologic map was published in 1964. This would demonstrate ERTS imagery as an effective tool for updating geologic maps. The only other explanation is that the image is not just showing the area which is physically occupied by the waste sights, but is showing the total area which is affected by these features: (Areas where vegetation may have been killed by adverse fumes or by acid seepage into the groundwater). In this case, ERTS imagery would be an effective source of data for environmental impact studies of mining dumps.

The enlarging of the ERTS image aided to some degree the interpretability of such. The alluvium/bedrock contact SE of the tailing pond, (2) on the overlay, was not detected on the original image. However, the enlargement did not improve the detection of many faults and other lithologic contacts present in the Mule Mountains.

Conclusions and Recommendations:

Except for the basaltic lava flows, no one lithologic unit could be completely mapped from the ERTS frame E-1317-17222. This lack of ability to discriminate between different rock types may be attributed to the facts that: (1) the mountain ranges, which contain practically all of the outcrops of the area, were heavily covered by vegetation, and (2) the bedrock in the basins was covered by thick accumulations of alluvium. Furthermore, the possible correlation between different types of alluviums and different colors on the image was made impossible by the lack of good supporting materials. It is therefore suggested that, if future studies of this nature are to be conducted, an area should be chosen in which there is a minimum of vegetation and superficial deposits covering the actual rock outcrops, and where there has been a considerable amount of detailed geologic mapping. The latter would assure the availability of ample amounts of good supporting materials which, in turn, would reduce the need for field checks. Also aerial photographic interpretation of the area may be used in place of field checks.

Section 6

CONCLUSIONS

Image Characteristics Related to Reflectance Spectra

The image density in the ERTS-I release positives was found to be indicative of the percent reflectance of the Willcox Playa, Arizona. Percent reflectance data of the twelve sampling stations within the Playa were averaged and compared to the mean value of 250,000 digital brightness measurements of the Playa obtained from ERTS-I release positives. These data are shown in Table 16 below.

Band	In Situ Spectra			ERTS Image Brightness	
	Incident $\mu w/cm^2/nm$	Percent Reflectance	Reflected $\mu w/cm^2/nm/sr$	$\bar{x}$	s
500-600	79	32	25	124.9	41.2
600-700	72	38	27	155.4	45.0
700-800	60	40	24	156.1	44.4
800-1100	35	42	15	152.8	34.0

Table 16. In situ spectral reflectance measurements and corresponding ERTS-I image density measurements.

These data were normalized with respect to average values at 950nm. The average digital brightness measurements were normalized to Band 7 and the average percent in situ spectral reflectance data normalized to 950nm. The results are plotted in Figure 62.

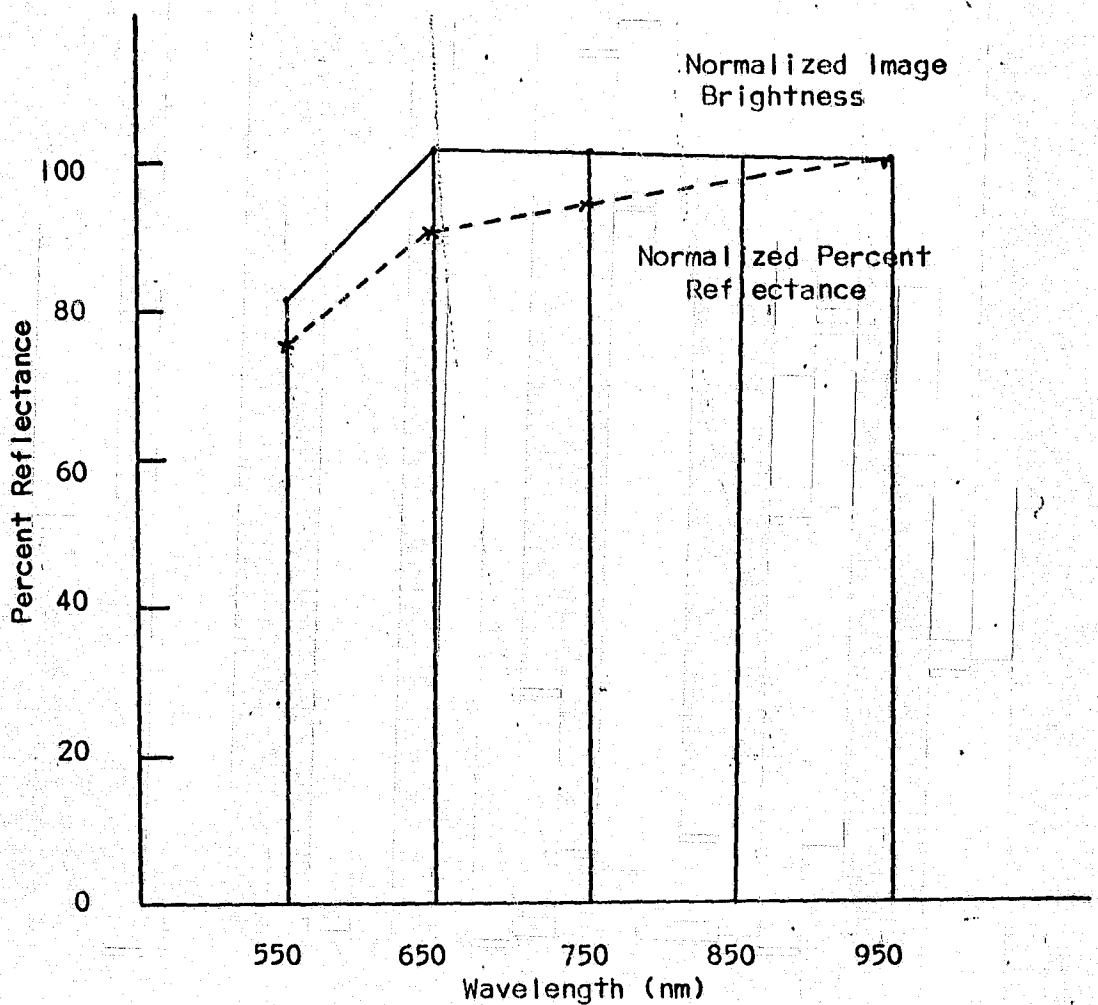


Figure 62. Comparison of in situ spectral reflectance measurements normalized to 950nm and ERTS-1 image brightness data normalized to Band 7.

While normalized ERTS-1 image brightness is related to spectral reflectance measurements normalized with respect to 950nm, calculated radiance values (viz. incident irradiance times percent reflectance) showed little correlation as can be seen from the above table which is probably due to the effects of the intervening atmosphere.

A comparison of the spectral reflectance data obtained at the Prescott National Forest and the in situ percent reflectance of Pinion Pine, Juniper and Manzanita showed no relationship whatever even though these species completely cover the ground in most of the Copper Basin Area of the National Forest.

Analysis of the ERTS-1 Image Brightness

Statistical analysis of 294,912 digitized pixels of ERTS-1 positive images showed that:

- the Willcox Playa is darker in Band 4 than any of the other ERTS-1 bands.
- the brightness of the Willcox Playa is approximately the same in Bands 5, 6 and 7.
- the variability of the brightness data is less in Band 7 than in any of the other ERTS-1 bands.
- the frequency distribution of brightness has two modes (peaks) in Bands 4 and 5 which are absent from Bands 6 and 7.

Statistical analysis of multidata ERTS-1 negatives and positives showed variations in the spectral reflectance of the imagery of the Willcox Playa between spectral bands and in the same spectral band on different dates. As is discussed below, this difference in image brightness between dates was due to standing water.

A statistical analysis of the difference in mean digital brightness measurements of cloud tops and shadows showed that the image contrast in each band increased as a percentage of Band 7 as follows:

$$\frac{\text{Band 4}}{\text{Band 7}} \times 100 = 74\%$$

$$\frac{\text{Band 5}}{\text{Band 7}} \times 100 = 79\%$$

$$\frac{\text{Band 6}}{\text{Band 7}} \times 100 = 88\%$$

The digital brightness of ERTS-1 images of the Prescott National Forest is not in any way related to the spectra of tree species growing there. It was not possible to differentiate Manzanita, Juniper and Pinion Pine.

Statistical analysis of digitized ERTS-1 negatives showed that the mean brightness difference between images of terrain in sunlight and in shadow expressed as a percent of that difference in Band 7 is:

$$\frac{\text{Band 4}}{\text{Band 7}} \times 100 = 34\%$$

$$\frac{\text{Band 5}}{\text{Band 7}} \times 100 = 60\%$$

$$\frac{\text{Band 6}}{\text{Band 7}} \times 100 = 76\%$$

It was also shown that these differences increased with decreasing relative brightness. A nomograph to correct for atmospheric conditions was derived using cloud tops, shadows and adjacent illuminated terrain areas. (Figure 54 on Page 85).

Additive Color Presentation and Analysis of ERTS Multidate Images

The dynamics of spectral reflectance changes over time were shown to be capable of presentation on an additive color viewer. The purpose was to establish if differences in standing water in the Willcox Playa could be detected in ERTS-1 imagery taken on different dates.

ERTS-1 images of the Willcox Playa acquired on September 27, October 14 and November 2, 1972 were used. The image of the Playa was located in different positives of the frame for each date so that only the intersection of the three images could be combined in color. Reprocessed positives were made from the NASA release negatives. The September 27 Band 5 was projected as blue, the October 17 Band 5 as green and the November 2 Band 5 as red. A copy of the recombined image is shown in Figure 63.

Ordinarily, the colors in a multispectral display are indicative of reflectance differences which exist as a function of wavelength. However, the vivid color differences which are seen in the multidate ERTS image on the next page, represent reflectance changes in the

ORIGINAL PAGE IS
OF POOR QUALITY

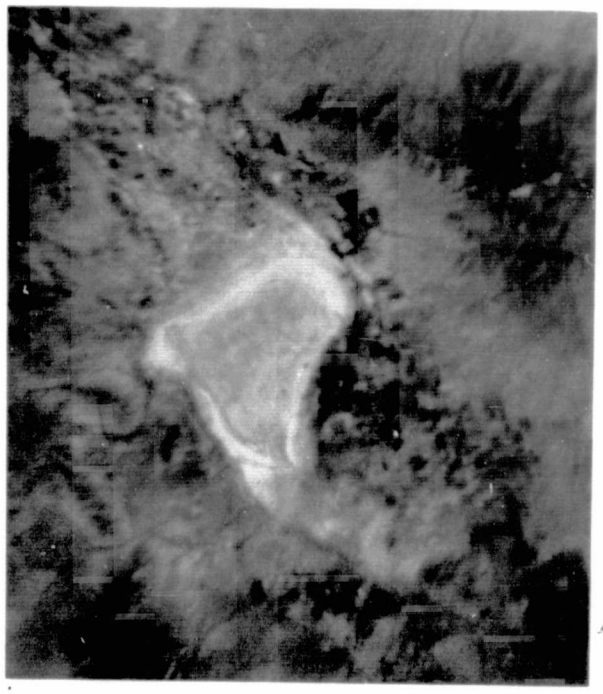


Figure 63. Multidate additive color image of the Willcox Playa showing changes in standing water.

600-700nm spectral band as a function of time. The colors within and surrounding the Playa are interpreted as follows:

- A colorless shade of white or grey indicates absence of any standing water between 27 September and 2 November 1972.
- Yellow indicates areas where a decrease in standing water occurred between 27 September and 14 October and little change from 14 October to 2 November.
- Orange also indicates a decrease in the amount of standing water between 27 September and 14 October, coupled with a reduced rate of decrease to 2 November.

- Cyan are areas where standing water changed little between 27 September and 14 October, then increased greatly by 2 November.
- Red indicates areas where surface water did not change between 27 September and 14 October, then decreased between 14 October and 2 November.
- Green indicates a reduction in surface water from 27 September to 14 October and an increase between 14 October and 2 November.
- Blue indicates the opposite effect from those areas that appear yellow; i.e., the amount of surface water increases between 27 September and 14 October with no change between 14 October and 2 November.

These procedures for using additive color analysis of multidate ERTS images developed under this study was the interpretation technique used to map standing water during the 1973 Mississippi Flood. A summary report of this flood mapping project using multidate ERTS imagery appears in Appendix G .

Section 7

New Technology

The research reported herein involves the multispectral analysis of ERTS scanner data.

The significant theories and the description of the interpretation techniques used have been given in Sections 2, 4, and 5 of this report.

APPENDIX A

"SYSTEM 800"

DESCRIPTIVE LITERATURE

A typical System 800 interactive display system using the Model 805 Color Display combined with the Model 810 Digital Processor is shown on the opposite page.

COLOR DISPLAY

The large screen color picture display is constantly refreshed at 60 fields per second from the refresh store and is constructed from a rectangular array of 512 by 512 picture elements. Each element, under individual program control, may be displayed in 32 colors, in a 32 level grey scale, in black, or in white.

COLOR KEYBOARD

The push-button keyboard in front of the display provides operator control of the picture elements according to their value. Thirty-two columns of keys, one column for each color or grey-scale value, change the display of all picture elements of a particular value from color to grey scale or to black.

In addition, under keyboard control, one or more equal-value sets of elements may be combined to reduce the number of colors or grey shades in the display.

Thus, the Color Keyboard speeds the analysis of displayed data by providing immediate operator control over the number of colors and grey-scale contrast.

DIGITAL PROCESSOR

The Processor and Magnetic Tape Units are supplied to meet the needs of specific applications or the Model 805 may be supplied alone with the proper interface for the customer's processor.

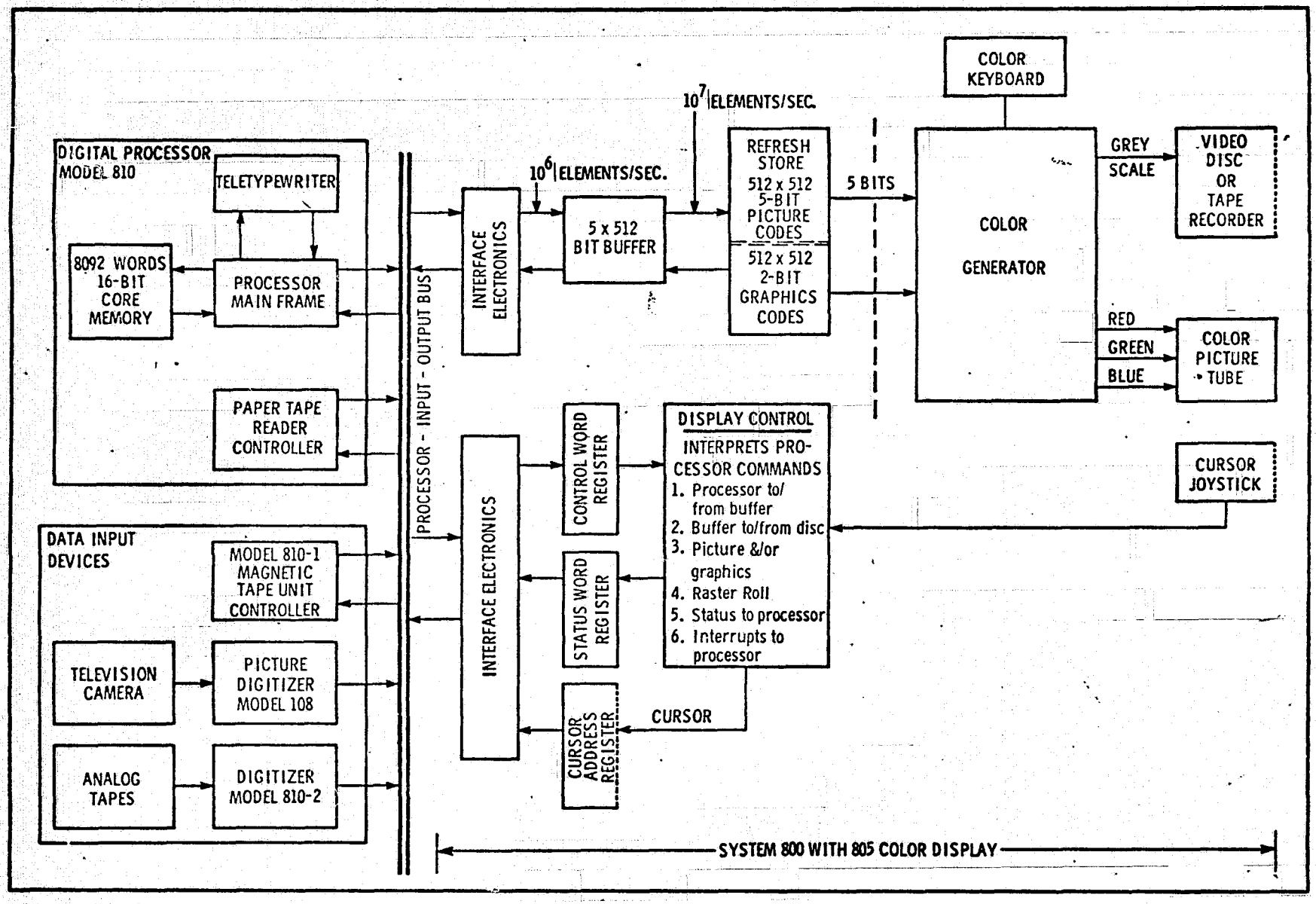
Operator control is provided through the Teletypewriter keyboard and results and programs are listed on the teleprinter. Program entry is rapid and convenient using the high-speed Photoelectric Tape Reader.

REFRESH STORE

The refresh store contains the 262,144 picture elements and continuously transmits them to the display at a peak rate of 10 million per second. At the request of the Processor program, the picture elements are transferred directly to or from core storage in blocks of 512 picture elements (one horizontal line). The transfers take place over the Processor input-output channel in a similar manner as other input-output devices, the magnetic and paper tape readers.

OPERATING SPEED

When operated with the System 800 Digital Processor, the entire 805 Display may be changed in less than eight seconds, new picture data may be added at the top or bottom and the picture moved up or down 60 horizontal lines per second, or the Display may be changed from a positive to a negative, from color to grey scale, or from picture to graphics only, in 1/30 second. The average access time for 512 elements is 1/60 second.


DIGITAL PROCESSOR MODEL 810
TELETYPEWRITER
8092 WORDS 16-BIT CORE MEMORY
PROCESSOR MAIN FRAME
PAPER TAPE READER CONTROLLER
DATA INPUT DEVICES
MODEL 810-1 MAGNETIC TAPE UNIT CONTROLLER
TELEVISION CAMERA
PICTURE DIGITIZER MODEL 108
ANALOG TAPES
DIGITIZER MODEL 810-2
PROCESSOR - INPUT - OUTPUT BUS
INTERFACE ELECTRONICS
INTERFACE ELECTRONICS
10^6 ELEMENTS/SEC.
5 x 512 BIT BUFFER
10^7 ELEMENTS/SEC.
REFRESH STORE 512 x 512 5-BIT PICTURE CODES
512 x 512 2-BIT GRAPHICS CODES
5 BITS
CONTROL WORD REGISTER
STATUS WORD REGISTER
CURSOR ADDRESS REGISTER
DISPLAY CONTROL
INTERPRETS PROCESSOR COMMANDS
1. Processor to/from buffer
2. Buffer to/from disc
3. Picture &/or graphics
4. Raster Roll
5. Status to processor
6. Interrupts to processor
CURSOR
COLOR KEYBOARD
COLOR GENERATOR
GREY SCALE
VIDEO DISC OR TAPE RECORDER
RED
GREEN
BLUE
COLOR PICTURE TUBE
CURSOR JOYSTICK
SYSTEM 800 WITH 805 COLOR DISPLAY

191 A3

SYSTEM OPERATION

The block diagram on the opposite page shows the major components of the complete Color Display System. The Model 805 Display is shown to the right of the input-output (I/O) bus of the Model 810 Processor.

The high resolution color picture refreshed at standard television rates is constructed from a rectangular array of 512x512 picture elements. Each picture element is specified by a 5-bit picture code and a 2-bit graphics code. The 32 picture values and the four graphics values are individually controlled from the processor to provide a wide variety of displays.

Two data paths are shown to the 805: one through the upper interface electronics to the Refresh Store for transfer of the picture and graphics codes, and one through the lower interface electronics to the Display Control for transfer of control words, status words, and cursor address.

The digital-to-analog converters in the Color Generator convert, under control of the Color Keyboard, the picture and graphic codes, which are continuously being circulated in the Refresh Store, to red, green, and blue video signals for the Color Picture Tube. According to the four possible values of the graphics code, the 32 possible values produce, for each picture element, either one of 32 colors, or one of 32 grey shades, or black, or white. The picture and graphics codes are separately accessed through the Buffer Store so that they may be modified independently.

DIGITAL PROCESSOR

The Model 810 Digital Processor and Model 810-1 Magnetic Tape Unit are designed to operate with the Model 805 Display as a stand-alone system for the analysis of picture information. The system can perform data editing and formatting, data analysis, and the production of graphics. Data is normally first entered by the 810-1 Magnetic Tape Unit. This data may have originally been digitized from a sensor (such as a thermal, radar, or sonar scanner) or may have been generated by a large-scale digital computer or the Model 810 itself.

The data on the magnetic tape is read, a block at a time, into the processor core storage, and, if not already formatted in a 512x512x5-bit matrix, is converted to 512x5-bit blocks of horizontal rows of picture elements for output to the Display. The data is transferred to the Buffer Store and then to the picture code section of the Refresh Store. The latter transfer takes place by a software-controlled output to the 805 control of a control word which contains the address of the line in the Refresh Store.

The transfer from the Buffer Store is made to one of the 512 horizontal rows of the Refresh Store specified by the control word placed in the Display Control by a programmed transfer.

The graphics codes, 2 bits for each picture element, are transferred to the Display in the same way as the picture data. Areas may thus be shown in grey-scale or color depending on parameters calculated by the Processor.

REFRESH STORE AND BUFFER

The picture and graphics are stored digitally in the Refresh Store. The horizontal lines, each containing 512 picture elements, are circulated, even lines followed by odd lines, so that they may be continuously read in synchronism with the standard interlaced scanning pattern of the color picture display. Successive lines (Y addresses) are read every 1/60 second.

The Refresh Store is addressed by line (Y) address from the control word and, at the proper time, the complete line of 512 picture elements is transferred to/from the Buffer Store. The Buffer Store then transfers to/from the Processor core using a high speed block transfer.

The Buffer Store may be used for transfer of picture or graphics data as specified by the control word sent to the Display Control.

COLOR GENERATION

The 5-bit picture codes and 2-bit graphic codes are read continuously from the Refresh Store. The Color Generator using special digital-to-analog matrix conversion circuits produces red, green, and blue color video signals to drive the three electron guns of the Color Picture Tube. Colors are produced by generating proper proportions of the red, green, and blue primaries on the screen. The color produced for each picture element is controlled by the 2-bit graphic codes as follows:

Binary 00: One of the 32 standard colors is assigned according to the 5-bit picture code (color picture).

Binary 01: White is generated regardless of picture code values (white graphics).

Binary 10: Black is generated regardless of picture code values (black graphics).

Binary 11: One of 32 shades of grey ranging from black to white are assigned according to the 5-bit picture code (B/W picture).

Thus, the graphic code determines the type of display for each element.

COLOR KEYBOARD

In addition to the software control of the display the colors are also under control of the Color Keyboard. Four interlocking push-keys are provided for each of the 32 colors and control the display of each color as follows:

1) Normal: Normal Operation, the picture-elements of this value are displayed on the screen as determined by the picture and graphics codes.
2) Black: Every picture-element of this value is now displayed in black.
3) B/W: Every picture element of this value is displayed in grey scale.
4) OUT: Every picture element of this value is displayed in the same mode as next higher order value. For example, the OUT key of value 10 displays value 11 in place of value 10 so that 10 and 11 are now the same color or grey level.

The black and B/W keys perform the same functions as the graphic codes on all elements of the same value or color and are a great help to the operator for recognizing particular colors and features.

The OUT keys eliminate colors so that the complexity of the color display may be reduced quickly without need for the processor to rewrite the picture data.

SYSTEM CONTROL

The system control accepts a control word from the Processor and supplies a status word to the Processor. When the cursor and joystick option is provided, a two-word X-Y address is also supplied to the Processor indicating the position of the cursor.

Program control of all picture elements simultaneously by a single 16-bit control word produces an all color display, an all grey scale display, graphics only, a complemented (negative) grey scale display, and roll up or roll down of entire picture. The latter command provides a rolling raster for display of continuous strip pictures.

The control word consists of an operation code and a line (Y) address. Only the Buffer to Refresh Store transfers require a line address. Specified bits in the operation code determine whether:

1) elements are displayed as specified by the graphics codes as described above.
2) all elements are displayed as specified by the graphics codes except color elements are displayed in grey scale.
3) all elements are displayed in color (without graphics control).
4) all elements are displayed in grey scale (without graphics control).
5) the graphics black and white elements only are displayed (without picture data).
6) any of the above are displayed with the picture data complemented.

These control functions require only one I/O instruction for operation and immediately switch the display from color, graphics, to grey scale under program control. Thus, the program may present ten types of information display to the operator without reloading the picture store.

In addition to the above operations, the operation code includes roll-up and roll-down. These operations immediately move the displayed picture up or down two horizontal lines. Continuous movement of the picture may be performed by writing new data at the top or bottom of the picture before each roll command. In this way new picture information can continuously replace the old, producing the effect of a continuous roll.

The status word provides the Processor program with updated information on the display status. An interrupt is given to the Processor at the completion of each operation that requires more than one Processor instruction time to complete, such as a buffer-disc transfer.

SOFTWARE

The Model 805 Display is provided with software on punched paper tape for operation with the Model 810 or customer's Processor. Included with the software package are:

1) Diagnostics for the Processor, core memory, and display system
2) Machine language assembler
3) Basic compiler
4) Load and Utility routines
5) Debug Program
6) Math Functions

The Processor is supplied with a software library including display diagnostic routines for checking the operation of the processor and display unit. User programs may be entered originally, edited, and assembled using the teletype keyboard. Programs are stored on paper tape and quickly loaded using the high-speed photoelectric tape reader. Operational activities are controlled through the teletypewriter keyboard and the Processor front-panel switch register.

SPECIFICATIONS

DISPLAY

TYPE: 19" Shadow Mask Picture Tube, 670x500 color-dot trios.

COLOR DISPLAY: Number of Colors - Selectable 1 thru 32.

Color Assignment - Any one of 32 colors assigned to any picture value. The colors are four shades of Yellow, Cyan, Green, Orange, Magenta, Violet, Red, and Blue. Colors are controlled by graphics data and keyboard to produce black, white, or monochrome.

MONOCHROME DISPLAY: Number of Grey Levels - 32. Monochrome superimposed on color under keyboard and program control.

GRAPHICS DISPLAY: Graphics displayed in black or white. Graphics display under program control.

RESOLUTION: 512x512 raster points stored, 512x489 displayed.

GEOMETRIC DISTORTION: Less than 2% overall.

SIZE: 16x12 (4/3 aspect ratio), 12x12 (1/1 aspect ratio).

REFRESH RATE: Standard 525-line television interlaced 2:1, 60 fields/sec., 30 frames/second.

DISPLAY KEYBOARD: 4x32 pushbuttons for selection of color, black, B/W, and Out.

COLOR PATCH PLUG: 64 pin plug for change in color order. Prewired plugs for normal and reverse order supplied.

CURSOR: Joystick control of cursor position. Activate switch. Maximum interrogation rate 30 times/second.

MODEL 810 DIGITAL PROCESSOR

CORE STORAGE: 8192 16-bit words.

NUMBER OF REGISTERS: 8

INSTRUCTION SET: Over 400 hardware instructions.

SPEED: Memory Cycle - 1.2 microseconds. Add/Subtract - 5.2 microseconds.

PERIPHERAL EQUIPMENT: Teletypewriter ASR 33, Photoelectric Paper Tape Reader (300 chars/second), Model 810-1 Magnetic Tape Unit - 9 track, IBM compatible, 800 bpi, 37½ ips, 10½" reels.

SOFTWARE: Diagnostics, Math Functions, Assemblers, BASIC, Debug.

POWER AND PHYSICAL

SYSTEM POWER REQUIREMENTS: 105/125 volts, 60 Hz, 20 amp circuit.

ENVIRONMENT: +15° to +30°C, 10% to 90% Humidity.

107 A7

APPENDIX B

"SYSTEM 800"

COMPUTER PRINTOUTS

WILLCOX, ARIZONA

SPECTRAL ANALYSIS

800 SYSTEM COMPUTER
PRINTOUT #8

(1)

SPECTRAL ANALYSIS
WILLCOX, ARIZONA

ERTS-1 POSITIVE IMAGES OF
WILLCOX PLAYA AND SURROUNDING
AREA; 4 SEPTEMBER 1973;
LOG DIGITIZATION

```
ERUN MARKER

 $RUN MARKER
**********************
$RUN DIGIT
#P0

#RUN DISPLY




$


 RUN DISPLY
#P0

$RUN DIGIT
#P0
```

READY!

```
$RUN DISPLY
#P0

$RUN HISTOR
```

ERTS-1 BAND 4
4 SEPT. 1973
WILLCOX, ARIZONA

```
SCAN
```

BAND 4 PERCENT AREA

107 B1

```
$RUN AREA
COLOR:      0        1        2        3        4        5        6        7
GRAY:     022      061      096      129      159      193      224      255
```

PERCENT: 04.32 04.10 10.02 20.30 31.10 18.20 01.04 00.00

#RUN DIGIT

(2)

P1

$RUN DISPLY
#P1

#RUN DIGIT

$RUN DISPLY
#P0

#RUN DIGIT

^C

RUN MARKER

ERTS-1 BAND 7
4 SEPT. 1973
WILLCOX ARIZONA

#RUN DIGIT

#RUN DISPLY

$RUN HISTOR
SCAN

$RUN MARKER
$RUN HISTOR
SCAN

$RUN MARKER
$RUN HISTOR
SCAN

$RUN AREA
COLOR: 0 1 2 3 4 5 6 7
GRAY: 032 064 096 128 160 192 224 255
PERCENT: 06.28 00.76 01.80 08.70 33.64 42.08 06.38 00.28

omit
(PUT IN FILE

$

101 B2

APPENDIX C

"SYSTEM 800"

COMPUTER PRINTOUTS

WILLCOX, ARIZONA

TEMPORAL ANALYSIS

DOS/BATCH V9-20C
DATE: 21-SEP-74
TIME:09:30

800 SYSTEM COMPUTER PRINTOUT # 8 (CONT.)

BASIC-08 V1-20P-74
TIME:-19:30:14
$

TEMPORAL ANALYSIS
WILLCOX ARIZONA

#RUN DISPLY
#RUN DISPLY
#RUNPROGER

#RUN DISPLY

ERTS-1 POSITIVE IMAGES OF WILLCOX PLAYA [ENLARGED]; BAND 4 ON FOUR DIFFERENT DATES.

$RUN MARKER
$RUN AREA

BAND 4, 4SEPT. 1973 PERCENT AREA

COLOR:	0	1	2	3	4	5	6	7
GRAY:	032	064	096	128	160	192	224	255
PERCENT:	03.12	01.98	04.30	10.04	26.30	35.76	17.62	00.76

$

ERTS-1 BAND 4
4SEPT. 1973
WILLCOX ARIZONA

RUN DIGIT
#P0

#RUN DISPLY

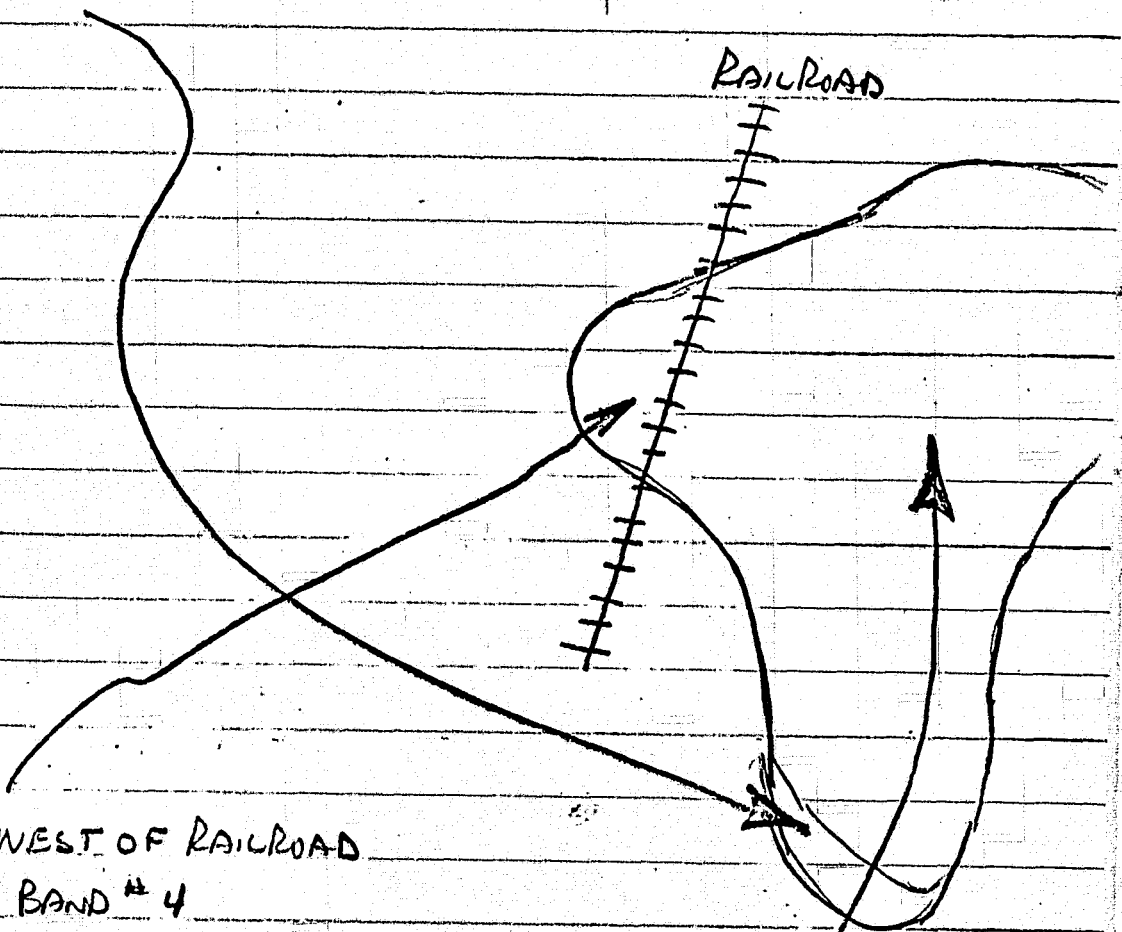
101 C1

#RUN HISTOR

SCAN

Z=225 AT (291, 442)
Z=225 AT (287, 434)
Z=222 AT (277, 432)
Z=224 AT (290, 428)
Z=226 AT (291, 442)

SOUTH END OF PLAYA
BAND #4
4 SEPT. 1973



Z=174 AT (207, 274)
Z=175 AT (210, 266)
Z=176 AT (210, 256)
Z=178 AT (214, 248)
Z=180 AT (217, 238)

WEST OF RAILROAD
BAND #4
4 SEPT. 1973

Z=164 AT (259, 224)
Z=165 AT (287, 218)
Z=159 AT (325, 200)
Z=165 AT (332, 238)
Z=178 AT (331, 284)
Z=191 AT (322, 324)
Z=184 AT (294, 346)
Z=177 AT (265, 314)
Z=182 AT (248, 290)
Z=181 AT (251, 252)

AT RANDOM IN PLAYA
BAND #4
4 SEPT. 1973

```
$RUN MARKER
ERDR3HBSTOR07,252)
```

ERTS-1 BAND 4
18 MAY 1973
WILLCOX ARIZONA.

```
$RUN HISTOR
SCAN
Z=229 AT (292,438)
Z=228 AT (279,424)
Z=233 AT (306,434)
Z=229 AT (292,442)
Z=224 AT (286,422)
```

SOUTH END OF PLAYA
BAND #4
18MAY 1973

```
Z=160 AT (204,278)
Z=157 AT (204,272)
Z=159 AT (207,260)
Z=152 AT (211,246)
Z=162 AT (211,236)
```

WEST OF RAILROAD
BAND #4
18 MAY 1973

ORIGINAL PAGE IS
OF POOR QUALITY

```
Z=163 AT (234,280)
Z=191 AT (241,252)
Z=158 AT (267,218)
Z=159 AT (297,216)
Z=161 AT (317,228)
Z=173 AT (324,260)
Z=181 AT (312,296)
Z=175 AT (293,346)
Z=153 AT (257,310)
```

AT RANDOM
IN PLAYA
BAND #4
18 MAY 1973

BAND #4, 18 MAY 1973, PERCENT AREA.

```
$RUN AREA
COLOR:      0       1       2       3       4       5       6       7
GRAY:     032     064     096     128     160     192     224     255
PERCENT: 05.50   05.92   21.84   30.04   19.70   14.72   01.98   00.22

$
```

ERTS-1 BAND 4
1 NOV. 1972
WILLCOX ARIZONA

```
#RUN DIGIT

#RUN DISPLY

$RUN MARKER
$RUN HISTOR
SCAN
Z=242 AT (291,442)
Z=238 AT (301,444)
Z=230 AT (284,450)
Z=236 AT (285,438)
Z=240 AT (296,446)
```

SOUTH END OF PLAYA BAND #4 1 NOV. 1972

ORIGINAL PAGE IS OF POOR QUALITY

```
Z=217 AT (203,288)
Z=227 AT (205,274)
Z=216 AT (205,262)
Z=217 AT (213,252)
Z=218 AT (213,238)
```

WEST OF RAILROAD BAND #4 1 NOV. 1972

```
Z=186 AT (241,260)
Z=190 AT (262,242)
Z=182 AT (289,230)
Z=191 AT (322,244)
Z=202 AT (324,274)
Z=210 AT (312,306)
Z=189 AT (282,312)
Z=179 AT (263,290)
Z=206 AT (268,270)
Z=182 AT (285,246)
```

AT RANDOM IN PLAYA BAND #4 1 NOV. 1972

```
$RUN AREA
```

BAND #4, 1 NOV. 1972, PERCENT AREA

```
COLOR:      0      1      2      3      4      5      6      7
GRAY:     032    064    096    128    160    192    224    255
PERCENT: 00.96  00.08  00.36  01.10  11.38  64.70  18.44  02.82

$RUN DIGIT
```

ERTS-1 BAND 4
18 FEB. 1973
WILLCOX, ARIZONA

```
$RUN DISPLY
#P2

$RUN MARKER
$RUN HISTOR
SCAN
Z=202 AT (283,438)
Z=190 AT (283,448)
Z=199 AT (284,428)
Z=204 AT (276,428)
Z=204 AT (288,440)
```

SOUTH END OF PLAYA BAND #4 18 FEB. 1973

Z=119 AT (203, 286)
Z=114 AT (204, 274)
Z=099 AT (209, 264)
Z=099 AT (209, 254)
Z=071 AT (212, 242)

WEST OF RAILROAD
BAND #4
18 FEB. 1973

Z=137 AT (258, 238)
Z=143 AT (287, 226)
Z=136 AT (331, 242)
Z=152 AT (316, 274)
Z=156 AT (304, 312)
Z=147 AT (297, 342)
Z=126 AT (263, 318)
Z=130 AT (280, 282)
Z=113 AT (243, 276)
Z=137 AT (282, 252)

AT RANDOM
IN PLAYA
BAND #4
18 FEB. 1973

BAND #4, 18 FEB. 1973, PERCENT AREA

```
$RUN AREA
COLOR:      0       1       2       3       4       5       6       7
GRAY:     032     064     096     128     160     192     224     255
PERCENT: 20.92   24.40   24.72   15.26   10.72   03.60   00.28   00.00

$RUN DIGIT
#P3

#RUN DISPLY
```

END!

#RUN DISPLY

APPENDIX D

"SYSTEM 800"

COMPUTER PRINTOUTS

PHOENIX, ARIZONA

SPECTRAL ANALYSIS

P1,P0

$RUN DISPLY

#P0

#RUN DIGIT

$RUN ADDER
#P1,P0

#RUN DISPLY

$RUN DIGIT
#P0

#RUN NEGATE

$RUN DISPLY
#P0

#RUN DISPLY

#RUN DISPLY

$RUN MARKER
#RUN DIGIT

$RUN HISTOR

SCAN

$RUN AREA

800 SYSTEM COMPUTER PRINTOUT #4

PHOENIX ARIZONA
SPECTRAL ANALYSIS.

ERTS-1 POSITIVE IMAGES OF CLOUDS AND SHADOWS ; 14 APRIL 1973, LINEAR DIGITIZATION

(1) THIS IS A SETUP TO DIGITIZE ALL IMAGES IN THE SAME RANGE STARTING WITH BAND 4 (IN FILE P2)

COLOR:	0	1	2	3	4	5	6	7
GRAY	032	064	096	128	160	192	224	255
PERCENT	14.72	22.24	27.78	29.24	05.42	00.50	00.00	00.00

OMIT

#RUN DISPLY

```
PIP  V10-02
#P4CP1
```

READY !

ART

ERTS-1 BAND 6
14 APRIL 1973
PHOENIX ARIZONA

```
#^C
.KI
$RUN MARKER

#RUN DIGIT

$RUN HISTOR

SCAN
Z=222 AT (168,292)
Z=202 AT (169,300)
Z=216 AT (171,290)
Z=204 AT (175,280)
Z=209 AT (162,250)
Z=208 AT (162,244)
Z=209 AT (162,238)
```

CLOUD BAND #6

```
Z=077 AT (152,246)
Z=069 AT (153,238)
Z=055 AT (151,248)
Z=063 AT (151,242)
Z=059 AT (152,238)
Z=079 AT (155,232)
Z=068 AT (155,282)
Z=084 AT (155,290)
Z=071 AT (154,284)
```

SHADOW BAND #6

```
$RUN AREA
```

BAND #6 PERCENT AREA

COLOR:	0	1	2	3	4	5	6	7
GRAY:	032	064	096	128	160	192	224	255
PERCENT:	01.98	04.54	12.62	24.80	31.82	20.60	03.50	00.08

```
#RUN DISPLY

$RUN MARKER

#RUN DIGIT

$RUN HISTOR
SCAN
Z=250 AT (165,304)
Z=227 AT (168,296)
Z=239 AT (166,292)
Z=240 AT (165,302)
Z=224 AT (163,312)
Z=208 AT (161,256)
Z=211 AT (161,248)
Z=207 AT (161,254)
Z=205 AT (160,262)
Z=074 AT (152,254)
```

ERTS-1 BAND 7
14 APRIL 1973
PHOENIX ARIZONA

CLOUD BAND #7

107 D2

```
Z=080 AT (152,250)
Z=073 AT (152,246)
Z=052 AT (152,240)
Z=071 AT (154,238)
Z=070 AT (154,234)
Z=068 AT (153,278)
Z=037 AT (153,284)
Z=054 AT (153,290)
Z=048 AT (153,292)
```

SHADOW BAND #7

```
$RUN AREA
```

BAND #7 PERCENT AREA

COLOR:	0	1	2	3	4	5	6	7
GRAY:	032	064	096	128	160	192	224	255
PERCENT:	02.52	05.62	15.44	30.68	28.78	13.48	02.94	00.42

ERTS-1 BAND 4
14 APRIL 1973
PHOENIX ARIZONA

```
#RUN DISPLY

$RUN MARKER
#RUN DIGIT

$RUN HISTOR
SCAN
Z=152 AT (164,300)
Z=172 AT (164,298)
Z=166 AT (165,292)
Z=192 AT (164,290)
Z=194 AT (162,290)
Z=187 AT (158,254)
Z=158 AT (161,250)
Z=155 AT (161,244)
Z=157 AT (162,240)
```

CLOUD BAND #4

```
Z=035 AT (153,238)
Z=066 AT (153,246)
Z=055 AT (151,256)
Z=046 AT (149,264)
Z=047 AT (153,278)
Z=052 AT (153,288)
Z=051 AT (152,294)
Z=066 AT (152,302)
```

SHADOW BAND #4

APPENDIX E

"SYSTEM 800"

COMPUTER PRINTOUTS

PRESCOTT, ARIZONA

SPECTRAL ANALYSIS

```
 KI
INV CMD!
$
```

800 SYSTEM COMPUTER PRINTOUT # 5

```
 RUN DISPLY
#P3/S
```

SPECTRAL ANALYSIS OF COPPER BASIN, PRESCOTT ARIZONA

```
$RUN DISPLY
#P3

$RUN HISTOR
SCAN
^C
IRUNCAREA
```

ERTS-1 NEGATIVE IMAGES OF COPPER BASIN AREA SOUTH OF PRESCOTT ARIZONA; 29 SEPTEMBER 1972; LINEAR DIGITIZATION

```
$^C
.^C
INV CMD!
$

 RUN AREA


COLOR:      0      1      2      3      4      5      6      7
GRAY:     012    024    036    048    060    072    084    255
PERCENT: 01.64  02.22  04.98  07.08  10.30  13.62  14.38  45.66

$RUN HISTOR
SCAN
Z=088 AT (132,131)
 COUNT= 002168 AT 049 GRAY.
 COUNT= 002631 AT 058 GRAY.
 COUNT= 002382 AT 047 GRAY.
 COUNT= 001433 AT 037 GRAY.
 COUNT= 001166 AT 032 GRAY.
0> COUNT= 001166 AT 032 GRAY.
 COUNT= 002423 AT 054 GRAY.
 COUNT= 002821 AT 060 GRAY.
 COUNT= 003380 AT 063 GRAY.
 COUNT= 003161 AT 064 GRAY.
1> COUNT= 003161 AT 064 GRAY.
 COUNT= 003469 AT 082 GRAY.
 COUNT= 002861 AT 091 GRAY.
 COUNT= 003176 AT 096 GRAY.
2> COUNT= 003176 AT 096 GRAY.
 COUNT= 001578 AT 118 GRAY.
 COUNT= 001163 AT 127 GRAY.
 COUNT= 001239 AT 130 GRAY.
 COUNT= 001526 AT 128 GRAY.
3> COUNT= 001526 AT 128 GRAY.
 COUNT= 000830 AT 143 GRAY.
 COUNT= 000650 AT 152 GRAY.
 COUNT= 000449 AT 158 GRAY.
 COUNT= 000370 AT 161 GRAY.
 COUNT= 000364 AT 159 GRAY.
 COUNT= 000370 AT 161 GRAY.
```

① THIS IS A SET UP OF THE PARTITION INTO EQUAL INTERVALS TO RUN AREA PROGRAM.

```
 COUNT= 000370 AT 161 GRAY.
 COUNT= 000367 AT 162 GRAY.
 COUNT= 000364 AT 159 GRAY.
 COUNT= 000370 AT 161 GRAY.
 COUNT= 000576 AT 160 GRAY.
4> COUNT= 000576 AT 160 GRAY.
 COUNT= 000183 AT 184 GRAY.
 COUNT= 000059 AT 191 GRAY.
 COUNT= 000182 AT 192 GRAY.
5> COUNT= 000182 AT 192 GRAY.
 COUNT= 000082 AT 209 GRAY.
 COUNT= 000087 AT 216 GRAY.
 COUNT= 000056 AT 221 GRAY.
 COUNT= 000034 AT 223 GRAY.
 COUNT= 000056 AT 225 GRAY.
 COUNT= 000056 AT 225 GRAY.
 COUNT= 000088 AT 224 GRAY.
6> COUNT= 000088 AT 224 GRAY.
 COUNT= 000024 AT 254 GRAY.
 COUNT= 003002 AT 255 GRAY.
7> COUNT= 003002 AT 255 GRAY.
```

READY!

```
$RUN AREA
```

BAND #7 PERCENT AREA

```
COLOR:      0       1       2       3       4       5       6       7
GRAY:     032     064     096     128     160     192     224     255
PERCENT: 07.00   23.38   36.10   20.06   08.56   02.52   00.84   01.44

$RUN MARKER

$RUN DIGIT
#P0

$RUN HISTOR
SCAN

$RUN AREA
C
```

BAND #4 PERCENT AREA

```
 OLOR:      0       1       2       3       4       5       6       7
GRAY:     032     064     096     128     160     192     224     255
PERCENT: 04.34   11.96   27.54   29.34   15.50   07.18   03.16   00.90

$RUN DISPLY
#P0

$RUN MARKER

$RUN DIGIT

$RUN HISTOR
SCAN

$RUN AREA
```

BAND #5 PERCENT AREA

```
COLOR:      0       1       2       3       4       5       6       7
GRAY:     032     064     096     128     160     192     224     255
PERCENT: 09.64   16.80   25.84   19.28   11.82   06.92   04.00   05.60

$RUN DISPLY
```

APPENDIX F

"SYSTEM 800"

COMPUTER PRINTOUTS

WILLCOX, ARIZONA

SPECTRAL ANALYSIS OF ATMOSPHERIC EFFECTS

①

```
#RUN NEGATE

$RUN ADDER
#P2,P3

#RUN DISPLY

#RUN NEGATE

#RUNP#DDER

#RUN DISPLY

.$
```

800 SYSTEM COMPUTER PRINTOUT RE 9 (CONT.)

```
 RUN HISTOR
SCAN

$RUN MARKER

$RUN HISTOR

SCAN
```

SPECTRAL ANALYSIS OF ATMOSPHERIC EFFECTS

```
$RUN MARKER
$RUN HISTOR

SCAN

$RUN MARKER
$RUN HISTOR
SCAN

$RUN HISTOR
SCAN
```

ERTS-1 POSITIVE IMAGES OF CLOUDS, SHADOW AND ADJACENT TERRAIN WILLCOX ARIZONA 4 SEPT. 1973 ; LOG DIGITIZATION

① THIS IS A SETUP TO DIGITIZE ALL IMAGES WITHIN THE SAME RANGE STARTING WITH BAND 4 (IN FILE P0)

```
Z=228 AT (116,315)
Z=230 AT (116,303)
Z=234 AT (121,289)
Z=224 AT (122,283)
Z=225 AT (114,277)
Z=220 AT (110,291)
Z=226 AT (109,297)
Z=224 AT (107,305)
Z=221 AT (106,313)
Z=229 AT (115,311)
```

CLOUD (OUT OF RANGE OF OTHER BANDS) HAD TO READJUST VIDEO RANGE SO THAT ALL BANDS FALL WITHIN 0-255 DIGITIZATION LEVEL

NOTE: IN THE PROCESS OF READJUSTING VIDEO LEVELS SO ALL BANDS FALL WITHIN 0-255 DIGITIZATION LEVEL

```
Z=005 AT (086,297)
Z=000 AT (086,293)
Z=000 AT (086,283)
Z=000 AT (086,275)
Z=000 AT (086,265)
Z=000 AT (079,265)
Z=000 AT (076,279)
Z=000 AT (076,289)
Z=000 AT (078,297)
Z=000 AT (068,291)

$RUN MARKER
$RUN*HISTOR
SCAN
```

```
Z=232 AT (155,270)
Z=236 AT (144,266)
Z=235 AT (144,256)
Z=233 AT (146,250)
Z=235 AT (149,244)
Z=230 AT (144,234)
Z=232 AT (144,250)
Z=23? AT (143,262)
Z=235 AT (142,270)
Z=232 AT (133,274)
```

```
Z=105 AT (109,266)
Z=104 AT (109,260)
Z=097 AT (109,254)
Z=095 AT (109,250)
Z=098 AT (111,244)
Z=098 AT (111,238)
Z=102 AT (111,232)
Z=101 AT (111,226)
Z=094 AT (107,220)
```

ALL DIGITIZED LEVELS EQUAL NOW IN ALL FOUR ERTS-1 BANDS

```
$RUN AREA
COLOR:      0       1       2       3       4       5       6       7
GRAY:     032     064     096     128     160     192     224     255
PERCENT: 01.22   00.42   01.14   08.58   55.32   29.86   02.42   00.98
```

```
$RUN MARKER
$RUN HISTOR
SCAN
Z=229 AT (148,278)
Z=233 AT (148,268)
Z=232 AT (148,262)
Z=231 AT (148,256)
Z=232 AT (151,248)
Z=230 AT (152,240)
Z=230 AT (151,234)
Z=226 AT (148,230)
Z=230 AT (152,240)
Z=230 AT (161,250)
```

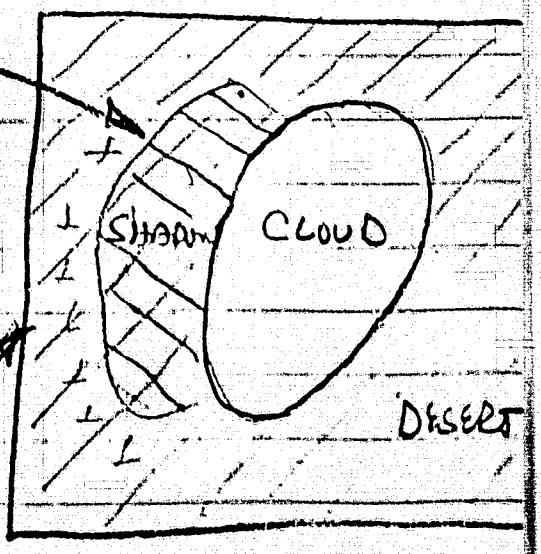
BRIGHT CLOUD BAND #5

ERTS-1 BAND 5
4 SEPT. 1973
WILLCOX ARIZONA.

```
Z=084 AT (117,260)
Z=072 AT (117,254)
Z=069 AT (119,248)
Z=060 AT (119,240)
Z=058 AT (119,234)
Z=057 AT (119,228)
Z=040 AT (114,220)
Z=056 AT (114,214)
Z=056 AT (110,208)
Z=044 AT (108,222)
```

TERRAIN IN SHADOW BAND #5

VIDEO IMAGE AS APPEAR ON 108 T.V. MONITOR




```
Z=142 AT (093,268)
Z=139 AT (085,256)
```

TERRAIN NOT IN SHADOW. BAND #5

107 F3

```
Z=140 AT (085,246)
Z=144 AT (085,238)
Z=145 AT (085,230)
Z=135 AT (086,220)
Z=141 AT (090,216)
Z=136 AT (090,212)
Z=146 AT (085,210)
Z=143 AT (116,270)
```

TERRAIN NOT IN SHADOW BAND #5

ERTS-1 BAND 5

BAND #5 PERCENT AREA

```
$RUN AREA
COLOR:      0       1       2       3       4       5       6       7
GRAY:     032     064     096     128     160     192     224     255
PERCENT: 01.56   01.80   04.80   09.42   49.28   30.34   02.14   00.58

$
```

```
 RUN MARKER
$RUN HISTOR
SCAN
```

ERTS-1 BAND 4
4 SEPT. 1973
WILLCOX ARIZONA

```
Z=229 AT (154,278)
Z=233 AT (154,270)
Z=231 AT (157,260)
Z=231 AT (158,252)
Z=230 AT (158,240)
Z=226 AT (153,234)
Z=233 AT (151,250)
Z=230 AT (144,252)
Z=234 AT (142,266)
Z=232 AT (141,278)
```

BRIGHT CLOUD BAND #4

```
Z=117 AT (117,266)
Z=103 AT (116,260)
Z=100 AT (116,254)
Z=096 AT (118,244)
Z=104 AT (118,234)
Z=099 AT (118,226)
Z=096 AT (112,238)
Z=094 AT (107,242)
Z=088 AT (106,254)
Z=097 AT (108,266)
```

TERRAIN IN SHADOW BAND #4

```
Z=155 AT (090,274)
Z=143 AT (088,264)
Z=145 AT (085,254)
Z=147 AT (085,242)
Z=143 AT (088,232)
Z=144 AT (087,224)
Z=143 AT (091,216)
Z=145 AT (091,208)
Z=145 AT (089,226)
Z=145 AT (086,240)
```

TERRAIN NOT IN SHADOW BAND #4

BAND #4 PERCENT AREA

```
$RUN AREA
COLOR:      0       1       2       3       4       5       6       7
GRAY:     032     064     096     128     160     192     224     255
PERCENT: 01.30   00.46   01.62   09.64   62.80   20.92   02.34   00.82

$
```

RUN MARKER

$RUN HISTOR

ERTS-1 BAND 6
4 SEPT. 1973
WILLCOX ARIZONA.

SCAN
Z=229 AT (152,276)
Z=231 AT (152,268)
Z=230 AT (152,264)
Z=230 AT (152,254)
Z=232 AT (152,248)
Z=229 AT (151,240)
Z=228 AT (144,240)
Z=227 AT (143,254)
Z=226 AT (138,262)
Z=228 AT (136,272)

BRIGHT CLOUD BAND #6

Z=067 AT (113,264)
Z=051 AT (112,256)
Z=052 AT (117,250)
Z=058 AT (117,244)
Z=058 AT (114,240)
Z=047 AT (114,234)
Z=035 AT (112,226)
Z=050 AT (111,224)
Z=045 AT (109,220)
Z=054 AT (107,216)

TERRAIN IN SHADOW BAND #6

Z=145 AT (093,206)
~~Z=139 AT (093,214)~~
Z=153 AT (088,216)
Z=152 AT (088,224)
Z=156 AT (085,232)
Z=155 AT (084,238)
Z=156 AT (080,246)
Z=152 AT (083,258)
Z=157 AT (085,268)

TERRAIN NOT IN SHADOW BAND #6

107 F 6

Z=157 AT (095,274)
Z=158 AT (098,276) TERRAIN NOT IN SHADOW

(7)

BAND #6

BAND #6 PERCENT AREA

```
$RUN AREA
COLOR:      0       1       2       3       4       5       6       7
GRAY:     032     064     096     128     160     192     224     255
PERCENT: 01.02   00.68   01.34   03.74   38.46   51.48   02.62   00.54
```

```
$RUN MARKER
$RUN HISTOR
SCAN
Z=233 AT (150,276)
Z=236 AT (150,270)  BRIGHT
Z=233 AT (157,266)
Z=235 AT (159,258)  CLOUD
Z=231 AT (159,252)
Z=232 AT (158,242)  BAND #7
Z=228 AT (151,242)
Z=232 AT (149,254)
Z=236 AT (146,262)
Z=233 AT (140,272)
```

ERTS-1 BAND 7
4 SEPT. 1973
WILLCOX ARIZONA

```
Z=040 AT (118,258)
Z=020 AT (117,250)  TERRAIN IN
Z=022 AT (118,240)
Z=031 AT (118,236)  SHADOW
Z=013 AT (116,228)
Z=020 AT (114,224)  BAND #7
Z=028 AT (112,216)
Z=004 AT (110,232)
Z=010 AT (107,242)
Z=013 AT (102,250)
```

```
Z=159 AT (102,274)
Z=147 AT (097,268)
Z=156 AT (089,266)
Z=153 AT (088,260)
Z=154 AT (085,254)
Z=154 AT (084,244)
Z=160 AT (085,234)
Z=159 AT (089,228)
Z=159 AT (089,218)
Z=163 AT (088,208)
```

TERRAIN NOT IN SHADOW BAND #7

BAND #7 PERCENT AREA

```
$RUN AREA
COLOR:      0       1       2       3       4       5       6       7
GRAY:     032     064     096     128     160     192     224     255
PERCENT: 01.24   00.58   01.30   03.04   24.78   65.38   02.84   00.74

$
```

APPENDIX G

MAPPING OF THE 1973 MISSISSIPPI RIVER FLOODS FROM ERTS

Remote Sensing and Water Resources Management